

**ANTIMICROBIAL PEPTIDE ADSORPTION AND STORAGE ON
OXIDIZED METAL SURFACES TO MITIGATE
BACTERIAL ATTACHMENT**

by

Jesús Héctor Morales Espejo

A Dissertation

Submitted to the Faculty of Purdue University

In Partial Fulfillment of the Requirements for the degree of

Doctor of Philosophy



School of Materials Engineering

West Lafayette, Indiana

December 2018

THE PURDUE UNIVERSITY GRADUATE SCHOOL
STATEMENT OF COMMITTEE APPROVAL

Dr. David Bahr, Chair

Department of Materials Science and Engineering

Dr. Yao Yuan

Department of Food Science

Dr. Lia Stanciu

Department of Materials Science and Engineering

Dr. Rodney Trice

Department of Materials Science and Engineering

Approved by:

Dr. David Bahr

Head of the Graduate Program

*To my beloved parents,
Clara and Héctor.*

ACKNOWLEDGMENTS

This work used samples which were originally created on a contract from Defense Threat Reduction Agency, Basic Research Award # IACRO 13-5897I, to Purdue University sub-contracted through Sandia National Laboratories. Sandia National Laboratories is a multiprogram laboratory managed and operated by Sandia Corporation, a wholly owned subsidiary of Lockheed Martin Company, for the U.S. Department of Energy's National Nuclear Security Administration under contract DE-AC04-94AL85000.

TABLE OF CONTENTS

LIST OF TABLES	8
LIST OF FIGURES	9
ABSTRACT.....	11
1. INTRODUCTION	12
2. BIOFILMS.....	17
2.1 Origin of biofilms	17
2.2 Development of biofilms	18
2.3 Presence of biofilms.....	20
2.4 Remotion of biofilms	22
2.5 Prevention of biofilms.....	23
2.6 Benefits of biofilms.....	25
3. THE ANTIMICROBIAL SYSTEM.....	26
3.1 The material surface.....	26
3.1.1 The chemistry of the surface.....	26
3.1.1.1 Stainless steel 304L	26
3.1.1.2 Titanium alloy Ti-6Al-4V	26
3.1.2 The surface topography	27
3.2 The antimicrobial agent	37
3.2.1 Nisin.....	43
3.2.1.1 Classification and chemical structure	43
3.2.1.2 Nisin as food preservative	46
3.2.1.3 Nisin activity.....	47
3.2.1.4 Nisin market	52
3.2.1.5 Future of nisin.....	53
3.3 The immobilization technique	56
3.4 The microorganism	59
4. SUBSTRATE CRACKING IN Ti-6Al-4V DRIVEN BY PULSED LASER IRRADIATION AND OXIDATION	62

4.1	Abstract	62
4.2	Introduction	62
4.3	Experimental	64
4.4	Results	65
4.4.1	Oxide film	65
4.4.2	Substrate	67
4.5	Discussion	68
4.5.1	Mechanics of the film fracture process	68
4.5.2	Mechanics of the substrate fracture process	71
4.6	Conclusions	74
5.	PEPTIDE INFUSION INTO MECHANICALLY INDUCED CRACKS IN OXIDE COATINGS TO CREATE AN ANTIBACTERIAL METALLIC SURFACE	76
5.1	Abstract	76
5.2	Introduction	76
5.3	Experimental	79
5.3.1	Titanium	79
5.3.2	Stainless steel	80
5.3.3	Nisin	81
5.3.4	Release test	81
5.3.5	Durability test	82
5.3.6	Antibacterial tests	82
5.4	Results and discussion	83
5.4.1	Determining the release of physisorbed nisin from oxidized metal surfaces	83
5.4.1.1	Ti64	83
5.4.1.2	SS	84
5.4.2	Detection of nisin on the surface of oxidized metals after mechanical scrubbing. ...	85
5.4.3	The antibacterial performance of nisin-coated oxidized metals	86
5.4.3.1	Tests using 2.5% nisin	86
5.4.3.2	Test using nisin ZP	88
5.5	Conclusions	89

6. APPLICATION OF AN OXIDIZED STAINLESS STEEL SURFACE AS A MEDIUM TO STORE BIOCHEMICAL AGENTS WITH ANTIMICROBIAL PROPERTIES	91
6.1 Abstract	91
6.2 Introduction.....	91
6.3 Experimental	94
6.4 Results and discussion	97
CONCLUDING REMARKS AND FUTURE WORK	103
REFERENCES	105
VITA	126

LIST OF TABLES

Table 3. 1 Summary for the different surface treatment techniques	36
Table 3. 2 Antimicrobial agents of potential use	41
Table 3. 3 Examples of worldwide use of nisin	47
Table 3. 4 Works about synergistic effects using nisin for food preservation	55
Table 4. 1 Chemical composition of the Ti alloy, obtained by EDS.....	65
Table 4. 2 Applied laser scan rates with resulting film thickness and color variation of the coupons. Irradiated area (colored centered square) is 6 x 6 mm.	65
Table 4. 3 Crack density and crack spacing obtained by laser scanning at different rates.	66
Table 4. 4 Mechanical properties for film and substrate.....	70

LIST OF FIGURES

Figure 2. 1	Different stages in the development of a biofilm: (1) Formation of the conditioning film, (2) Adhesion of cells, (3) Formation of microcolonies, (4) Biofilm formation, and (5) Detachment and dispersal, and the cycle goes on.....	18
Figure 3. 1	Peptide structure of nisin, with three rings on the “N” terminus, the hinge region (positions 20, 21 and 22), and two more rings on the “C” terminus.....	44
Figure 4. 1	Backscattered electron images of the oxide film formed after PLI. (a) At 110 mm/s and (b) At 300 mm/s. Lines in the background, parallel to the arrows in the figures, are the result of the scanning direction of the laser path. There is no clear relationship between the laser direction and the formation of cracks.....	67
Figure 4. 2	FIB images of cross sections. (a) Crack grows perpendicular to the interface but with some wobbling, probably due to the alternate expansion/contraction cycles between each laser pulse and the next. (b) The presence of a branch coming from the main crack.	68
Figure 4. 3	Decay of available driving force with increasing crack depth	72
Figure 4. 4	Variation in stress intensity factor vs relative crack depth (penetrating into the substrate). Shaded area represents the relative crack depth for the films used in this study.	73
Figure 5. 1	Microstructure of (a) cracked Ti64 and (b) uncracked SS.....	80
Figure 5. 2	Nisin release from SS uncracked oxide layer. (a) Colorimetric test showing the color variation in samples taken at different times (in days), (b) Linear relationship between time and nisin concentration estimated from absorbance values.	84
Figure 5. 3	FTIR spectra for Ti64 oxide layer: A = pristine oxide layer, B = nisin ZP coated, C = after 1 scrub movement, D = after 2 scrubs, E = after 3 scrubs, F = after multiple scrubs. The infrared bands observed when coating with nisin reappear after multiple scrubbing, indicating that there is still nisin on the surface, likely coming out of the cracks.....	85
Figure 5. 4	Antibacterial tests performed on (a) uncoated Ti64 oxide layer, (b) nisin-coated Ti64 oxide layer, (c) uncoated SS oxide layer, (d) nisin-coated SS oxide layer.	87
Figure 5. 5	Antibacterial test on nisin-coated Ti64 oxide layer scrubbed using a wet sponge....	88
Figure 5. 6	Antibacterial tests performed on nisin-coated Ti64 cracked oxide layer after being immersed in water at 50°C for 24 hours (up), and on nisin-coated SS uncracked oxide layer after being immersed in water at room temperature for 21 consecutive days (down).	89

Figure 6. 1 Microstructures corresponding to: (a) U-SS, in which only some scratches and polishing lines are observed on the surface, and (b) C-SS, in which cracks may be observed all over the surface and the areas with more cracks are marked in ovals95

Figure 6. 2 Summary of the tests performed on the stainless steel coupons, changing temperature and pH. It can be seen that nisin release is mainly driven by pH, while rise in temperature only accelerates the reaction. Interesting to notice that slow release was obtained when U-SS was tested at room temperature and pH 6, while there was no release at all when C-SS was submitted to the same conditions; this means that for U-SS there was a slow detachment of nisin nanoparticles from the surface, while for C-SS nisin is immobilized inside the cracks, taking much longer times to travel until the aqueous solution. 97

Figure 6. 3 U-SS at room temperature and pH 6. (a) Linear relationship between time and the accumulative nisin release, but even after 21 days there is still desorption; (b) According to calculations, only 34% of the total nisin retained by the oxide film has been released after 21 days, meaning that, if the linear behavior is maintained, all nisin would be released after 63 days of immersion under these conditions. 98

Figure 6. 4 U-SS at 50°C and pH 2. (a) Linear relationship between time and the accumulative nisin release; (b) According to calculations, it would take approximately 14 hours to release all the nisin retained on the oxide layer..... 99

Figure 6. 5 Microstructures corresponding to: (a) C-SS before nisin coating, and (b) C-SS after nisin coating and immersion into solution at 50°C and pH 2, corroded surface, cracks are not there anymore. 100

Figure 6. 6 Test for C-SS immersed at 50°C and pH 2. (a) BCA reagent is originally green in color, (b) when in contact with the release solution, a purple-colored complex is formed. 101

ABSTRACT

Author: Morales Espejo, Jesús Héctor. Ph.D.

Institution: Purdue University,

Degree Received: December 2018.

Title: Antimicrobial Peptide Adsorption and Storage on Oxidized Metal Surfaces to Mitigate Bacterial Attachment.

Major Professor: David Bahr.

In the pursuit to create more natural, chemical-free antibacterial surfaces, fracture mechanics and the ability of laser-modified surfaces to store an antimicrobial agent have been investigated through the combination of scanning electron microscopy coupled with focused ion beam, infrared spectroscopy, bactericidal tests and a colorimetric method. It was found that the irradiation of a nanosecond pulsed laser on Ti-6Al-4V and 304L stainless steel surfaces creates colored oxide layers with 100-150 nm in thickness and, by using the adequate parameters, it is possible to obtain surfaces with cracks of 1-6 μm deep that not only penetrate the film but also the substrate. Physisorption was used to immobilize nisin, an antimicrobial agent, to the walls of those cracks. Antibacterial tests show that nisin-coated oxide layers exhibit antibacterial activity against *Listeria monocytogenes* even after immersion in water or the application of mechanical scrubbing, and release kinetics tests demonstrated that nisin desorption is promoted by acidic pH and that nisin is effectively stored into the cracks of stainless steel. The immobilization into the cracks of the titanium oxide layer seem to reveal that there is an excellent anchor between the peptide and the crack walls, but future research is still required.

1. INTRODUCTION

Food safety has become an important issue worldwide due to increasing foodborne diseases and changes in food habits. The occurrence of illness due to consumption of foods contaminated by bacteria has a great impact on public health [1].

The true cost of foodborne illnesses is difficult to determine. Estimates in the United States vary widely. A report stated that there were between 6.5 and 33 million cases per year, resulting in 9,000 deaths and costing \$6.5-34.9 billion annually [2, 3], and although tremendous efforts have been made by governments and the food industry to reduce foodborne illnesses, there are still sporadic outbreaks due to post-production contamination by foodborne pathogens [4]. For instance, in 2007, there was a recall by a New Jersey company of a total of 21.7 million pounds of ground meat patties [3]. Effective food preservation has become an important subject of research because of improving standards of food quality and increasingly stringent requirements for microbial control [5].

Antimicrobial food preservatives are employed in many food products to prevent post-processing contamination, extend shelf-life and keep food quality [4] but, on the other hand, consumers do not want high levels of chemical food preservatives in their food and yet they increasingly look for convenient food that is of high quality without excessive processing [6]. Thus, a number of antimicrobial agents are allowed by regulatory agencies to minimize the deterioration of food quality but a growing interest in using natural additives in the food industry restricts the preservatives allowed to be used, especially those needing high concentrations to be effective [7].

However, pathogens may not only contaminate the food matrix, but they can also be present on surfaces that make contact with food [8]. Microbial contamination of foods during

processing/storage is a major cause of foodborne illnesses and reduction in shelf-life [7]. Adhesion, accumulation and growth of microorganisms on artificial surfaces, designated as biofouling, can have severe negative consequences not only in food processing but also in other industrial processes (textile, paper, etc.), medicine (nosocomial infections, medical implants) [9] and in equipment in contact with seawater (pipelines, cooling and filtration systems, fishing nets, ship hulls and bridge pillars) [10, 11]. Bacterial colonization has an adverse effect on the functionality of the surface, resulting in the contamination of manufacturing surfaces in the food industry, less performance or loss of medical implants in the medical field, or clogging of pipes and tubing in other industries [12].

The attachment of bacteria followed by development of biofilms in food processing environments is a potential source of contamination that may conduct to food spoilage or transmission of diseases [13]. Products like disinfectants and sanitizers are used in specific cleaning routines in the food industry to decontaminate the food contact surfaces [8], but these products usually contain chemical compounds which represent a great burden for nature since they are not environmentally friendly [14]. Additionally, they usually contain acids and alkalis which are quite destructive of natural or synthetic materials used in the food processing plant, causing erosion, cracking, hardening and shrinking [3].

The prevention of bacterial adhesion by inactivation of bacteria when contacting the surface (contact killing) or alternatively, by repelling bacterial cells from attachment (antibacterial), has gained more prominence in the last years [12]. Inhibiting initial bacterial colonization will avoid the subsequent formation of a biofilm [15].

Antimicrobial surfaces are promising materials for effectively controlling microbial contamination on various substrates by impeding the growth of microorganisms [16]. Nevertheless,

the design of an antimicrobial surface is not an easy task given that the bacterial attachment to surfaces is influenced by many factors such as the cell surface charge, surface chemistry, surface hydrophobicity, surface roughness/topography, surface energy, pH, temperature, and presence of flagella and extracellular polysaccharides [17, 18].

The creation of an effective antimicrobial surface involves the interplay of four main elements: The surface, the chosen antibacterial agent, the immobilization technique employed, and the microorganism(s) involved. In this study, the overall goal was to demonstrate that, by using surface modification by a pulsed laser, it is possible to create microcracks in which, without significantly altering the mechanical properties of the surface material, an antibacterial agent can be immobilized, conferring antibacterial properties to the surface for a longer time.

With this purpose, the materials selected were 304L stainless steel and Ti-6Al-4V titanium alloy. Stainless steel is ideally suited to the construction of food manufacturing plants because of its heat transfer efficiency, cleanability [19], strength and corrosion resistance [3]. Ti-6Al-4V was chosen given its importance in medical instrumentation [20].

Concerning the agent, antimicrobial peptides (AMPs) are a new and promising class of antimicrobial agents with a low tendency to induce resistance and little known side effects [16]. From the gamma of AMPs that have been discovered, nisin was chosen as a model antimicrobial for this study since it is naturally produced, has a broad spectrum against Gram-positive bacteria and, especially, for being the only bacteriocin allowed in foods as a preservative [4].

Regarding the immobilization technique, in the pursuit of a more natural, chemical-free surface, physisorption was the method selected.

Listeria monocytogenes was chosen as the model bacterium due to the incidence and morbidity related to this microorganism.

The objectives of this research were threefold: (1) Determine the presence of cracks (after pulsed laser) and their geometry through the characterization of metallic surfaces, (2) demonstrate that an antimicrobial agent (nisin) can be stored inside these cracks, and (3) evaluate the antibacterial efficacy of the stored agent under different treatments to verify stability.

Given that this work constitutes an amalgam between materials science and microbiology, the following two chapters are dedicated to introduce microbiological concepts that are necessary to explore before proceeding to the experimental tests.

Chapter 2 will introduce the problematic that biofilms represent especially for the food industry, how they develop, how to remove and how prevention against biofilms is currently done; all this is as a prelude to introduce the concept of antimicrobial system, its four components and how they interact, which is explained in Chapter 3.

Chapter 4 explores the characterization of the oxide layer formed on the surface of a titanium alloy after being submitted to pulsed laser irradiation. The geometry of the artificially created cracks is determined, emphasizing that these penetrate into the substrate. Additionally, by applying some equations from literature, an estimation of the fracture toughness up to the point where cracks arrest is presented. This chapter was originally published as a paper in the journal *Surface and Coatings Technology*.

Antibacterial tests were carried out on the oxide layer of a titanium alloy in Chapter 5, with the purpose to verify the biocidal activity displayed by an infused antimicrobial peptide in tandem with the laser-modified oxide surface.

Finally, Chapter 6 presents an analysis of the kinetics of the antimicrobial peptide desorbing from cracked and uncracked laser-modified oxide layers of stainless steel,

demonstrating that the peptide is effectively immobilized into the cracks and is only released under specific medium conditions.

2. BIOFILMS

2.1 Origin of biofilms

Bacterial adhesion depends on environmental factors (such as pH, temperature or ionic strength), properties of bacterial cell surface, and the chemical and physical characteristics of the surfaces, including elemental composition, hydrophobicity, charge, free energy, roughness, and the presence of pores [21].

Bacteria generally exist in one of two types of population: planktonic, freely existing in bulk solution, and sessile, attached to a surface [22]. Bacteria attach firmly to solid surfaces, passing from planktonic to sessile state, and they can grow forming microcolonies [16]. Biofouling refers to the unwanted formation of a layer of living microorganisms and their decomposition products as deposits on the surfaces in contact with liquid media [23, 24]. By growing, bacteria finally organize into biofilms, in which bacterial cells are embedded in a viscous matrix of extracellular polymeric substances (EPS) that protects them efficiently from physical and chemical biocidal agents (disinfectants, sanitizers, antibiotics), and makes them very difficult to remove [16, 22, 25–27]. It has also been demonstrated that mixed biofilms (formed by different bacterial species) are even more stable than monospecies biofilms [3].

Glycocalyx (also known as EPS, slime, capsule or sheath) is the term used to refer to the extracellular polymeric substance associated with the biofilms. It protects the bacteria from dehydration by retaining more water than its own mass and only slowly becomes desiccated. The biofilm polysaccharides are critical for the survival in hostile environments. It also protects the bacterial cells from the effects of antimicrobial agents [23].

2.2 Development of biofilms

The development of biofilms can arise on almost any surface in any environment in which microorganisms are present. Biofilm formation is a process involving a series of steps (Fig. 2.1) [23, 28]:

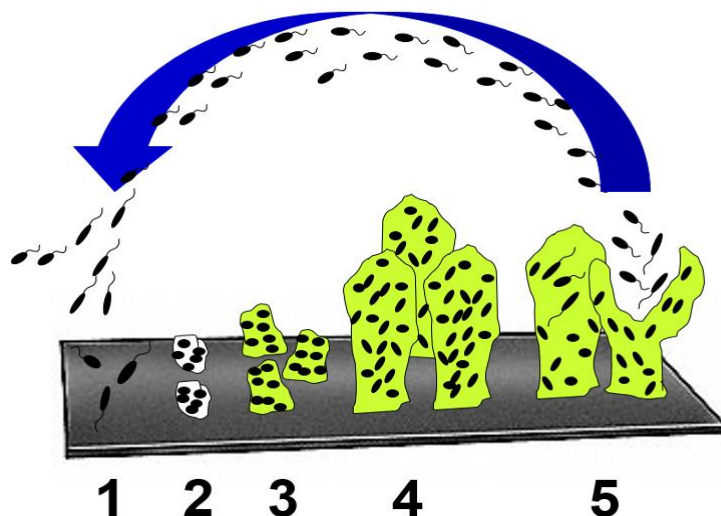


Figure 2. 1 Different stages in the development of a biofilm: (1) Formation of the conditioning film, (2) Adhesion of cells, (3) Formation of microcolonies, (4) Biofilm formation, and (5) Detachment and dispersal, and the cycle goes on.

- (a) Conditioning of a surface: Bacteria along with other organic and inorganic molecules get adsorbed to the surface forming a conditioning film. The accumulation of molecules at the solid-liquid interface on food-contact surfaces leads to a higher concentration of nutrients compared to the fluid phase. The conditioning changes the physicochemical properties of the surface. The microtopography of the food-contact surface also plays an important role to favor bacterial retention, especially if the surface is made of profound channels and crevices to trap bacteria. Scanning electron micrographs have revealed that foodborne pathogens and spoilage microorganisms pile up as biofilms on stainless steel, aluminum,

glass and polytetrafluoroethylene seals and nylon materials typically found in food-processing environments [23].

- (b) Adhesion of cells: The physicochemical properties of the bacterial cell surface are important for the adhesion of cells during this initial attachment. Initial weak interactions (van der Waals attraction forces, electrostatic forces and hydrophobic forces) developed between the bacterial cells and the substrate are referred to as reversible adhesion. During this stage, bacteria will show Brownian motion and can easily be removed by fluid shear forces (like rinsing). The irreversible attachment of cells comes next. Repulsive forces mainly avoid the bacterial cells in making a direct contact with the surface, however, the contact still occurs due to the production of surface appendages by the bacteria such as flagella, fimbriae and pili [29]. These polymeric structures form a bridge between the bacterial cell and the substrate, enabling the irreversible association with the surface, unless stronger forces such as scrubbing or scrapping are applied. Hydrophobicity, pH and temperature of the contact surface have also influence on the amount of adhered microorganisms [23].
- (c) Formation of microcolonies: Attached cells grow and divide by using the nutrients present in the conditioning film. This leads to the formation of microcolonies, building blocks of biofilm structure [29], which grow and coalesce to form a layer of cells on the surface. Simultaneously, the attached cells also produce more polymer (EPS) which helps to anchor the cells to the surface and to stabilize the colony from the changes of the environment, becoming thicker with time to form a matrix [23]. The microcolony may be composed of 10 – 25% cells and 75 – 90% EPS matrix. Bacterial cells within the matrix are characterized by their lack of Brownian motion, and usually by having a mushroom-like shape [22].

- (d) Biofilm formation: This is normally a slow process and may reach a few millimeters thick in a few days depending on the conditions. A mature biofilm requires 2 to 4 weeks to be formed [8]. The microorganisms within the biofilm are not uniformly distributed. Composition of biofilms can be heterogeneous, because of the colonization of different microorganisms with diverse nutritional requirements. The structure of the microbial biofilm is profoundly impacted by the interaction of the various microbial populations present in the initial stages of biofilm formation. The initial colonization species may potentially promote the colonization of species which are physiologically compatible, while hindering the binding of others [23]. Many other organic and inorganic substances and particles may get entrapped in the biofilm matrix too.
- (e) Detachment and dispersal: As the biofilm ages, some of the bacteria from the biofilm get detached individually. Sloughing is a discrete process in which periodic detachment of relatively big particles of biomass from the biofilm occurs. The released bacteria may be taken to new locations and start the biofilm process again [23, 30].

Some of the advantages of biofilm formation for bacteria are: (a) Protection from antibiotics, disinfectants and dynamic environments; (b) Intercellular communications within a biofilm rapidly stimulate the up and down regulation of gene expression enabling temporal adaptation; (c) Ability to survive in nutrient deficient conditions [22], (d) Reduced turbulence and scouring [3].

2.3 Presence of biofilms

Biofilm growth has been observed in many industrial and domestic domains, and in most cases this growth is detrimental [31]. Industries such as maritime, food, water systems, oil, paper,

opticians, dentistry and hospitals suffer the effects of biofilm growth, resulting in heavy costs in cleaning and maintenance [22].

In the food industry, biofilms cause serious engineering problems such as blocking the flow of heat across a surface and increases in the corrosion rate of surfaces leading to energy and production losses [22], as well as reduction in the service life of industrial devices such as tanks, pipelines and heat exchangers, among others [21]. Growth and cross-contamination of pathogens like *Listeria monocytogenes*, *Escherichia coli* and *Salmonella spp.* on the surface of food contact materials (work tables, conveyor belts, processing equipment) as well as noncontact materials (joints, valves, gaskets, ventilation ducts, door knobs, floor drains, etc.) represent a risk to public health [32, 33]. However, the major risk is when biofilms are present on food processing surfaces or the food itself, offering potential for cross-contamination and even post-process contamination [3]. Bacterial biofilms have been encountered on food products, beverage processing devices, packaging equipment, etc. [34].

In hospitals, bacteria present in the operating room or bacteria that normally populate the skin may contaminate an implant during its insertion, and then evolve to a biofilm [35]. Biofilms are also common in catheters and needles. [34]. Infections associated with medical surgical tools (catheters, stents, heart valves, arthroprostheses, etc. [35]) and supporting parts, are responsible for at least 1.5% - 7.2% post-operational complications [36].

In drinking water distribution systems, biofilms lead to decrease in water velocity and carrying capacity, clogging of pipes, increase in energy utilization and loss in efficiency of operations. Biofouling in heat exchangers and cooling towers has been a major problem for many years because the bacterial attachment greatly reduces the heat transfer and operating efficiency of the processing equipment. In filtration systems, biofilm formation also greatly reduces the

permeability of membranes. The microbial activity in biofilms, especially by the sulfate-reducing or acid-producing bacteria, causes corrosion of metal surfaces. The fouling of ship hulls are mainly caused by growth of biofilms consisting of algae, diatoms and bacteria. Many antifouling paints have been created to prevent such colonization, however, none of them has been especially designed to avoid biofilm formation [23].

2.4 Remotion of biofilms

Because of its three-dimensional structure a biofilm is able to develop antimicrobial resistance, but this is lost as soon as the structure is broken. It has been observed that disinfectants like peracetic acid and formaldehyde have no effect on biofilms. It has been reported that *L. monocytogenes* attached to food-contact surfaces also displayed increased resistance to traditional sanitizers like quaternary ammonium compounds [23].

The best disinfectants for planktonic cells are not necessarily the suitable ones for biofilm cells. The relatively short application time and concentration of common sanitizers are not sufficient to remove or kill all bacteria in a biofilm. For instance, active chlorine concentrations of at least 1,000 ppm are needed to achieve a significant reduction of biofilm cells which is much higher than the suggested 200 ppm in 1 to 2 min. For planktonic cells, only 10 ppm in 1 min is sufficient [30].

Bacteria embedded in the biofilm exhibit diverse physiological patterns and show nutrient and oxygen variations across the biofilm. Within the biofilm, bacterial cells are found to receive less oxygen and fewer nutrients than those cells at the surface. In addition, some studies with foodborne bacteria have proved that older biofilms (more than 1 day old) are more resistant to various disinfectants compared to the young ones [23].

Methods to remove biofilms may be classified in three kinds:

- (a) Physical methods: Super-high magnetic fields, high pulsed electrical fields on their own or in combination with organic acids, ultrasound treatment, low electrical fields on their own and as magnifiers of biocides [23].
- (b) Chemical methods: Before applying a disinfectant, it is crucial to get rid of as many microorganisms as possible. If no mechanical treatment is given, the disinfectants leave the slime intact, favoring biofilm growth in crevices and seams, after the cleaning procedure. Detergents containing chelating agents like ethylenediaminetetraacetic acid (EDTA) and ethylene glycol-bis (β -aminoethyl ether) N,N,N',N'-tetracetic acid (EGTA) help in removal of biofilms. The chelators, by binding calcium and magnesium ions, also destabilize the outer membranes of the bacterial cells [37]. Monolaurin (glycerol monolaurate) was also found to be lethal to bacteria like *L. monocytogenes* at low concentrations [23].
- (c) Biological methods: Bacteriocins are antimicrobial compounds exhibiting bactericidal properties. Nisin, a well-known bacteriocin, has demonstrated to be a very well inhibitor of many food pathogens and spoilage bacteria. Enzymes (like α -amylase and β -glucanase) have also demonstrated to be effective in cleaning the extracellular polymers which form the matrix and thus helping in removal of biofilms [23].

2.5 Prevention of biofilms

Many strategies rely on the prevention/intervention of initial bacterial adhesion rather than on the removal of mature biofilms [10, 33, 38].

Currently, incorporation of metal nanoparticles (such as those from silver, copper, zinc oxide and many others) is gaining prominence as a new approach to generate antimicrobial activity because of their noticeable biocidal activity and their higher stability even under extreme conditions [36, 39, 40].

Some of the reasons why the incorporation of nanoparticles in a coating matrix is a very attractive technique are the fast deposition rate and high bonding between the nanoparticles and the matrix. Unfortunately, there is a disadvantage: the poor control over the release of antimicrobial agents. In order to overcome this barrier, nanoparticle films with a multilayer structure were proposed [36], to prevent detachment of nanoparticles from the substrate.

Marine equipment has been protected against biofilm formation using paints [33, 41] containing metal or organometallic compounds such as tributyl tin or copper complexes. However, the use of eco-toxic tin based coatings is nowadays prohibited in some countries [24].

In the medical field, there is considerable interest in developing biomaterials with inherent properties to prevent and also kill bacteria [42]. Antibiotics have been inserted in catheters and other indwelling devices to reduce biofilm development; however, bacteria are evolving to resist antibiotics faster than scientists can develop new classes of drugs [43] and, for this reason, it is widely accepted that, in the very near future, healthcare professionals will have no effective therapies for bacterial infections [44]. Silver ions have been inserted as well, but several studies report on the toxicity of silver [45, 46, 47].

In the food industry, factors such as complicated food matrix composition, the variation of materials used in equipment manufacture (from polymers such as HDPE to various types of steel), pH and temperature extremes, exposure to mechanical or chemical stresses, cost, and regulatory compliance must be taken into account in translating antimicrobial materials research from other

industries to a food processing application [48]. Development of packaging materials containing antimicrobial compounds have gained practical relevance in the last years for the biocontrol of foodborne pathogenic and spoilage microorganisms on food-contact surfaces [23].

2.6 Benefits of biofilms

Not all biofilms generate problems and in many natural environments the maintenance of water quality is achieved by using the microbial metabolism in biofilms.

Biofilms represent a natural form of cell immobilization, which has been employed in bioreactors to improve the productivity and stability of the fermentation processes. Industrial production of acetic acid, ethanol and some polysaccharides and for metal ore leaching require the application of biofilms [23]. Some biofilms of particular bacterial species are useful in certain applications such as biomineralization, wastewater treatment, and bioremediation of oil and gasoline spills [29].

3. THE ANTIMICROBIAL SYSTEM

An effective antimicrobial system is composed of four elements: The material surface, the antimicrobial agent, the immobilization technique, and the microorganism(s) involved.

3.1 The material surface

3.1.1 The chemistry of the surface

3.1.1.1 Stainless steel 304L

Stainless steel 304L is an alloy currently widely used for most furniture for facilities (kitchen, operating room, cold room, ventilation system, storage tanks, food preparation benches) due to their good aesthetical and mechanical properties of forming, welding, corrosion resistance, toughness, and easy cleaning [49]. It is an ideal material for food processing because it is chemically and physiologically stable at a variety of processing temperatures [8]. However, their use can be limited when hygiene (cleaning and disinfecting) is of extreme importance, because of their lack of antibacterial property [50, 51]. Stainless steel surfaces with antibacterial properties would be very beneficial [52].

Stainless steel also forms a passive film when in contact with the atmosphere, mainly composed of iron(III) and chromium(III) oxides and typically 2 – 5 nm thick in most acidic and neutral environments at room temperature [53].

3.1.1.2 Titanium alloy Ti-6Al-4V

Ti-6Al-4V is an α/β titanium alloy, each phase being stabilized with aluminum and vanadium, respectively. The low temperature α phase has a hexagonal closed packed structure while the high temperature β phase has a body centered cubic structure [54, 55]. Microstructure of the alloy is related to the processing conditions, as temperature, annealing time or cooling rate,

together with the distribution of alpha or beta phases (usually equiaxed α with stable β at the grain boundary triple points) [56]. Once exposed to atmosphere, the surface of the alloy develops a passive layer almost instantaneously [57]. This layer is mainly composed by titanium dioxide (TiO_2), but other oxides of titanium and of the alloying elements are also present [58], mainly Al_2O_3 and some hydroxyl groups, while vanadium is hard to detect [59]. It is one of the few completely biocompatible materials and is the most common metal used in dental and hip implants because of its excellent strength, fracture toughness, fatigue and corrosion resistance, and Young's modulus [60, 61, 62, 63, 64]. Titanium and its alloys have a more similar elastic modulus compared to bone and can reduce bone resorption. The Ti-6Al-4V alloy is the first titanium alloy registered as an implant material in terms of ASTM standards and is attractive because of its high specific strength [65, 66].

In vivo, stainless steel is colonized more easily than titanium, maybe because its capacity for osseointegration is not the same [67].

3.1.2 The surface topography

One approach to prevent microbial surface colonization is the preparation of surface topographies which are unfavorable for bacterial attachment [15], usually called surface modification.

Surface treatments can be classified into four categories: mechanical, physical, chemical and biochemical surface modifications [65].

- (a) Mechanical: Machining, grinding polishing, blasting, attrition. Usually used as surface pretreatments to break the surface oxide layer [68].

- (b) Physical: Thermal spraying, laser-based techniques, physical vapor deposition (PVD, thermal evaporation or sputtering [69]), ion implantation and deposition, and glow discharge plasma treatment.
- (c) Chemical: Chemical treatment (acid, hydrogen peroxide, alkaline, etc.), anodic oxidation, sol-gel processes and chemical vapor deposition (CVD).
- (d) Biochemical: Photochemistry, self-assembled monolayers (SAM), bio-coating deposition [70].

Surface modification by texturing can have a profound impact on the growth and adhesion of bacterial cells on surfaces [60]. Topographical features that limit cell-surface interactions have been shown to reduce biofilm formation [71, 72]. Structural features of substrates, such as size, spacing, aspect ratio and roughness can have both deterrent and attractive effects on the settlement of fouling organisms [10].

Diaz et al. [73] showed that ordered groove microstructures can have a tiny (but measurable) effect in decreasing biofilm growth rates, probably due to microfluidic flow effects at the surface, but still under research. There is an important study, based on the reproduction of shark skin surface morphology, suggesting that these structures can reduce bacterial biofilm growth, although the mechanism for this is not well developed yet [74].

Ivanova et al. [75] suggested that high aspect ratio (defined as the ratio between the structure depth and the ridge width [12]), sharp nanoscale features, such as those found on Clanger cicada wings, dragonfly wings and black silicon can physically damage and kill bacterial cells; these results are promising, but the details still remain unclear [15, 74, 76].

Helbig et al. [10] found that topographies with structure periods smaller than the size of individual bacterial cells (around 500 nm) restrict the cell-substrate contact area, leading to scarce cell retention; for topographies with structure periods close to bacterial cell size (around 1000 nm) the retention was the highest; and for topographies with structure periods larger than cell size (around 5000 nm) cell retention strongly depends on the bacterial cell morphology (for example, if the bacterium is spherical or rod-shaped). This trend was independent of the contact time between the bacteria and the substrate, the structure type and the substrate chemistry, demonstrating that surface topography is indeed a strong trigger influencing cell adhesion.

Puckett et al. found that nano-rough titanium surfaces produced by electron beam evaporation decreased the adherence of Gram-negative bacteria compared to nano-smooth surfaces [77].

Additionally, there is a clear link between topographical surface modification and superhydrophobicity, one unique property which is widely present in many animal skins, plants and insect wing surfaces among others, that reduces the wettability of the surface, and is attributed to the presence of hierarchical and non-hierarchical micro/nano-structured surfaces [78].

Patterned surface wettability has been shown to affect bacterial retention. Bos et al. used a surface patterned with hydrophobic and hydrophilic patches of 10 μm size to test bacterial adhesion, finding that the adhesion rates were similar for all surfaces, but the strength of cell adhesion was much less for hydrophobic surfaces [74].

Genzer and Efimenko [79] have analyzed the applications of superhydrophobic surfaces, which are non-wetting surfaces with $>150^\circ$ contact angles [80], to prevent biofouling. The Cassie-Baxter superhydrophobic condition keeps the liquid interface at the tips of rough, hydrophobic

topological features. Although this should prevent biofilm formation, it has been found that this wetting state is metastable and does not last for long [74].

Another approach consists in using these nano- and micro-topographical features to store or immobilize compounds that reduce bacterial cell adhesion. Some researchers have designed microstructured surfaces containing a thin, inert lubricant liquid layer that is energetically bound to the surface, known as slippery liquid-infused porous surfaces or SLIPS. A few studies on different SLIPS have demonstrated a real resistance to protein and bacterial cell adhesion [74, 81, 82].

Hitherto the vast knowledge bases on cell retention and orientation on materials with structures covering the nano- and micro-scale are inconsistent, maybe because different ranges of structure dimensions as well as structure types with periodically arranged or randomly distributed structures were applied [10]. The effects of surface modification on bacterial attachment and biofilm formation are complicated and not completely understood. These are new areas of research and still underway [74].

In this work, nanosecond pulsed laser irradiation is the technique used to modify the surfaces of Ti-6Al-4V and 304L stainless steel. Laser-based techniques have emerged as a promising method for creating micro- and nanoscale features because of its inherent fabrication advantages. Lasers are able to accurately deliver large amounts of energy into specific regions of a material in order to achieve an expected response. For materials which are opaque, this energy is absorbed near the surface, modifying its chemistry, crystal structure, and/or multiscale morphology without modifying the bulk [60].

Laser processing offers a number of advantages over traditional processing:

- (a) It is versatile and able to modify diverse substrates.
- (b) It can be applied to materials with high melting points, hardness, or resistance to corrosion and brittleness [65, 83].
- (c) It is a one-step, direct maskless, nonc-oncontact technique, which permits the manipulation of sensitive molecules without losing cellular activity [65].
- (d) Does not require harsh production environments. It can be performed in gaseous and liquid environments, from air to water or even sulfur hexafluoride. It does not require cleanroom operation either [65].
- (e) Lasers produce precise surface features that may be tailored through parameters such as frequency of light and exposure time [60]. High-resolution features, micro- and nanoscale, may be produced on two- and three-dimensional scales. The arrival of femtosecond (fs) lasers has significantly improved the precision at the nanoscale [65, 84].

Concerning the response of the material to interact with light, if laser induced excitation rates are slow compared to the thermalization time, then the process is considered as photothermal, in which the absorbed laser energy is directly transformed into heat. Material heating rates can get as high as 10^9 K/s for nanosecond (ns) pulses and even higher for femtosecond lasers, reason why significant changes to the material can arise [60], falling into three categories:

- (a) Thermally activated processes: Diverse temperature dependent processes in the solid material may be activated when laser heating operates with fluences below the threshold of melting. The high temperatures generated can enhance diffusion rates promoting impurity doping, the reorganization of the crystal structure, and sintering of porous

materials. Energy barriers for chemical reactions can overcome as well. The large temperature gradients achieved with localized laser heating can lead to rapid self-quenching of the material [85], trapping in highly non-equilibrium structures. Also, the rapid generation of large temperature gradients can induce thermal stresses which may contribute to the appearance of warping, or cracking on the material [60, 86].

- (b) Surface melting: Fluences above the threshold of melting can lead to the formation of short-term pools of molten material on the surface, resulting in a rapid material homogenization. At temperature above the melting point, hydrodynamic motion can reshape and redistribute material. Radial temperature gradients on the order of $10^2 - 10^4$ K/mm can develop in melt pools, causing convective flows to circulate material. For most materials, the liquid's surface tension is inversely proportional to the increasing temperature and the liquid is pulled from the hotter to the cooler regions [60]. This effect of surface tension driven convection is known as the Marangoni effect and becomes dominant if sufficiently high temperature differences between maxima and minima happen; this reduces the quality of the pattern, especially in metals with low thermal conductivities such as titanium and stainless steel [87].
- (c) Ablation: This is the removal of material from substrate by direct absorption of laser energy [12], normally related to pulsed lasers. The onset of ablation occurs above a threshold fluence, which depends on the absorption mechanism, microstructure, morphology, the presence of defects, and on laser wavelength and pulse duration. Typical threshold fluences for metals are between 1 and 10 J/cm², for inorganic insulators between 0.5 and 2 J/cm², and for organic materials between 0.1 and 1 J/cm² [60].

Laser exposure of metals such as vanadium, copper, titanium and stainless steels in air results in the growth of highly colored layers [88, 89]. Surface laser-irradiation promotes a pyrolytic reaction in which a metal substrate undergoes a high-temperature chemical reaction with the ambient atmosphere enhancing the growth of a film composed of elements from the substrate and mixed with gases from the environment [90]. Diverse process gases have been used, like air and nitrogen, resulting in the growth of oxides or nitrides on metal substrates after gas-phase transport, chemisorption, diffusion, and chemical reactions at the surface. Those highly colored films have found use as unique authenticity markings in welded components [91, 92], counterfeit protection, information encoding [93], as well as for other applications in the fields of solar energy, light absorption, detectors, catalyzing chemical reactions or decorative architecture [94, 95, 96].

Previous studies about laser marking of stainless steel have demonstrated that a diversity of colors can be obtained and that a multi-phase structure may turn out from surface pyrolytic reactions. Laser parameters determine the thickness, composition and phase of oxide films grown on austenitic stainless steel 304L. Thicker oxides result in a “duplex” phase structure with a Cr-rich interface and an Fe-rich overlayer. Thinner oxides consist only of a single Cr-rich layer. In general, laser-heating causes melting of the stainless steel 304L substrate and Cr diffuses from the substrate to the oxide layer, generating a Cr-free zone [91].

Surface channel cracking has been observed on stainless steel oxide layers created by pulsed lasers, with thicknesses greater than 100 nm. These cracks divide the film into a series of islands in a pattern often seen in drying mud [97]. Pervasive, interconnecting cracks normally develop in a strained film [98, 99, 100] as a way to relieve residual film stresses due to differences in coefficients of thermal expansion between the substrate and the film [101, 102]. It is expected that residual stress increases as oxide thickness increases, as has been observed in laser-fabricated

films on titanium substrates; however, it is also possible that stress is constant and strain energy increases with thickness, given that fracture can be an energy driven process [91].

Laser heat treatments do not have difficulties associated with coatings as no additional material is added to the surface, and allow for similar changes in wetting characteristics of the surface by changing roughness, microstructure and surface chemistry, affecting corrosion resistance and cell adhesion [60].

Pulsed lasers, especially fs lasers, have proved to be useful for various applications in which modifying surface characteristics is required [65, 103]. Traditionally in the ns range and mostly evolving into the fs range, pulsed lasers have been used to directly modify physical surfaces of metals. Laser beams with pulse energies over 1 mJ, optical intensities over 10 TW/cm², and pulse repetition rates greater than 100 GHz have been developed. Lasers, when applied straight on metal surfaces, can etch through them, although increased pulse durations lead to thermal ablation. Thus, many researchers and investigators have a profound interest in using ultrafast pulsed lasers, such as fs lasers, to diminish thermal ablation while simultaneously increasing spatial resolution. Laser-based techniques have successfully modified surface wettability using a wide range of materials (silver, silicon, steel, etc.) and recent groups have taken advantage of advances in laser technology to achieve precise topographical control using fs lasers. Hitherto, fundamental knowledge about laser thermodynamics and phase transformations is still not enough and more research is needed [65].

Laser texturing of nano- and micron-sized features such as grooves, ridges, craters and mountains can increase surface area, providing more available spots for attachment [60]. Ulerich et al. investigated the effects of multiscale laser texturing of a Ti-6Al-4V substrate on the adhesion of cells by rastering a focused beam from a nanosecond pulsed UV laser across the surface to

pattern linear grooves, finding that groove width was not significantly affected by the number of passes or the distance between pulses, but can be accurately manipulated by controlling the pulse energy, because when this energy increases, a larger fraction of the beam exceeds the ablation threshold. Groove depth, on the other hand, was affected by the translation distance and the number of passes as well as the laser pulse energy. Decreasing the distance between pulses or making multiple passes would increase groove depth without affecting the width. Processing conditions also affected the roughness and sub-micron features created on the surface [104]. Small-scale features (nodules, ripples, ledges and nano-textures) would form on the surface of the grooves depending on the specific nature of the material ablation and redeposition [60]. Decreasing the translation distance between laser pulses tended to increase surface roughness due to the increased interaction with the residual heat left from previous pulses. Surface chemical composition was also modified by the laser texturing. With a small translation distance between pulses, there was some depletion of aluminum in the valleys of the grooves and an enrichment of aluminum on the ridges, mainly because aluminum evaporates preferentially by its higher vapor pressure [60, 61].

Guenther et al. [12] used direct laser interference patterning (DLIP) for direct fabrication of periodic micrometer and submicrometer structures on polymeric materials, finding that topographies have a remarkable impact on bacteria adhesion; on the one side, one-dimensional line-like structures especially with dimensions of the bacteria enhanced microbe attachment, while on the contrary, complicated three-dimensional patterns prevented biofilm formation even after implantation and contamination in living organisms.

A summary of surface treatment techniques can be seen in Table 3.1.

Table 3. 1 Summary for the different surface treatment techniques

Technique	Type	Advantages	Disadvantages
Laser	Physical	Precise control of surface modification One-step fabrication technique No cleanroom required	High initial cost Produces homogenous surfaces that do not mimic the more graded architecture in nature
Plasma spray	Physical	Versatile process for most ceramics and metals Good deposition rate Uniform coating Good control of coating	High initial cost and scale-up issues Ion damage on surface May cause residual stress
Physical vapor deposition	Physical	Deposition for a large range of materials Rapid solidification process Low cost	Cannot control thin film and produces amorphous coatings Capacity limited for large-diameter wafers
Anodization	Chemical	Controlled way to create nanofeatures Commonly used technique to increase thickness and oxide layer of atmosphere Promotes high corrosion resistance Good control of oxidation	Choice of electrolytes must be carefully chosen and requires prior expertise
Chemical vapor deposition	Chemical	Used to prepare inorganic nanostructures Good control of nanofeatures	Fast gas flow is required Reactors must be cleaned frequently Deposition occurs everywhere Fragile substrates can be damaged Film properties highly dependent on surface homogeneity
Chemical etching	Chemical	Inexpensive High precision Low chemical deposition Applicable to small features	Poor anisotropy Poor process control because of high sensitivity to temperature Low control over particle size High cost of chemical disposal

Source: Verissimo, Chung and Webster [65]

3.2 The antimicrobial agent

In order to select an antimicrobial agent several factors such as the mechanism of action, availability for repeated use, stability to drastic changes in pH and temperature, and cleaning and sanitization regimes must be taken into consideration [48].

Antimicrobial agents may be divided as:

- (a) Metal-based materials: A variety of metal ions are being studied because of its toxicity to bacteria (Gram-positive and Gram-negative) as well as fungi, like vanadium, titanium, copper, silver, zinc, nickel, cobalt, chromium and mercury. The antimicrobial effectiveness depends on migration of the metal ion or particle from a coating. Because of this migration and frequent washings employed in the food industry, coatings hardly retain effectiveness for long periods of time [48].

Silver is probably the metal-based antimicrobial agent that has been more commercially manufactured, especially for consumer goods and healthcare industries, followed by copper. Silver application in food contact materials is to some extent restricted, especially because of public health and environmental issues [48]. In 2014, the US Environmental Protection Agency issued an order against Pathway Investment Corporation, from New Jersey, to stop selling plastic food containers made using nanosilver, which presages that commercial production of silver-based antimicrobial materials is plausibly to undergo increased regulatory surveillance [105].

- (b) Quaternary ammonium compounds (QACs): These compounds include a nitrogen atom linked to a halogen and several alkyl groups. Some examples include benzalkonium chloride, benzethonium chloride, cetalkonium chloride, tetraethylammonium bromide, and domiphen bromide. Biocidal activity relates to the chain length of the alkyl groups bound to the nitrogen. Usually between 5 and 17 carbons in length are required to be biocidal

toward Gram-positive and Gram-negative bacteria as well as yeasts and fungi; however, their antimicrobial activity may be impacted if QAC's react or precipitate with other organic molecules, especially proteins [48], and they are degraded by Sommelet-Hauser rearrangement when in contact with a strong base.

- (c) Cationic polymers: This includes substances like polylysine, chitosan and polyamines. Their antimicrobial effectiveness has been extensively demonstrated against Gram-positive and Gram-negative bacteria (even some evidence against viruses using chitosan), and they are usually coated using layer-by-layer (LbL) deposition [48]. Their antimicrobial efficacy is diminished by the presence of particulates or organic matter, probably a result of fouling by anionic compounds in suspension [48].

- (d) Antimicrobial peptides (AMPs): These peptides are synthesized generally by microbial cells as an innate immune response against the environment. More than 800 AMPs have been studied [48, 106], from those coming from insects (andropin, moricin, melittin, etc.), rabbits (CAP18), cattle (indolicidin), amphibians (bombinin, brevinin-1, magainin) to those coming from humans (LL-37, defensins).

Amines, carboxylic acids and thiols inherent in AMP's structure are the functional groups used to attach these peptides to food contact material surfaces, via covalent links. They can also be deposited through LbL or another technique on different material surfaces such as silicon, glass, titanium, polystyrene and stainless steel [107]. The main drawback is that these coatings can be affected by hydrolysis and/or degraded under pH and temperature extremes, which inhibits their antimicrobial effect [48].

- (e) Essential oils: Natural concentrated hydrophobic liquids possessing groups such as phenols, alcohols, hydrocarbons, aldehydes and ketones. They are produced by plants (containing

the “essence” or aroma of the plant from which they are extracted) for protection against microorganisms and have been found to be antimicrobial against Gram-positive and Gram-negative bacteria as well as yeasts, fungi and viruses [48].

Commercial application of essential oils is impeded because of their own odor, which drastically impacts taste of foods processed on equipment coated with essential oils. Moreover, these coatings would lose effectiveness over time [48].

- (f) Light-activated antimicrobials: Compounds that can be organic and aromatic (like porphyrin) or inorganic oxides (like titanium dioxide, TiO_2) and have the particular characteristic of photoactivation. Their antimicrobial activity is the result of exposure to light of a specific wavelength, generating free radical species (mainly associated to oxygen) that can react with cell membranes, enzymes and/or nucleic acids, and affecting microbial viability [48]. The so-called photodynamic antimicrobial chemotherapy (PACT) has been developed following this technique.

However, these antimicrobials are nonspecific against organic matter, which can drastically diminish effectiveness. There are not exhaustive stability studies conducted to evaluate the robustness of light-activated antimicrobials after being included into coating structures either [48].

- (g) N-halamines: Compounds with one or more nitrogen atoms that can be reversibly halogenated, mainly with chlorine. Researchers generally agree that the mechanism of biocidal action includes an oxidizing effect on microorganisms' membrane functions conferred by the nitrogen-stabilized halogen. One special characteristic that makes N-halamines attractive for is that after imparting their antimicrobial effect, they can be

recharged by exposure to a halogen source (commonly chlorine) and again used for disinfection [48].

N-halamines display biocidal efficacy towards Gram-positive and Gram-negative bacteria, although usually a lower antimicrobial effect compared to free chlorine, but N-halamines are less reactive toward organic matter.

The stability of N-halamine coatings has been investigated more deeply compared to other antimicrobial materials and coatings, especially because of interest in their rechargeable nature. However, researchers work in the development of high molecular-weight N-halamines to counteract toxicity issues attributed to the low molecular-weight ones [48].

Table 3.2 contains examples of antimicrobial agents from different classes that have been used in research works.

The present work is focused on antimicrobial peptides.

Antimicrobial peptides can be classified in three major categories [109]:

- (a) Class I or lantibiotics, which are posttranslationally modified peptides containing (methyl-)lanthionines, and are usually less than 5 kDa in size.
- (b) Class II includes heat-stable non-modified peptides between 37 and 58 amino acids, with a typical size of less than 10 kDa.
- (c) Class III contains peptides that are sensible to heat and with size larger than larger 30 kDa.

Table 3. 2 Antimicrobial agents of potential use

Organic acids	Benzoic acid, lactic acid, malic acid, sorbic acid, succinic acid, tartaric acid
Organic acid salts	Potassium sorbate, sodium benzoate
Organic acid anhydrides	Benzoic anhydride, sorbic anhydride
Inorganic acids	Phosphoric acid
Inorganic gases	Sulfur dioxide, chlorine dioxide
Alcohols	Ethanol
Amines	Hexamethylenetetramine (HMT)
Ammonium compounds	Silicon quaternary ammonium salt
Antibiotics	Natamycin
Antimicrobial peptides	Defensin, magainin, attacin, cecropin, melittin K14
Antioxidants	Butylatedhydroxyanisole (BHA)
Bacteriocins	Bavaricin, brevicin, carnocin, lacticin, mesenterocin, nisin, pediocin, sakacin, subtilin
Chelators	Citrate, conalbumin, EDTA, lactoferrin
Enzymes	Chitinase, β -glucanase, lysozyme, ethanol oxidase, glucose oxidase
Fatty acids	Lauric acid, palmitoleic acid
Fatty acid ester	Monolaurin
Fungicides	Benomyl, imazalil
Metals	Copper, silver, zirconium titanium oxide
Plant and spice extracts	Grapefruit seed extract, bamboo powder, cinnamic acid, caffeic acid
Essential oils	Carvacrol, citral, estragole, geraniol, linalool, thymol, oregano, lemongrass
Natural phenols	Catechin, hydroquinones, p-cresol
Phenolic compounds	Butylatedhydroxytoluene (BHT)
Parabens	Ethyl paraben, methyl paraben
Polysaccharides	Chitosan, konjac glucomannan
Oligosaccharides	Chitooligosaccharide
Miscellaneous	Reuterin, triclosan, probiotics, nitrites

Source: Adapted from Karam, Jama, Dhuslter and Chihib [108]

Antimicrobial peptides are naturally produced as important immunity agents in a broad spectrum of living organisms, from plants to insects to mammals, including humans; as such, they have become very well recognized in current research as initiators for prospective antibiotic agents. They are cationic (positive net charge), medium length (12 – 50 residues), and have good solubility in water. AMPs constitute a viable alternative to traditional antibiotics because they also have the ability to penetrate bacterial cell membranes, disrupting them, causing membrane lysis and

eventually cell death. The advantages of AMPs are: (a) Highly selectivity against the negatively charged bacterial membrane and (b) no specificity in targeting, as the peptides function by disrupting the bacterial membrane and therefore hardly arousing bacterial resistance [110].

AMPs are a key component of the immune system of most living organisms and protect them against pathogen microorganisms. So far, almost 3,000 AMPs have been reported in the antimicrobial peptide database (<http://aps.unmc.edu/AP/main.php>) [35].

The selectivity of AMPs can be explained by the distinct composition and topological arrangement of the lipids of cytoplasmic membranes in prokaryotic and eukaryotic cells. The outer layer of the membranes of animals and plants is entirely composed of electrically neutral and zwitterionic phospholipids; the negatively charged head groups of most lipids are segregated into the inner side, in contact with the cytoplasm. On the other hand, bacterial membranes contain big amounts of negatively charged phospholipid head groups. The low propensity to develop microbial resistance and the fast killing exhibited by AMPs can both be explained by their site of action, the bacterial membrane. A microorganism would have to redesign its membrane, changing the composition and/or organization of its lipids, which probably represents a ‘costly’ solution for most micro-species [35].

Nevertheless, aminoarabinose in lipid A [111], a positive compound which reduces the anionic nature of the cell surface and also the electrostatic interactions with AMPs [112], is the main reason why Gram-negative bacteria are not susceptible to these peptides.

Lactic acid bacteria (LAB) are Gram-positive, non-sporulating microaerophilic bacteria whose main fermentation product from carbohydrates is lactate and they occur naturally in raw milk [113]. LAB have been used for centuries in the fermentation of food, not only for flavor and texture, but also due to the ability of starter-derived inhibitors to prevent the growth of spoilage

and pathogenic microorganisms. They produce a number of antimicrobial substances, such as organic acid, hydrogen peroxide, and bacteriocins. Among these inhibitors, bacteriocins are antimicrobial peptides (or proteins) that inhibit other bacteria, often closely related species, in environmental niches [114].

Bacteriocins, which are ribosomally synthesized by several lactic acid bacteria (unlike antibiotics), exhibit antimicrobial activity and offer potential applications in food preservation [115]. Hitherto, the only bacteriocin legally allowed as food preservative is nisin [1], the antimicrobial agent used in this work. Nisin, a low molecular weight peptide ($3,500 \text{ g mol}^{-1}$), was selected because of its high activity against a broad range of Gram-positive bacteria, its approved use as a food preservative, its lack of toxicity for humans, and its high stability when involved in films and coatings [51].

3.2.1 Nisin

3.2.1.1 Classification and chemical structure

Lantibiotics are small ($<5 \text{ kDa}$) bactericidal peptides characterized by the presence of the atypical amino acids lanthionine (Ala-S-Ala), β -methyl-lanthionine (Abu-S-Ala) and some other dehydrated amino acids coming from enzyme-mediated post-translational modifications [116]. Nisin (or group N inhibitory substance [113], $\text{C}_{143}\text{H}_{230}\text{N}_{42}\text{O}_{37}\text{S}_7$) is a small, cationic, hydrophobic, and 34-amino acid peptide that contains one lanthionine and four β -methyl-lanthionine rings, and uncommon residues as dehydroalanine and dehydrobutyrine. There are two natural variants, nisin A and nisin Z; in which the only change in structure is at the amino acid at position 27, because nisin A possesses a histidine, while nisin Z has an asparagine [114, 117]. These variants have similar properties but it has been shown that nisin Z has better diffusion properties than nisin A in agar [118]. The peptide structure of nisin is shown in Figure 3.1.

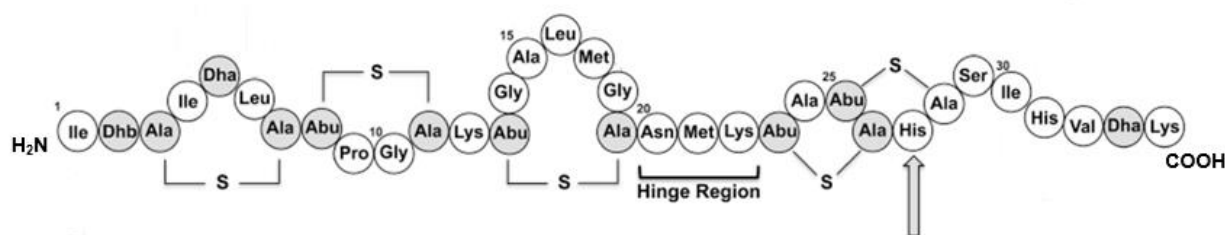


Figure 3. 1 Peptide structure of nisin, with three rings on the “N” terminus, the hinge region (positions 20, 21 and 22), and two more rings on the “C” terminus.

Discovered in 1928 in England by Roger and Whittier [113], nisin is one of the oldest known antibacterial agents produced by *Lactococcus lactis*. It belongs to type A of lantibiotics family, with overall positive charge [+4]; and has amphipathic properties [114, 118] due to its structure, with N-terminal containing several hydrophobic residues (3 lanthionine rings A, B and C), whereas the C-terminal is more hydrophilic (rings D and E) [6]. Both terminals are linked by a flexible hinge region consisting of 3 amino acids (Asn20 – Met21 – Lys22) [116, 119]. The characterization of nisin was first done by Mattick and Hirsch (1947), who coined its name from “N inhibitory substance”.

The hydrophobic face of nisin A is composed of the residues Ile4, Leu6, Pro9, Leu16 and Met17 and the hydrophilic Lys12 is located at the opposite face. In addition, the region from residue 21 to 28 is amphipathic [117]. Most of the charged and hydrophilic amino acids can be found in the C-terminal extreme of the molecule, while the N-terminal possesses the hydrophobic residues and only one of them is charged, Lys12 [117].

Nisin as a powder is extremely stable when temperatures do not exceed 25°C, is kept away from direct sunlight and without moisture ingress. pH affects the solubility and stability of nisin in solution. Optimum heat stability occurs at pH 3 to 3.5. Heinemann et al. studied the effect of processing temperature and pH on the stability of nisin in diverse foods, finding that in low-acid

foods at pH 6.1 to 6.9, heating for 3 minutes at 121°C destroyed 25% to 50% of the added nisin. Nisin is, however, successfully used in high-pH/heat-treated food products such as canned-vegetables and pasteurized liquid-egg, implying that the molecule is somewhat protected by food components [6].

Liu and Hansen [120] reported nisin solubility at pH 2.2 as approximately 56 mg/ml, but only 1.5 mg/ml at pH 6 and even lower (around 0.25 mg/ml) at pH 8.5. Solubility in foods is never a problem because nisin levels are always very low, with levels in food rarely above 0.025 mg/ml. In vitro studies have shown that nanomolar concentrations of nisin were sufficient to display antibacterial activity [121]. However, research in Danisco laboratories has demonstrated that care must be taken when preparing high-concentration nisin solutions from nisin commercial preparations (such as Nisaplin®, 2.5% nisin), because exceeding a concentration of approximately 250 µg/ml may lead to loss of activity as a consequence of salt precipitation and/or filtering [6].

Nisin is tasteless and imparts no negative taste to foods in which it is applied. Danisco conducted triangle taste trials in which volunteers could not detect 200 mg/L Nisaplin® in mineral water (approximately equal to 5 µg pure nisin/g) [6].

Some sources have confused nisin with an antibiotic, but there are clear differences between this bacteriocin and pharmaceutical antibiotics. In the past, there were several trials to use nisin as a medication, but they failed because of nisin's lack of activity against Gram-negative bacteria and its fast breakdown within the body. Generally antibiotics are secondary metabolites; nisin is a primary metabolite produced by a process involving ribosomal transcription and translation. Nisin (and other bacteriocins) should be considered as antimicrobial peptides and not considered as antibiotics [6].

Nisin, being a lantibiotic peptide with positive charge [122], is able to attach to negatively charged cytoplasmic membranes. It has been broadly used in food given that it is approved as a food preservative and is effective in suppressing Gram-positive bacteria such as *L. monocytogenes*. Nisin kills bacteria by forming pores on cell membranes [123, 124].

3.2.1.2 Nisin as food preservative

Lactococci, producers of nisin, occur naturally in milk; for this reason, nisin can be present naturally at low levels in both milk and cheese [6].

Nisin was approved for use in food in 1969 and remains the only bacteriocin licensed to be used in food [6]. The first commercial extract of nisin was obtained by Aplin & Barrett Ltd. (now part of Danisco) in 1957 [6].

Nisin has shown bactericidal action against Gram-positive bacteria and very low toxicity in humans. It can be ingested in quantities of up to 3.3×10^7 U/kg of body weight with no adverse effects [125, 126]. It has been approved as generally recognized as safe (GRAS) [127, 128, 129, 130] for food use by both the Food and Agriculture Organization and the World Health Organization since 1969. In 1983, nisin was added to the European food additive list, as E234 [131, 132]. It has been used as a safe alternative to chemical reagents to control food pathogens during food shelf-life in more than 40 countries [118], including the United States, France, Belgium, Italy, Netherlands and China. National laws concerning the presence and maximum levels of nisin in different food produces vary greatly [133] (see Table 3.3).

Table 3. 3 Examples of worldwide use of nisin

Country	Food in which nisin is permitted	Maximum level (IU/g)
Argentina	Processed cheese	500
Australia	Cheese, processed cheese, canned tomatoes	No limit
Belgium	Cheese	100
Brazil	Cheese, canned vegetables and sausages	500
France	Processed cheese	No limit
Italy	Cheese	500
Mexico	Nisin is a permitted additive	500
Netherlands	Factory cheese, processed cheese, cheese powder	800
Peru	Nisin is a permitted additive	No limit
Russia	Dietetic processed cheese, canned vegetables	8,000
United Kingdom	Cheese, canned foods, clotted cream	No limit
United States	Pasteurized processed cheese spreads	10,000

Source: Juncioni, Faustino, Gava and Vessoni [113].

Nisin has been used as food preservative in a wide range of products, for instance dairy and bakery products, liquid egg, vegetables, meat (especially deli meats [134, 135]), fish [117], sauces and salad dressings [129]. Typical concentrations of nisin used by the food industry are between 2.5 and 12.5 ppm [128].

Combined with other inhibitory factors, nisin can become an obstacle for the growth of undesirable bacteria, thereby reducing the amount of chemicals included in the food and diminishing the impact of the processing conditions [21].

The effectiveness of nisin is often affected by factors such as pH, temperature and, when applied on food, it may also be affected by food composition, structure, as well as food microflora [1]. Nisin is more stable at lower pH, while it is unstable and insoluble at neutral and alkaline pH values [26].

3.2.1.3 Nisin activity

Nisin exerts fast bactericidal effects against a wide spectrum of Gram-positive bacteria and food pathogens, such as *Listeria monocytogenes*, *Staphylococcus aureus*, *Bacillus cereus* and

Clostridium botulinum [136]. It has also shown stable activity when adsorbed on films against Gram-positive bacteria including *Brochothrix thermosphacta*, *Lactobacillus helveticus*, *Listeria monocytogenes*, *Mariniluteicoccus flavus* and *Pediococcus pentosaceus* [137]. Nisin shows promising activity towards clinical isolates of the *Methicillin-resistant Staphylococcus aureus* (MRSA) bacterium [43, 138], *Streptococcus pyogenes*, and some of the most severe human pathogens, such as the multiresistant *Streptococcus pneumoniae* and vancomycin-resistant *Enterococcus faecium* or *Enterococcus faecalis* [109]. Nisin can induce cell autolysis and inhibit the outgrowth of spores as well [1].

Nisin kills bacteria mainly by pore formation in the cytoplasmic membrane. By attaching to the peptidoglycan precursor lipid II, nisin performs two killing mechanisms: it permeabilizes the membrane and stops the cell wall synthesis [109]. Nisin utilizes lipid II as a docking molecule. For bacteria, lipid II is a crucial constituent of the cell membrane because it delivers peptidoglycan units for the cell wall synthesis [121].

Breuknik et al. found that the presence of lipid II in liposomes drastically diminishes the concentration of nisin needed for liposome permeabilization. In consequence, only nanomolar concentrations of nisin are enough to permeabilize cell membranes, whereas micromolar concentrations are needed for the permeabilization of artificial membranes, in which lipid II is absent [118]. Lipid II and nisin form a mixed pore, formed by eight nisin molecules and four lipid II molecules; inhibition of cell wall synthesis results from nisin displacement of lipid II [117, 122].

Lipid II is present in all eubacterial membranes, where it fulfills the function of transporting peptidoglycan units [139]. When bounded to lipid II, nisin effectively permeabilizes the membrane through the formation of pores, causing a collapse of the vital ion gradients across the membrane [43, 140, 141, 142, 143], with efflux of intracellular material [138, 2, 144] and disruption of the

proton motive force [145]. Nuclear magnetic resonance (NMR) spectroscopy has shown that the N- terminus of nisin is involved in the interaction with lipid II, but the flexible hinge between rings C and D is also important. Mutations in this hinge region cause a reduction in the antimicrobial activity but a far larger inhibition of the ability of nisin to permeabilize the membrane [122].

Hasper et al. concluded that nisin and lipid II form uniformly sized pores, which display drastically increased lifetimes compared with nisin pores in the absence of lipid II. These properties of the hybrid pores strongly contrasts the characteristics of pore-forming AMPs that do not have a fixed target. These AMPs show a much lower affinity for their target, and upon binding of enough peptide molecules, they will form only temporal pores, which are neither stable nor uniform, like those formed by magainin [122].

The net positive charge of cationic antimicrobial peptides also plays a fundamental role in peptide-membrane interactions, especially in attracting the AMP to the anionic surface of bacterial membranes [110]. Balancing peptide hydrophobicity and charge distribution promotes effective antimicrobial activity.

Nisin is not good against Gram-negative bacteria, yeasts and molds [146], or microorganisms that should be eliminated by pasteurization treatments. The outer membrane of Gram-negative bacteria acts as a permeability barrier for the cell and avoids nisin from reaching the cytoplasmic membrane. Combination of nisin and chelating agents such as sodium salts of ethylenediaminetetraacetate (disodium EDTA) represents an effective approach to improve the antimicrobial activity of nisin against Gram-negative bacteria [147] (such as *Escherichia coli* O157:H7 and *Salmonella tryphimurium* [148]) by attaching metal ions to the lipopolysaccharide layer of the bacteria [147].

Disodium EDTA is already used as a direct food additive in a broad variety of food products particularly to avoid color and flavor detriment.

The antimicrobial activity of nisin is also strongly driven by the pH of the nisin solution. The highest activity is achieved at acidic pH (2-3) followed by dramatic loss of activity at higher values. On the other hand, the stability of a metal-chelator complex (disodium EDTA), is favored by neutral or alkaline pH. Therefore pH should be optimized in order to get an adequate antimicrobial formulation to inhibit both Gram-positive and Gram-negative bacteria [147]. Adhikari et al. [149] found that biocompatible organic acids and citrate-stabilized gold nanoparticles may interact with nisin to generate robust antimicrobial agents that exhibit remarkable nisin activity even at high pH [149].

Another possible influencing factor is nisin conformation on the surface. Nisin possesses sections which are predominantly hydrophobic, and would likely experience a major change in conformation when doing to a hydrophobic surface than when adsorbing to a more hydrophilic one. If greater molecular distortion occurs when nisin adsorbs to a hydrophobic surface, then a lower effectiveness of nisin could be expected. According to Bower et al., the activity of nisin lowered significantly on high hydrophobic surfaces and the amount of attached bacterial cells went up, as compared to less hydrophobic surfaces, in which the conformational change of nisin may be less [2]. The hydrophobic residues (located in the N-terminal) of nisin are identified as to be responsible for its antimicrobial activity [147].

However, the orientation of nisin on a variety of hydrophilic and hydrophobic surfaces has been controversial. It is usually accepted that on hydrophilic surfaces the hydrophilic domain of the nisin is pointing towards the substrate, while on a hydrophobic substrate the opposite happens. Bower et al. [2] found that multiple layers of nisin adsorbed on silanized hydrophobic silica

surfaces were easily eluted by washing in buffer or could be displaced by other proteins. They also noted that the antibacterial activity was significantly reduced even if the hydrophobic surface had adsorbed higher concentrations of nisin. It was confirmed that nisin undergoes a conformational change upon adsorption which stopped interaction with the bacterial cell membrane. Chihib et al. observed a similar behavior on low density polyethylene substrates. However, in both cases, nisin is just physisorbed onto the surfaces and susceptible to leaching [26].

The effectiveness of nisin also depends on the bacterial load. Nisin will be less effective in a processed food with a high spore content; this would commonly be the result of poor quality in the ingredients. Nisin gives the opportunity (within safety limits) of energy saving and, as a result, cost cutting. Thermally injured spores are more sensitive to nisin, and extended shelf life can be achieved using nisin in conjunction with a reduced heat treatment [6].

Concerning concentration, it has been shown that increasing nisin concentration from 1-2 mg/ml to 5 mg/ml causes no further rise in antibacterial activity, which suggests that higher concentrations may create steric hindrance and that higher densities of immobilized peptides may not penetrate the bacterial cell wall as efficiently [26].

Another factor that could decrease nisin activity is competitive adsorption. Competitive adsorption refers to the introduction of a second peptide/protein to an already-adsorbed film, which may result in some degree of displacement if the second molecule has a better electrostatic interaction with the surface [2].

When applied directly on food, migration of nisin to food bulk lowers its effect at the surface. Compounds such as proteases, titanium dioxide, and sodium metabisulphite can severely affect nisin stability. In order to extend its efficacy, nisin has been embedded in packaging films

or coatings [150], with challenges that lie in the cost of film-design on an industrial scale and in the tailoring of nisin desorption [123].

Some authors have pointed out that some bacterial strains are able to develop resistance to nisin by the production of the enzyme nisinase [1, 151]. For this reason, the assembly of nisin to other antimicrobial agents, such as silver nanoparticles [152] and chitosan/alginate nanoparticles [153], has been explored, displaying a superior antibacterial efficacy of nisin.

3.2.1.4 Nisin market

The global nisin market was valued at USD 442.3 million in 2015, and is estimated to grow at a compound annual growth rate (CAGR) of 4.3% between 2015 and 2020, reaching USD 545.5 million by the last year. The growth of nisin market has been especially fueled by the increasing demand in North America (in the pursuit of more safe and convenient food) as well as the increasing population and awareness in emerging economies, such as China, in Asia-Pacific [154].

Meat, bakery and dairy products, canned vegetables, beverages and others are the major application areas of nisin as preservative. The largest market share for meat is mainly due to the extensive consumption of meat products in North America and Europe, while the dairy products segment comes as second-largest share of nisin market because of the growing consumption of products such as cheese, processed cheese, milk, and so on [154].

Nisin market in North America accounts for the largest share and is expected to grow at an even faster pace. Nisin market is driven by the growing demand of convenience and RTE products. Asia-Pacific has become the second-largest share of nisin market mainly due to the increasing population [154].

The production of nisin is sensitive and vital. The finished product is severely affected if there is an increase in lactate concentration over a standard level. Nisin, as a natural preservative, is at least ten times more expensive than chemical preservatives [154].

Various companies, such as Danisco A/S (originally from Denmark, now part of DuPont), Royal DSM N.V. (Netherlands), Siveele B.V. (Netherlands), Galactic (Germany), Shandong Freda Biotechnology Co., Ltd. (China), Zhejiang Silver-Elephant Bio-engineering Co. Ltd. (China), and Chihon Biotechnology Co., Ltd. (China) are the key players in this market [154].

3.2.1.5 Future of nisin

Nisin continues to be at the vanguard of bacteriocin-related research.

It is expected that future antimicrobial applications in food would not come from the invention of new antimicrobials but rather from the effective combinations of existing ones to achieve additive or synergistic effects [145]. Synergism is a positive interaction achieved when two combined compounds exert an inhibitory effect that is bigger than the sum of their individual effects [155]. Microbial control can be achieved most efficiently using more than one method of preservation, sequentially or simultaneously. The more ‘barriers’ with different mechanisms of action are presented to a pathogen, the lower the chances are of a significant amount of cells surviving [5]. Table 3.4 shows a summary of different research works that have been done with nisin in synergism with other antimicrobial agents.

In healthcare, several recent studies highlight the multiple manners in which nisin could potentially be used as a therapeutic agent. Nisin was shown to be effective in the treatment of head and neck squamous cell carcinoma [116, 156], and there is increasing evidence indicating that nisin may influence the growth of tumors and exhibit selective cytotoxicity towards cancer cells [130].

Nonetheless, the widespread use of nisin has not yet been fulfilled in part due to its low solubility and stability at the pH in the human body. Fortunately, the nature of nisin allows strategies that can modify the structure of the peptide in a more direct fashion than for other types of antimicrobials, and generate modified peptides with potentially beneficial biological, chemical and physical properties [116].

Nisin has been used in certain applications in the veterinary field thanks to its efficacy against pathogens causing diseases such as bovine mastitis. However, for the treatment of human infections (like human mastitis), its potential has been scarcely explored in the last few years and there is still a lack of knowledge in this regard [116].

In the industrial aspects for the efficient production of nisin, a better understanding on the molecular mechanism and regulatory characteristics of the nisin biosynthesis seems to be required to obtain improved nisin yields. Hitherto, several attempts to increase nisin yields by genetic manipulation have been tested [114].

Table 3. 4 Works about synergistic effects using nisin for food preservation

Authors	Year	Antibacterial agents	Model bacteria	Result
Brumfitt et al. [157]	2002	Nisin Antibiotics (bacitracin, ramoplanin, chloramphenicol)	Methicillin-resistant Staphylococcus aureus Vancomycin-resistant enterococci	High synergism with ramoplanin Antagonistic effect with chloramphenicol
Najjar et al. [5]	2007	Nisin A ϵ -poly-L-lysine	L. monocytogenes B. cereus	Synergistic activity
Sivaroooban et al. [158]	2007	Nisin Grape seed extract	L. monocytogenes	Synergistic effect
Tokarsky et al. [145]	2008	Nisin Lactic acid Monolaurin	L. monocytogenes	Synergistic effect
Brandt et al. [159]	2010	Nisin Lauric arginate ester Acidic calcium sulfate ϵ -poly-L-lysine	L. monocytogenes	Synergistic for nisin + acidic calcium sulfate Antagonistic for ϵ -poly-L-lysine + acidic calcium sulfate
Esteban et al. [128]	2012	Nisin Carvacrol (heat treatment)	Salmonella enteritidis Salmonella senftenberg	1.2 μ M nisin with 0.77 μ M carvacrol significantly delayed growth of heat treated cells
Liu et al. [146]	2015	Nisin ϵ -polylysine	E. coli B. subtilis Staphylococcus aureus	Synergistic effect
Bag et al. [160]	2017	Nisin Linalool p-coumaric acid	B. cereus S. typhimurium	A combination of the three antimicrobials caused >50% antibiofilm efficacy
Shi et al. [155]	2017	Nisin p-anisaldehyde	S aureus	Synergistic effect
Sun et al. [7]	2017	Nisin SipB (a protein from Lactobacillus crispatus)	Staphylococcus saprophyticus	Synergistic effect
Sangcharoen et al. [37]	2017	Nisin Ascorbic acid EDTA	Salmonella Enteritidis ATCC 13076	Synergistic effect optimum at 500 ppm nisin, 1515 ppm ascorbic acid and 250 ppm EDTA

3.3 The immobilization technique

Immobilization can be defined as the binding of molecules to a surface resulting in reduction or loss of mobility [161]. One challenging task is immobilizing antimicrobial agents onto surfaces in such a way that their three-dimensional structure, function and binding sites are kept [161].

Immobilization methods and chemistries vary significantly depending on immobilization surface and the properties of the antimicrobial agent. Recent intelligent immobilization methods include the use of light, electrochemical, thermal and mechanical stimuli to attach and detach with high-precision spatial control [162]. Some of the immobilization techniques that have been employed are:

- (a) Physical immobilization: By adsorption on surfaces via intermolecular forces, especially ionic bonds and hydrophobic and polar interactions. The resulting layer tends to be heterogeneous and randomly oriented, since each molecule can form many contacts in different orientations to minimize repulsive interactions with the substrate and previously adsorbed agents. In addition, high-density packing may sterically block active sites, interfering with functional properties [161]. Buffers or detergents may be able to remove adsorbed agents.
- (b) Graft polymerization: Surface chemistry of a solid substrate (usually a polymer, but could also be steel or another inorganic material) is modified by grafting polymer chains with desirable characteristics from or onto it. Two approaches may be applied: grafting from, in which the surface is modified to introduce active sites so that a monomer can be incorporated and then perform polymerization attaching more monomers, and grafting to, in which a backbone chain with randomly distributed functional groups is used to attach

monomers and form a copolymer [48]. The method has been applied mainly on polyethylene, polyvinylchloride and polyisobutylene.

- (c) Cross-linkable coatings: Polymers able to bond each other after deposition by adding chemical cross-linkers or subsequent exposure to irradiation. The most commonly used crosslinkers are polyaziridines, polycarbodiimides and polyisocyanates for systems based on water [48].
- (d) Self-assembled monolayers (SAMs): Formed spontaneously by adsorption of organic molecules on a surface, creating a single layer (from one to a few nanometers in thickness) of relatively ordered groups on it via strong interactions involving an anchoring group (called head group), generally a thiol, silane or phosphonate. SAMS are inexpensive and have found applications in control of wetting and adhesion, as in the creation of a hydrophobic monolayer on car windshields to keep them clear of rain. The main drawback is that SAMs' stability under aqueous (especially when acid or basic) conditions has not been well established and remains challenging [48].
- (e) Layer-by-layer (LbL): In this technique, alternating layers of oppositely charged species – usually polyelectrolytes – are deposited on a solid substrate to create thin functional films, applying some wash steps in between [48]. The alternate layers and wash steps can be performed using methods such as dip coating, spin coating, spray coating or electromagnetic techniques. Antimicrobial agents can be applied and entrapped between layers.

LbL is a rapid coating technique that can create lasting layers on many surfaces, from polymers to stainless steel, which are stable due to the presence of many noncovalent

electrostatic and Van der Waals interactions. The films are thin, usually between 1 and 100 nm, depending on the amount of bilayers. [48].

LbL has been the most explored technique to immobilize AMPs on surfaces, and it has found applications in corrosion control, biomedicine, protein purification, etc.; nevertheless, this approach is constrained to the use of highly charged and water-soluble AMPs, which are not so frequently encountered [35, 163].

- (f) Chemical vapor deposition (CVD): A thin film is formed on a heated solid support from a gaseous phase in a closed chamber typically under vacuum, followed by removal of unreacted gas and chemical by-products. The process is mainly used in the semiconductor industry, but also to produce materials such as silicon nitride or synthetic diamond. A commercial drawback to use CVD on food processing equipment is the complexity of the apparatus employed, and the fact that the size and throughput of the materials to be coated is limited [48].
- (g) Electroplating and electroless plating: Electroplating is a solution-based process that uses an electrical current to create a thin coherent metal coating on an electrode made of another metal. On the other hand, electroless plating is a plating method which employs a chemical reducing agent in the bath instead of electricity (no external source). Examples of these reducing agents are hypophosphite (used for nickel plating) and low-molecular weight aldehydes. Antimicrobial character can be conferred either by electroless plating of antimicrobial metals, like silver and copper, or by codeposition of antimicrobial particles within an inert metal (e.g. nickel). The existence of large-scale commercial plating outfits has constituted a major advantage of plating with coating technologies for antimicrobial food equipment coatings [48].

Several researchers have been working on nisin (and other AMPs) immobilization by using diverse techniques. Duday et al. [16] used dielectric barrier discharge (DBD) plasma deposition to immobilize nisin molecules on stainless steel surfaces, obtaining good bactericidal action (nearly $4\log_{10}$ reduction of Gram-positive strain according to ISO 22196) and good resistance to several cleaning conditions (film stability).

Aveyard et al. [26] immobilized nisin on polystyrene substrates and, using XPS, they confirmed the immobilization of the peptide when the C1S spectra of the grafted surfaces clearly showed a characteristic peptide O=C-N at 289.0 eV, confirming that nisin has adhered to the surface and no other adventitious contaminants.

Humblot et al. [164] used a self-assembled monolayer (SAM) to graft the antimicrobial peptide magainin I on gold surfaces, reducing the adhesion of bacteria by more than 50% and killing the already-adhered cells, no release of the peptide was observed, and the activity persisted for up to six months.

3.4 The microorganism

Microorganisms are divided into six major classes: bacteria, archaea, fungi, protozoa, algae, and viruses. Nonetheless, for the purpose of this work, only bacteria and, most precisely, pathogenic bacteria, are considered.

Pathogenic bacteria are unicellular microorganisms able to cause disease. There are fewer than 100 bacterial species that cause disease in humans, and some of the most common are in the genera *Salmonella*, *Campylobacter* and *Listeria*.

In this work, *Listeria monocytogenes* was used as a model organism to demonstrate antimicrobial activity due to its importance in food safety. It has been reported to be one of the pathogens responsible for the most foodborne illness related deaths [32, 165].

L. monocytogenes is a ubiquitous pathogen in the natural environment [145] that has been implicated in several recalls and outbreaks of foodborne illness [2]. It can cause disease conditions ranging from stillbirth and premature delivery in perinatal cases to meningitis and septicemia in adults [159].

L. monocytogenes is a Gram-positive food borne microorganism that grows even at refrigerated temperatures (psychrotrophic), and survives for a long period of time in industrial plants and on food surfaces. According to the Center for Disease Control and Prevention (CDC), listeriosis is a serious public health problem [123]. The mortality rate following an infection by *L. monocytogenes* is much greater than that by other pathogens, including *E. coli* O157:H7 [21].

In 2005, it is estimated that 300,424 pounds of ready-to-eat (RTE) meat products were recalled for possible *L. monocytogenes* contamination in U.S. [158]. Something similar happened in 2008 in Canada when this bacterium was responsible for a RTE meat product outbreak that claimed the lives of 20 Canadians [147]. The food processing plant environment appears to be a greater source of *L. monocytogenes* contamination of finished product than of raw materials [134]. In consequence, the U.S. Food and Drug Administration (FDA) and USADA Food Safety and Inspection Services (FSIS) maintain a zero-tolerance policy for detection of *L. monocytogenes* in RTE food products [159].

Lewis et al. [166] demonstrated that the presence of one single *L. monocytogenes* cell on a substrate, such as stainless steel, can propagate to form biofilms when grown at 30°C for 72 h. Works from Herald [167] and Kryszinski [168] also supported the attachment of this bacterium to stainless steel.

Brewer et al. [169] found that the inactivation of *L. monocytogenes* in the presence of nisin was undoubtedly dependent on the nisin concentration. A concentration of 10 IU/ml reduced

counts by 1 log unit in 20 min, while a concentration of 50 IU/ml reduced viability by 4 log units in the same period and, in addition, the sensitivity of *L. monocytogenes* to nisin was particularly increased by the presence of ethanol (synergistic effect).

Thomas and Wimpenny [170] determined that increasing NaCl concentration, and when pH falls between 7.92 and 5, nisin action is higher against *L. monocytogenes*, while the effect of temperature difference was not so obvious.

Once that the problematic of biofilms has been explained and that the four components of an antimicrobial system have been explored in detail, it is time to fully start the experimental part in which the modified oxide layers of the chosen materials will be proven in order to determine their capability to store the antimicrobial agent while keeping the antibacterial property.

4. SUBSTRATE CRACKING IN Ti-6Al-4V DRIVEN BY PULSED LASER IRRADIATION AND OXIDATION

Previously published by Journal Surface and Coatings Technology,
Vol. 322, pp. 46 – 50 in May 2017.

4.1 Abstract

Oxide layers grown on Ti-6Al-4V using pulsed laser irradiation to thicknesses between 100-150 nm result in a variation in color of the films, but also exhibit a two-dimensional network of cracks (i.e. mudflat cracking). The crack densities increase with laser scan rate. Focused ion beam sections showed that the cracks not only occur within the oxide film (through thickness) but also penetrate into the titanium alloy substrate to depths between 1-6 μm . With this information and the elastic and fracture properties of the film and the substrate measured using nanoindentation, the residual tensile stress and strain undergone by the oxide film while cooling after the application of a laser pulse was estimated; this is the same stress that is relieved through cracking. The possibility that the fracture toughness of the substrate has decreased by embrittlement is also discussed.

4.2 Introduction

Crack formation drives material failure and is often regarded as a process to be avoided [171] and a menace for the microfabrication industry [172]. Such cracking can happen over a wide range of length scales – from the macroscopic, like geological and biological systems, to the microscopic, like cracking thin films for a particular technology [173].

Arresting crack propagation is important for the prevention of material failure, however, in specific cases, cracks may find useful applications such as in cryptography. The tailoring of

controlled cracks can find use in engineered structures as well. If the stress drops during the propagation of a crack, the crack registers the disturbance of the driving force and, when this one decreases to a value comparable to the crack resistance, the crack stops propagating [171].

Metallic titanium, in contact with the atmosphere, develops a passive oxide film, (generally 2–3 nm thickness [174, 175]), which gives titanium its excellent corrosion resistance [176]. Thicker titanium oxide coatings attract particular interest in applications such as optical and decorative coatings, catalysts and medical implants. A good technique to produce such coatings is pulsed laser irradiation (PLI) of a metallic titanium surface in a reactive (oxidizing) atmosphere [177, 178].

In order to produce colored oxide films on titanium through laser irradiation, the pulse must heat the surface to an elevated temperature within a certain time needed for chemical reactions to take place [177]. Nevertheless, when the laser pulse stops, the material cools down and, due to the difference in coefficients of thermal expansion between the metallic substrate and the film (oxide), the latter is often susceptible to through thickness fracture (cracking) from high residual stresses [174, 179]. These residual stresses are in-plane tensile stresses if the coefficient of thermal expansion of the film exceeds that of the substrate ($\alpha_f > \alpha_s$) [180]. Sometimes the cracking phenomenon is not limited only to the film. Film debonding or decohesion may accompany the channeling crack if the interface fracture toughness (Γ_i) is sufficiently low compared to that of the film and substrate.

Cracking may also extend into the substrate. If the substrate is very stiff compared to the film, the channeling crack may not reach the interface with the substrate. Conversely, depending on the elastic mismatch and the toughness of the substrate relative to the film, the crack may penetrate into the substrate [180]. It has also been demonstrated that a brittle film may cause a

premature fracture of a ductile substrate and that crack penetration depends on the number of dislocations emitted from the crack tip [181]. Each of these effects can influence film crack interaction and the paths that cracks follow. There are cases, for example, in which a propagating film crack induces an interface debond on one side of the crack but not on the other, creating a strong asymmetry with respect to the crack tip, causing the crack to follow a curved trajectory [180].

For this current study, oxides fabricated by pulsed laser irradiation on a commercial titanium alloy substrate were characterized using electron microscopy to determine the geometry and depth of the cracks, as understanding the scope of substrate cracking would explain either detrimental behavior (i.e. crevice corrosion) or the possibility of increasing adhesive bonding via mechanical interlocking with adhesives. From prior studies of the mechanical properties of the film and the substrate, it is possible to make estimations of the energy required to extend the crack and the stress intensity factors (K_I) in the system. The possibility that the fracture toughness of the substrate has decreased by embrittlement (reason why the cracks penetrate into the substrate) will be discussed.

4.3 Experimental

Five Ti-6Al-4V (henceforth Ti alloy) coupons (12 x 12 x 3 mm) with a chemical composition shown in Table 4.1, were irradiated using an Er-doped, glass-fiber laser ($\lambda = 1.54 \mu\text{m}$) from SPI Lasers, Inc., at 7.6 W average power, pulse frequency of 225 kHz and pulse duration of 120 ns, in air, scanning a 6 x 6 mm area of the sample surface, line by line, with parallel laser traces at a controlled scan velocity [182]; more complete processing parameters are described in an earlier publication [183].

Table 4. 1 Chemical composition of the Ti alloy, obtained by EDS.


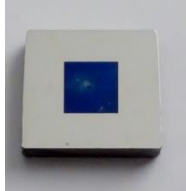

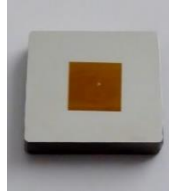
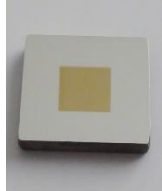
	% Ti	% Al	% V	% Others
Ti-6Al-4V	89.4	7.4	3.1	< 0.1

After laser exposure, the irradiated (colored) area of the coupons was characterized by scanning electron microscopy (SEM) combined with focused ion beam (FIB) machining, using a FEI Nova 200 NanoLab DualBeamTM-SEM/FIB. SEM images were helpful to perform measurements of crack density and crack spacing, while FIB cuttings were used to observe the cross section of the Ti alloy, estimate the oxide thickness and crack depth into the film.

4.4 Results

Ti alloy coupons were superficially melted by the laser promoting oxygen diffusion through the molten material and, thus, to the oxidation of the Ti alloy [182]. These oxide layers (henceforth the oxide film) vary in color depending on the oxide thickness [183] as shown in Table 4.2.

Table 4. 2 Applied laser scan rates with resulting film thickness and color variation of the coupons. Irradiated area (colored centered square) is 6 x 6 mm.

Laser scan rate (mm/s)	90	110	170	200	300
Film thickness, h (nm)	148	139	124	119	110
Color	Blue 	Purple 	Brown 	Brown 	Golden 

4.4.1 Oxide film

The oxides produced by laser irradiation are composed of non-stoichiometric TiO and Ti₆O [184]. The latter is mainly present in the interfacial layer, essentially intercalated in the HCP α -Ti

substrate [174]. The film thickness, determined using images of the cross sections, is on the order of 100–150 nm, depending on the applied scan speed (Table 4.2). A cross sectional micrograph showing the $\alpha+\beta$ Ti alloy microstructure of the oxide layer and underlying substrate after pulsed laser irradiation on films grown under the same conditions has been previously published (see Fig. 9 in [183]), and suggests that a martensitic transformation to a lath morphology of hexagonal Ti can occur. Adams and co-workers [183] have noted (but not explicitly measured) cracks in the oxides grown by PLI can penetrate this transformed region, and suggested that the cracks penetrate into regions that contain detectable O concentrations. However, it is important to note here that Adams and co-workers found transformation zones to martensitic Ti to extend to depths up to 25 μm under the oxide.

A collection of interconnected cracks, resulting in the formation of oxide islands, covers the surface. This mudflat cracking (Fig. 4.1) indicates the oxide film is stress relieved; residual stresses that developed during fabrication, likely due to difference in coefficients of thermal expansion between oxide and substrate, have been relieved through cracking. The average island diameter, or spacing between cracks, determined from line averages of SEM images, is on the order of 5 – 14 μm , and it decreases when the film thickness (h) decreases (Table 4.3).

Table 4. 3 Crack density and crack spacing obtained by laser scanning at different rates.

Laser scan rate (mm/s)	90	110	170	200	300
Crack density, C (cracks/mm)	74.5	78.8	126.0	126.6	150.0
Average Crack spacing, S (μm)	13.4	12.7	7.9	7.9	6.6

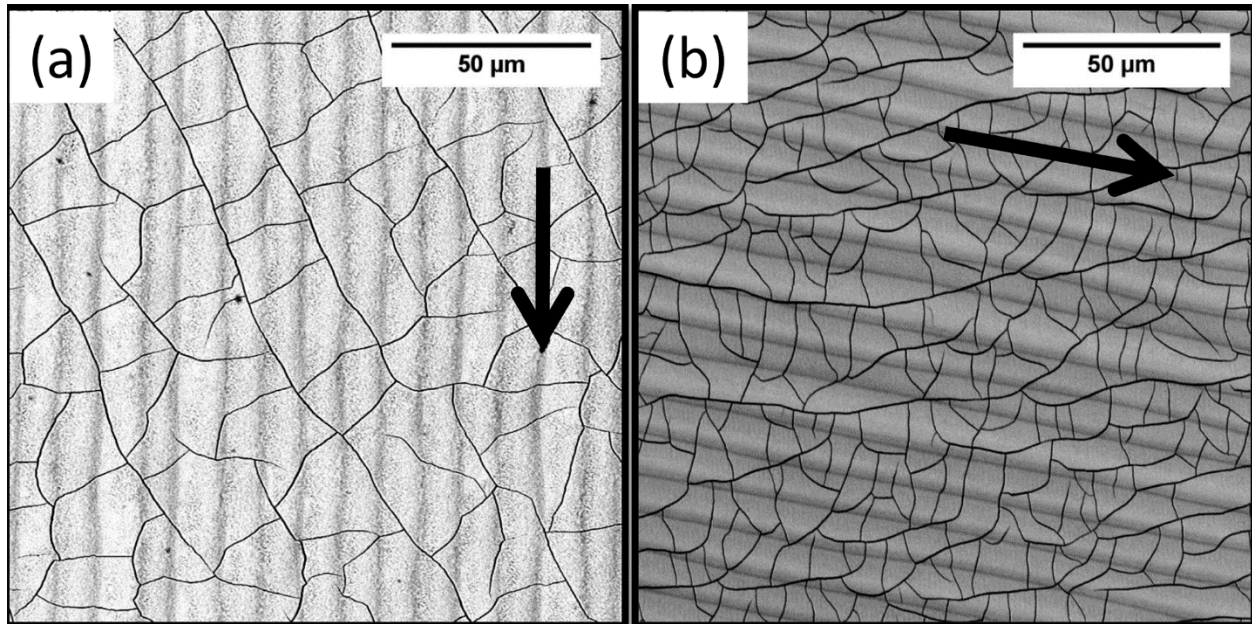


Figure 4. 1 Backscattered electron images of the oxide film formed after PLI. (a) At 110 mm/s and (b) At 300 mm/s. Lines in the background, parallel to the arrows in the figures, are the result of the scanning direction of the laser path. There is no clear relationship between the laser direction and the formation of cracks.

4.4.2 Substrate

FIB images of the cross section revealed that the cracks present in the film penetrate into the substrate (Ti alloy). The penetration is significant, mostly on the order of 1–6 μm beneath/below the interface.

For all five Ti alloy coupons, cracks mostly grow perpendicular to the surface, with a few variations like the branch shown in Fig. 4.2(b). No evidence of significant bifurcation within the substrate was observed, nor was there any evidence that the crack directions were altered significantly at the oxide-metal interface.

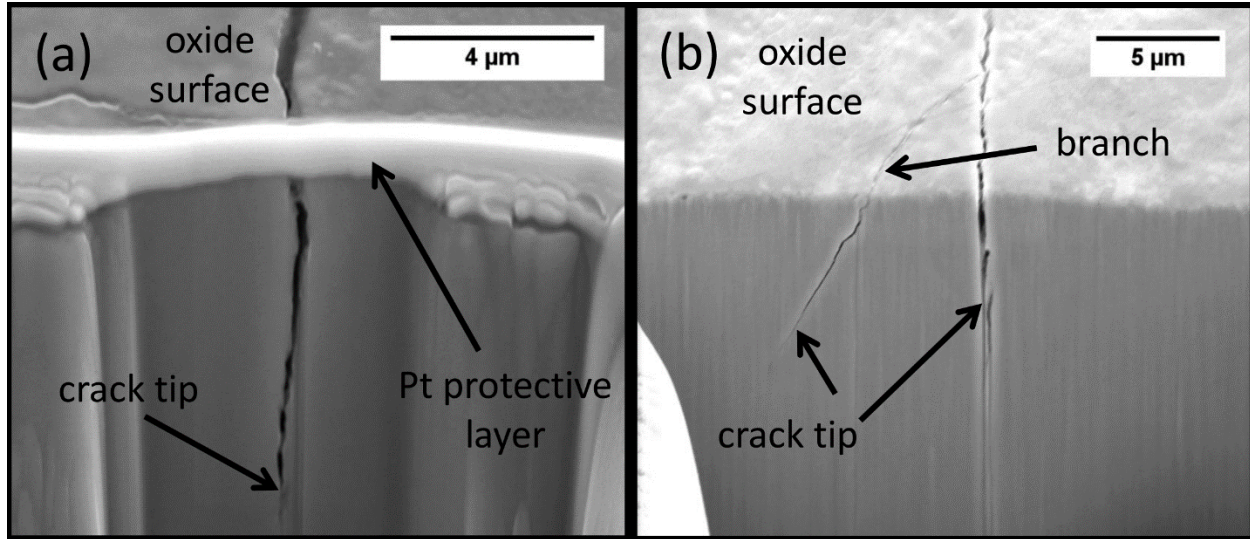


Figure 4. 2 FIB images of cross sections. (a) Crack grows perpendicular to the interface but with some wobbling, probably due to the alternate expansion/contraction cycles between each laser pulse and the next. (b) The presence of a branch coming from the main crack.

4.5 Discussion

Crack formation in materials is controlled by (a) the mechanical properties, including modulus (stiffness), toughness (energy required to break the material) [185], and thermal expansion, (b) the geometrical properties (dimensions and flaw population), and (c) the loading (applied and residual strain, and temperature excursions) [186].

4.5.1 Mechanics of the film fracture process

Every time that the native oxide layer is irradiated by a laser pulse, the local thermal excursion leads to the generation of local stresses and strains. The irradiation generates a change in temperature which drives to an expansion of the whole system (film + substrate), but film and substrate expand at different rates because the coefficient of thermal expansion of the film is different to that of the substrate. When a thin film is deposited on a substrate, a composite is formed in which the presence of the substrate affects the film and vice versa [187].

After the few nanoseconds of irradiation, the whole system cools down. Film and substrate contract but, again, they do it at different rates. In the particular case of this study, the oxide film must have a higher coefficient of thermal expansion than the substrate; this way, the film contracts faster than the substrate but, because the substrate is substantially thicker than the film, even if the latter tends to shrink, the former restricts it from doing so, and thus the film experiences a tensile residual stress (σ_0) that can be relieved by film cracking. However, at the same time, the interaction with laser promotes specific chemical reactions that change the chemistry in the oxide film; more oxygen (and probably other chemical species) diffuse into the film, creating a mixture of different oxides (TiO , Ti_6O) and a thicker film. Because the chemical composition of the oxide layer is different depending on the thickness of the film, it is assumed that the fracture toughness of the film (Γ_f) is not of the same magnitude for all the samples.

The first cracks appear with uniform spacing and only when the stress in the film reaches a critical value. Once the first cracks are formed, the distribution of stress transferred across the interface that causes more fracture is different from that which originally existed when the film was continuous [187]. The cracking produces a stress relaxation in the film that lowers the stress to a value below that of the critical stress, especially in the regions very close to the crack. As the substrate is strained further, the stress in the cracked oxide segments (islands) will increase and, to relieve this added stress, more cracks will form, generally in the midpoints of the unbroken islands, those points being the farthest from the cracks and thus experiencing the least stress relaxation (maximum stress) [187]. In the case of this study, the process may be repeated several times with a laser pulse irradiating the surface every few nanoseconds. We begin with the assumption that the film would not have undergone multiple fracture (mudflat) if it were not bonded to a more pliable material as substrate beneath it [187].

Once the laser irradiation process has been completed, crack density (C) in the oxide film may be estimated using SEM images. Then the average spacing between cracks can be calculated with the equation:

$$S = \frac{1}{C} \quad (Eq. 4.1)$$

where S is the crack spacing. Values of crack density and crack spacing for each one of the samples are shown in Table 4.3.

With the application of nanoindentation, Lawrence [174] determined that residual stresses in oxide films grown using similar laser scan rates are in the order of 6.7 to 10.3 GPa. Using this data and

$$\sigma_0 = \frac{E_f \varepsilon_0}{(1 - \nu_f)} \quad (Eq. 4.2)$$

the applied strain in the film (ε_0) may be calculated. With the parameters in Table 4.4, ε_0 is estimated in the 0.022-0.034 range. E_f and ν_f are the Young's modulus and the Poisson's ratio of the film, respectively.

Table 4. 4 Mechanical properties for film and substrate

	Film	Substrate
Young's modulus, E (GPa)	215 [174]	110 [187]
Poisson's ratio, ν	0.3	0.3
Shear modulus, μ (GPa)	90	44
Residual stress, σ_0 (GPa)	6.7–10.3 [174]	-----

According to Thouless [188], the crack spacing is proportional to the square root of the film thickness by

$$S \simeq 5.6h \sqrt{\frac{\Gamma_f(1-v_f)}{(1+v_f)E_f\varepsilon_0^2h}} \quad (Eq. 4.3)$$

where Γ_f is the fracture toughness of the film (in J/m²).

Using Eq. 4.3, it is estimated that Γ_f should be between 4600 J/m² and 7500 J/m².

4.5.2 Mechanics of the substrate fracture process

Channel cracks in the film have developed at some stage during the cooling of the film/substrate system and their growth may be stopped either because the substrate is much tougher or because sufficiently large substrate surface defects are not readily available [189]. Hu et al. [190] demonstrated that Cr films subject to tensile intrinsic stress first split generating a mudflat cracking pattern, and then the cracks subsequently can extend into glass substrates, growing along the plane for which $K_{II} = 0$. Guo et al. [181] also found that cracks penetrate into the substrate when a brittle TiN film is placed on brass substrate due to dislocation shielding.

In this current study, the film is stiffer than the substrate ($E_f > E_s$). A compliant substrate provides less constraint for crack propagation [179]. Because the laser pulses are directly applied to the oxide film, the stress and strain reside in the film, not in the substrate. The available driving force (G_a) decays significantly for deep cracks, implying stable propagation. The crack arrests at a certain depth due to this decline.

Since cracks can propagate in a stable fashion below the film-substrate interface when they are driven by a residual tension in the film [191], the energy-release rate (driving force) at the tip of a single crack of depth a , where $a \gg h$, tends to a limit of

$$\frac{G_a}{\bar{E}_s h \varepsilon_0^2} = 2.14 \left(\frac{1+\alpha}{1-\alpha} \right) \left(\frac{a}{h} \right)^{-1} \quad (Eq. 4.4)$$

where \bar{E}_s is the Young's modulus of the substrate and α is the Dundurs' parameter [192, 193, 194],

$$\alpha = \frac{\bar{E}_f - \bar{E}_s}{\bar{E}_f + \bar{E}_s} \quad (Eq. 4.5)$$

where $\bar{E} = E/(1 - \nu^2)$ in plane strain. If α is positive, means that the film is stiffer than the substrate; if negative, then substrate is stiffer than the film.

For the film/substrate system in this study, $\alpha = 0.32$, while G_a depends on the crack depth according to Fig. 4.3. It can be observed that the decay is very significant in the first 500 nm, therefore there is enough driving force to cross the interface and penetrate into the substrate.

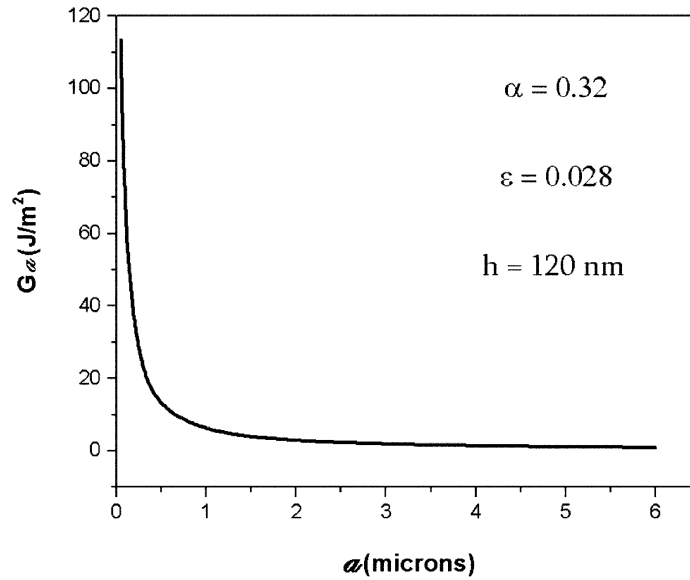


Figure 4. 3 Decay of available driving force with increasing crack depth

Drory and Evans [195] determined that for a semi-infinite substrate, the opening mode stress intensity factor K_I for a line force on a crack surface is given by

$$\frac{K_I}{\sigma_0 \sqrt{h}} = \frac{2.6}{\sqrt{\pi \lambda}} \quad (Eq. 4.6)$$

where λ is the relative depth and is defined as $\lambda = (a - h)/h$. So, K_I is inversely proportional to the square root of the relative depth as shown in Fig. 6 from [195] for λ up to 10.

In this study, the average crack depth is around 30–35 times larger than the film thickness, and the behavior of K_I vs λ is shown in Fig. 4.4. It is important to remark that the K_I values of the Ti alloy are in the order of $1 \text{ MPa}\sqrt{m}$. This value is considerably lower than the average fracture toughness for Ti-6Al-4V, which is on the order of $65 \text{ MPa}\sqrt{m}$ [196]. Fracture toughness values between 16 and $28 \text{ MPa}\sqrt{m}$ have been reported in literature [197] for a martensitic microstructure of Ti-6Al-4V (i.e. the expected microstructure from [183]), which is much higher compared to the value obtained in this study, which makes us believe that an embrittlement process is involved here.

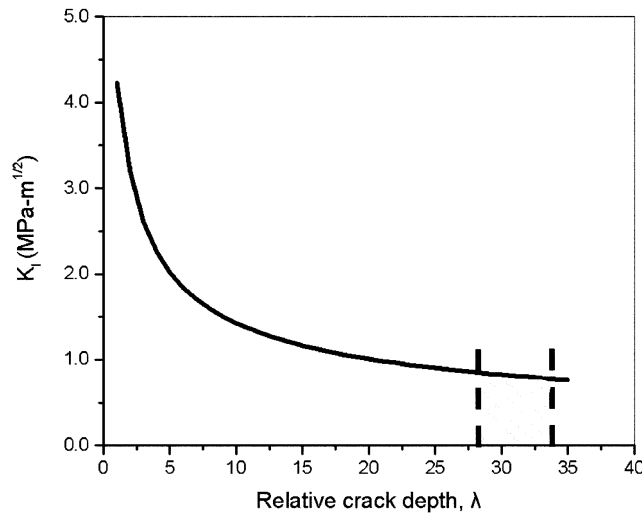


Figure 4. 4 Variation in stress intensity factor vs relative crack depth (penetrating into the substrate). Shaded area represents the relative crack depth for the films used in this study.

Embrittlement of the substrate would be most likely caused by solute oxygen or hydrogen. As the laser irradiates the film several chemical reactions occur; the main one is the diffusion of oxygen which creates a mixture of oxides. As the growth is in ambient atmosphere both oxygen and water vapor are present, and the harsh environment of the pulsed laser could lead to dissociation of water, making it possible that either embrittling species could be present. Literature

reports of O embrittling α -Ti [198] or H embrittling Ti [199, 200, 201] can lead to substantial decreases in toughness. Unfortunately, given the rapid diffusion of H in Ti, the time between fabrication and analysis would be prohibitive to identify if H had been the embrittling species; similarly the fact that the oxide intermixes with the matrix in the current samples makes identifying the actual concentration near the end of the crack tip challenging. Future analysis will be required to identify the particular species responsible for this behavior; at the current time we have not been able to identify O gradients at sufficient resolution to verify this hypothesis.

4.6 Conclusions

The following structure and proposed mechanism leads to substrate cracking, driven by tensile stresses, in an oxide film grown by PLI on Ti-6Al-4V

- (a) The oxide film, which is composed of a mixture of different Ti oxides and approximately 100-150 nm in thickness exhibits a strong presence of mudflat cracking with cracks that not only penetrate the film but also the substrate, attaining depths between 1–6 μm in the substrate.
- (b) Given that the oxide film is stiffer than the substrate and $\alpha > 0$, the energy release rate in the film increases when the ratio a/h increases, which helps the cracks reach the interface.
- (c) When cracks start to penetrate into the substrate, the energy release rate (driving force) considerably decays because the stress forms in the film. At some depth, the energy is not sufficient to continue to fracture the substrate, and the cracks arrest.
- (d) The toughness at which cracks arrest in this system (on the order of $1 \text{ MPa}\sqrt{m}$) is significantly lower than the bulk toughness of Ti-6Al-4V or of any possible martensitic form of Ti; one likely cause is embrittlement caused by the diffusion of chemical species (e.g. hydrogen or oxygen) during oxide growth due to the interaction between the laser

pulse and the atmosphere. When coupled with the likelihood of martensitic transformations due to thermal processing in Ti [183] suggest that oxide induced substrate cracking in this type of system is a combined effect of substrate structure and solute impurities.

5. PEPTIDE INFUSION INTO MECHANICALLY INDUCED CRACKS IN OXIDE COATINGS TO CREATE AN ANTIBACTERIAL METALLIC SURFACE

5.1 Abstract

A nanosecond pulsed laser was used to create oxide films on a titanium alloy, Ti-6Al-4V, and 304L stainless steel. Laser conditions employed created a mudflat cracked surface on titanium samples, but no cracks on the steel ones. An antimicrobial peptide, nisin, was infused into the cracked and uncracked oxide surfaces to provide antimicrobial activity against Gram-positive bacteria; *Listeria monocytogenes* was chosen as the model microorganism. Durability and release tests were used to estimate the degree of immobilization of the peptide on the modified surface of both materials. Release tests in distilled water at room temperature show that nisin is slowly liberated from the uncracked stainless steel surface, while there was no evidence of nisin liberation from the cracked titanium alloy surfaces, likely due to immobilization of the peptide into the artificially created micro-cracks on the surface of this alloy. Concerning the bactericidal tests, surfaces treated with nisin became active against *L. monocytogenes*; this behavior is mostly retained after scrubbing/washing and simple immersion in water.

5.2 Introduction

There is an increasing awareness of the importance of minimizing post-processing contamination occurring through the contact of a product with contaminated surfaces in food-processing plants, where bacteria attach to a surface (gaskets, conveyor belts, slicing, dicing and packaging machines, containers, knives, tables, floors, walls, etc.) and can persist for months, even for years [202]. A sessile bacterial cell attached on a substrate surface is functionally distinct from a planktonic cell in the liquid [78], and tends to form biofilms.

Biofilms are microconsortia of surface-adhering cells encased in a self-produced matrix of extracellular polymeric substances (EPS or “slime”) [29, 203]. This extracellular matrix is mainly comprised of water, polysaccharides, proteins and extracellular DNA [35, 204]. Mature biofilms only require two to four weeks to fully develop [8].

Several directions in research have been proposed to mitigate the formation of biofilms on surfaces. These include using polymers [21, 136], nanoparticles [123, 205], and flat metallic surfaces [16, 21, 206]; however, the techniques used to confer antibacterial properties to the material are very diverse. Duday et al. [16] demonstrated that dielectric barrier discharge (DBD) plasma deposition can be used to create an organosilicon interlayer in which biomolecules can be attached and protect stainless steel against bacteria. Several successful studies have used antimicrobial peptides (AMPs) to create an antibacterial surface. Some examples of these efforts include those of Qi et al. [124], who created antimicrobial multi-walled carbon nanotubes using polyethylene glycol (PEG) as a linker [207] between the nanotubes’ surface and an AMP. Peyre et al. [208] used PEG to attach another AMP to a titanium oxide surface. Lee et al. [137] created an antimicrobial paper by using a copolymer as a binder to attach an AMP to the surface, and Héquet et al. [34] protected stainless steel by attaching an AMP using chitosan and a combination of aldehydes. A common thread in these studies is using bioaffinity or covalent bonding to immobilize the antibacterial agent, thus preparing or functionalizing a material surface against biofilm formation using chemical processes, however, investigation using physisorption between AMPs and surfaces is less common.

Physisorption is usually considered a weak method to immobilize an antimicrobial agent because it depends mostly on intermolecular forces (electrostatic, hydrophobic, van der Waals, etc.) on the surface. Particles of the antimicrobial agent in physisorbed systems may not attach

with the same orientation, which may create steric hindrance [162] and non-uniformity in the antimicrobial coating. However, surface modification, by fabrication of micro- and nanoscale structures, is a very promising technique for immobilization of antimicrobial agents [209].

Creating micro- and nano-features such as ridges, grooves, trenches or dimples, may increase anchoring between an antimicrobial agent and a surface.

Laser irradiation provides a unique method of generating surface patterns because lasers are capable of modifying physical and chemical properties over multiple length scales [61]. They have the ability to accurately deliver large amounts of energy into confined regions of a material in order to achieve a desired response. For opaque materials, like metals, this energy is absorbed near the surface, modifying surface chemistry, surface energy, crystal structure, and/or multiscale morphology without altering the bulk [60]. Because material heating rates can be extreme, reaching as high as 10^9 K/s for nanosecond pulses (and even higher for femtosecond pulses [210]), significant changes to the material can occur [60]. The large temperature gradients achieved with localized laser heating can lead to rapid self-quenching of the material, creating non-equilibrium structures; thermal stresses also occur and they can contribute to mechanical response of the material in the way of work hardening, warping or even cracking [60]. Crack appearance is considered by several publications [61, 65] as one of the main drawbacks for the use of laser technology in surface modification given that cracks are commonly detrimental features that have the potential to grow over time and eventually lead to material failure [61]; however, depending on the intended application and by using suitable laser parameters, special cracks which may be beneficial rather than detrimental to the material may be concocted.

A few studies [211, 212, 213] have been published trying to infuse chemicals (liquid state) to improve bactericidal properties of the surface. Most of them are based on the so-called slippery

liquid-infused porous surfaces (SLIPS) that work by increasing the hydrophobicity of the surface, making it repellent to liquids and, therefore, reducing substantially biofilm formation. However, to the best of our knowledge, no research has been done trying to infuse physisorbed antimicrobial nanoparticles into artificially modified surfaces.

In this work, nanosecond pulsed laser irradiation (PLI) in ambient atmosphere was used to create oxide layers on metal surfaces; some of these layers developed an interconnected network of cracks, while others remained uncracked, depending on the laser parameters employed. Nanoparticles of the antimicrobial peptide nisin were infused on those layers by using vacuum. Nisin, produced by *Lactococcus lactis*, is currently used as a food preservative in a broad range of products, including dairy products, liquid egg, bakery products, vegetables, meat and fish [117], and in more than 50 countries, including the United States, countries in the European Union, and the People's Republic of China [133]. The materials tested were 304L stainless steel, the most common contact material in the food industry because it is chemically and physiologically stable at a variety of processing temperatures, easy to clean and has a high resistance to corrosion [8] and Ti-6Al-4V, used mainly for orthopedic and dental implants in the biochemical industry [214]. The challenge remains in the immobilization of nisin while keeping their accessibility and durable activity towards the surrounding bacterial cells [106].

5.3 Experimental

5.3.1 Titanium

Five Ti-6Al-4V (henceforth Ti64) coupons (12 x 12 x 3 mm) were irradiated using an Er-doped, glass-fiber laser ($\lambda = 1.54 \mu\text{m}$) with the conditions described in [215]. Only the laser scan speed was modified, varying from 90 to 300 mm/s. After irradiation (only an area of 6 x 6 mm

was irradiated on each coupon surface), the fabricated colored oxide coatings were characterized by SEM/FIB revealing the presence of an interconnected network of cracks 2 – 6 μm deep, 100 – 200 nm width (high aspect ratio), and an average spacing on the order of 15 – 20 μm (Fig. 5.1a). The oxide layer grown on Ti64 is on the order of 100's of nm thick; thus these cracks penetrate the metallic substrate.

5.3.2 Stainless steel

One austenitic 304L stainless steel (henceforth SS) coupon (12.5 x 12.5 x 3.4 mm) was irradiated using the same laser employed for Ti64, with the conditions described in [91]. The scan speed was 500 mm/s, significantly higher than the one used for Ti64. After irradiation, the fabricated colored oxide coating was characterized by SEM, with no presence of cracks (Fig. 5.1b). The oxide on this sample is also on the order of 100 nm thick.

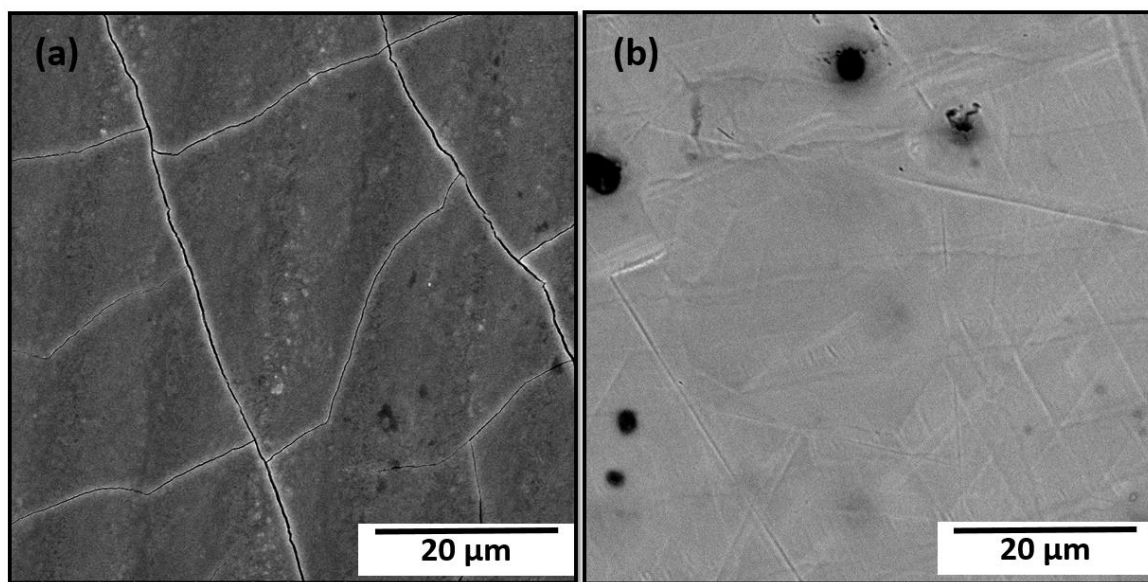


Figure 5. 1 Microstructure of (a) cracked Ti64 and (b) uncracked SS.

5.3.3 Nisin

Two types of nisin were employed for this work. The first was an unpurified “2.5% nisin A” stabilized in NaCl and denatured milk solids (henceforth 2.5% nisin, from Sigma-Aldrich, USA, available as a lyophilized powder). The second was “ultrapure nisin Z” (henceforth Nisin ZP, from Handary SA, Belgium). Each was used separately to prepare a solution of 1 mg/mL in sterile deionized water. This solution was spread on the fabricated oxide coatings and then the sample was placed in a vacuum chamber for 10 min to infuse the nisin solution into the cracks. After this treatment, release, durability and antibacterial tests were performed on the samples.

5.3.4 Release test

The samples with oxide coatings were immersed in 4 ml of HCl 0.01M at room temperature (release solution) with the purpose to observe how much nisin was liberated from the surface with time. Nisin concentration was quantified in release solutions at different time intervals. This concentration of nisin diffused in the release solution was determined through the bicinchoninic acid assay (BCA) using a BCA kit from G-Biosciences (St. Louis, MO). Bovine serum albumin was used as a standard. A volume of 0.3 mL was taken at each time interval and placed into refrigeration at 4°C. Once all samples were collected, a volume of 0.1 mL (taken from the 0.3 mL previously sampled) at each time interval was vigorously mixed with 1 mL of the BCA kit's working reagent. For this assay, the reagent color is green and turns purple when reacting with the peptide. The more purple the coloration, the higher the nisin concentration. Absorbance was measured at 562 nm, no more than 10 min after mixing the working reagent with the 0.1 mL of release solution, in a SpectraMax 384 Plus UV/vis spectrophotometer [216].

5.3.5 Durability test

Oxide coatings were analyzed on a Perkin Elmer Spectrum 100 spectrophotometer using the attenuated total reflection (ATR) technique, with the purpose to characterize the oxide layers before and after being coated with the nisin solution, and also trying to assess what sort of changes the treated oxide layer undergo when it is scrubbed using a commercial sponge. This sponge, prior to use, was washed to remove all traces of preservatives or other chemicals that may have an undesired effect when running spectra. The sponge was placed into a bag with 100 ml distilled water and 2 ml washing-up liquid ($\text{Na}_2\text{CO}_3 + \text{Na}_2\text{SO}_4$, no phosphate), and the bag contents were mixed for 60 s. The sponge was removed from the bag, rinsed thoroughly with cold water and squeezed to remove excess liquid, then dried [217]. During the test, the sponge was slightly wet and doing scrubs on the oxide (1 scrub = 1 movement back and forth on the surface). The aim of this test is to evaluate how well anchored is nisin to the surface and try to elucidate if nisin might remain in the cracks after scrubbing (simulating a washing process).

5.3.6 Antibacterial tests

The antibacterial assays were carried out against *L. monocytogenes*, bacterium responsible for listeriosis [169]. According to the Center for Disease Control and Prevention's (CDC) estimations, the annual incidence of death caused by listeriosis is about eight times greater than that caused by *Escherichia coli* O157:H7 [202]. Metallic oxide coupons were cleaned using an ultrasonic bath for 20 min, followed by cleaning with isopropyl alcohol. The antibacterial activity was measured by comparing the survival of bacteria on the nisin-coated coupons versus their survival on the uncoated ones [206]. All coupons, coated and uncoated, were immersed in 10 ml of Brain Heart Infusion (BHI; Bacto™, Sparks, MD) broth containing 100 µl of an overnight culture of *L. monocytogenes* (1×10^7 CFU/mL) and placed into an orbital incubator shaker

(instrument reference) at 37°C and 120 rpm for 48 hours, with the purpose to reach the threshold cell density required to induce the quorum sensing chemical signaling responsible of biofilm-phenotype expression, leading to adhesion to the surface and further formation of a biofilm on the oxide. After incubation with bacteria, the coupons were removed from the broth and washed with sterile deionized water in order to remove the unbounded or weakly attached bacteria to the surface [209]. The biofilm-covered side of each coupon was scraped with a sterile wooden stick for approximately 20 s [206]. This wooden stick was then immersed in a phosphate buffer to disperse the bacteria collected from each sample (stock bacterial solution). Following the standard method for bacteria enumeration, a whole set of 7 serial dilutions, 1:10 was prepared from the stock solution, in order to quantify the bacteria concentration recovered from the biofilm formed on the surface. 100 µl from each dilution were inoculated on Oxford agar base (Difco) supplemented with modified Oxford antimicrobial supplement (Difco) plates, and incubated at 37°C for 48 hours.

5.4 Results and discussion

5.4.1 Determining the release of physisorbed nisin from oxidized metal surfaces

5.4.1.1 Ti64

Two Ti64 coupons (one irradiated at a scan speed of 90 mm/s and the other at 300 mm/s) coated with 2.5% nisin were immersed separately into 10 mL of deionized water, showing no nisin release even after 21 days of continuous immersion (no purple coloration, no UV absorbance). The same process was repeated but coating with Nisin ZP, obtaining the same results. In consequence, a third test was performed using Nisin ZP but also increasing the water temperature to 50°C (with the purpose to accelerate any diffusive processes) for 24 hours and, again, no nisin release was detected. However, it is important to note that the BCA test was also used in the remaining

immersion solution (the release solution that was not sampled) and, again, no color change is detected. So, if no peptide is present in the sampled release solutions at different times nor in the remaining release solution, this suggests that nisin is still anchored to the metallic oxide or bound within the cracked surfaces.

5.4.1.2 SS

The results for SS were quite different when using nisin ZP. Even at room temperature, purple coloration could be seen at naked eye after 3 days (Fig. 5.2a). This figure proves that nisin release is not immediate, but a time-dependent process. The nisin concentration is still increasing even after 3 weeks of immersion. The relationship between time and cumulative nisin concentration is clearly linear as shown in Fig. 5.2b.

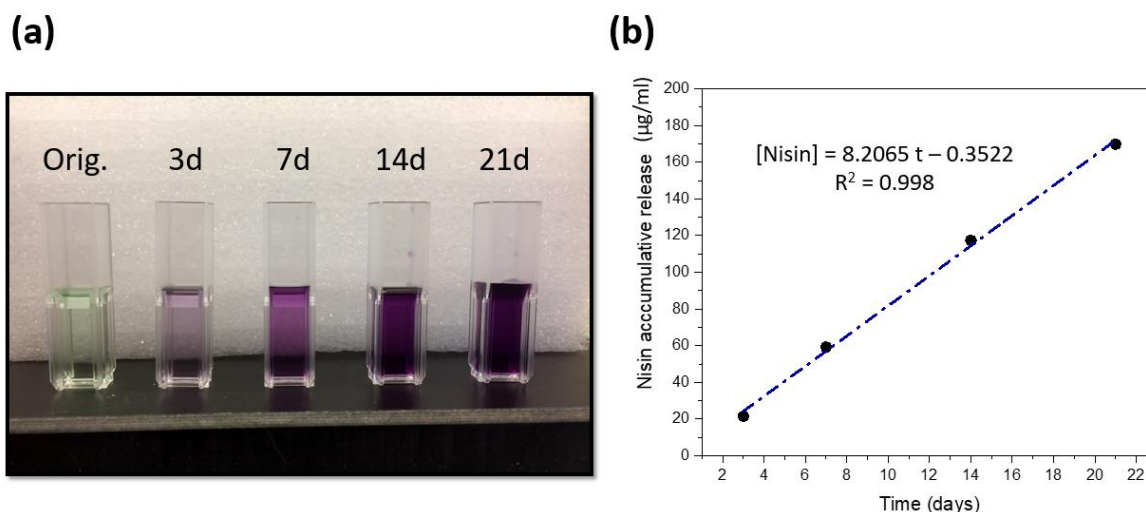


Figure 5. 2 Nisin release from SS uncracked oxide layer. (a) Colorimetric test showing the color variation in samples taken at different times (in days), (b) Linear relationship between time and nisin concentration estimated from absorbance values.

5.4.2 Detection of nisin on the surface of oxidized metals after mechanical scrubbing.

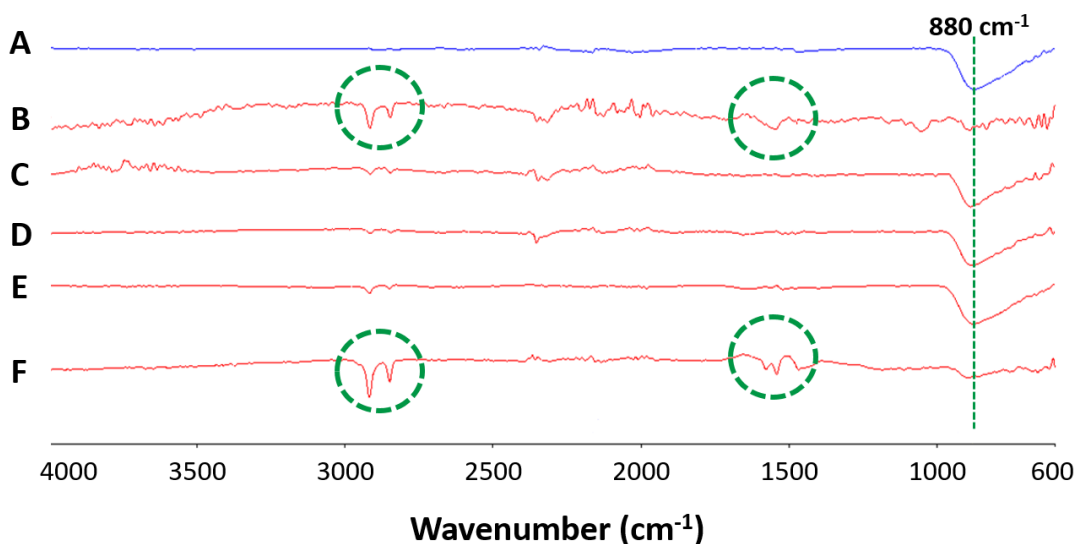


Figure 5. 3 FTIR spectra for Ti64 oxide layer: A = pristine oxide layer, B = nisin ZP coated, C = after 1 scrub movement, D = after 2 scrubs, E = after 3 scrubs, F = after multiple scrubs. The infrared bands observed when coating with nisin reappear after multiple scrubbing, indicating that there is still nisin on the surface, likely coming out of the cracks.

Fig. 5.3 shows the FTIR spectra of a typical Ti64 oxide (in this case one irradiated at 90 mm/s) at different stages of analysis. Spectrum A corresponds to the pristine Ti64 oxide; the broad band at 880 cm^{-1} is attributed to the Ti-O stretching. Spectrum B corresponds to the oxide surface after infusing the nisin ZP solution; it is important to notice the two narrow bands in the $2800 - 2900\text{ cm}^{-1}$ range, which correspond to the C-H symmetric and asymmetric stretchings, while the band at 1580 cm^{-1} is due to the presence of amine groups in the peptide, and the band at 880 cm^{-1} now is hidden. These features confirm the presence of nisin on the surface and suggest the coating is thick enough to suppress the signal from the underlying Ti64 oxide.

Spectra C, D and E correspond to the application of 1, 2 and 3 scrubs on the surface, respectively. As can be seen, the C-H stretching and the amine bands now have a weak signal,

while the Ti-O band reappears at 880 cm^{-1} . This suggests that nisin from the surface is being removed by scrubbing with the sponge and for this reason the titanium oxide is visible again.

However, spectrum F, measured after doing more than 20 consecutive scrubs on the surface, resembles spectrum B. The C-H stretchings and the amine bands re-appear at the same positions and, at the same time, the Ti-O band is practically hidden. This is an indication that nisin is still present. While the first three scrubbing motions removed some nisin from the surface, there is clearly more nisin present which re-appears on the surface with continued exposure to cleaning. It appears the mechanical impact of the sponge, in conjunction with water, is causing some wear of the surface. Concurrently, it is very possible that nisin is coming out of the microcracks, and is spread on the surface by the same sponge. The disappearance of the Ti-O band indicates the oxide surface is covered, but yet optically the color related to the oxide is still present, suggesting the coating is thin and optically transparent.

5.4.3 The antibacterial performance of nisin-coated oxidized metals

5.4.3.1 Tests using 2.5% nisin

First, as a negative control, the growth of bacteria on the oxidized metals with no applied nisin was assessed. The Ti64 oxide layer showed growth of nine CFU for the 10^{-1} dilution, and the SS showed growth of two CFU at the 10^{-1} dilution (Fig. 5.4a and 5.4c). Conventionally, only spread plates with colony counts in the range 30 – 300 CFU are used because high colony counts might prevent accurate counting, while low colony counts might lead to high variability (as observed here) [218], however in this work both materials displayed considerably less than 30 CFU which suggest that Ti64 and SS oxide layers (created by PLI) exhibit some degree of antibacterial activity by themselves, even before being treated with the nisin solution.

In the case of the oxide layers coated with nisin, for both metals there was no bacterial growth in any of the dilutions, likely due to the presence of nisin (Fig. 5.4b and 5.4d). There is no certainty if nisin is deposited on the surface, into the cracks or on both locations but, independently of the location, nisin is effective conferring antibacterial properties to both oxide layers.

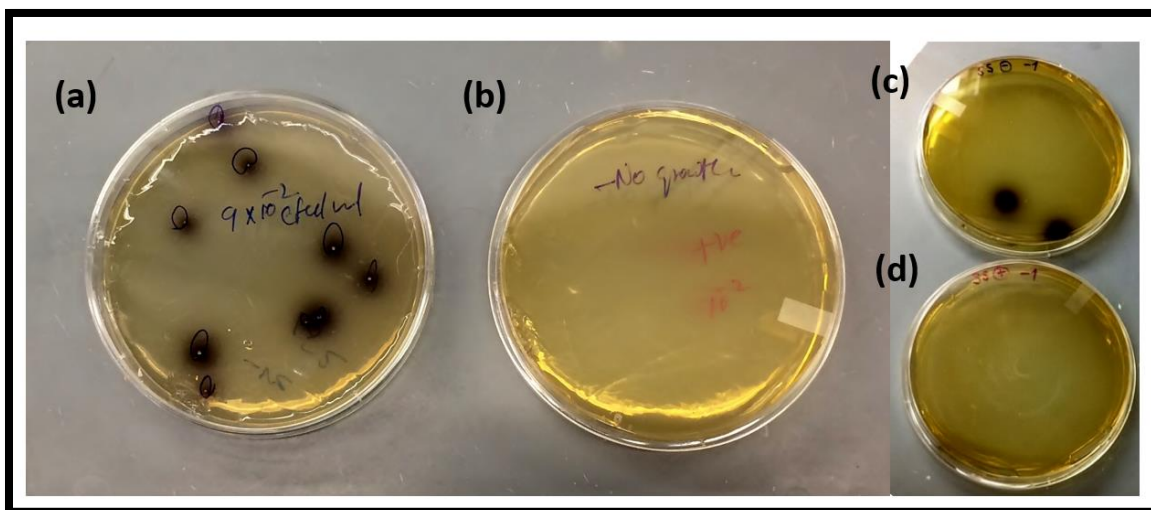


Figure 5. 4 Antibacterial tests performed on (a) uncoated Ti64 oxide layer, (b) nisin-coated Ti64 oxide layer, (c) uncoated SS oxide layer, (d) nisin-coated SS oxide layer.

Our hypothesis is that oxidized samples with cracks will provide a “storage” facility for AMPs, and therefore Ti64 oxide was subjected to treatment with the nisin solution followed by sponge scrubbing. After mechanically scrubbing the Ti64 surface and subsequently exposing the system to bacteria, no bacterial growth was displayed on any of the dilutions. Assuming that the sponge removed nisin partially or totally from the metallic surface, this suggests that the antibacterial activity after scrubbing is likely coming from nisin infused into the microcracks on Ti64 oxide layer (Fig. 5.5).

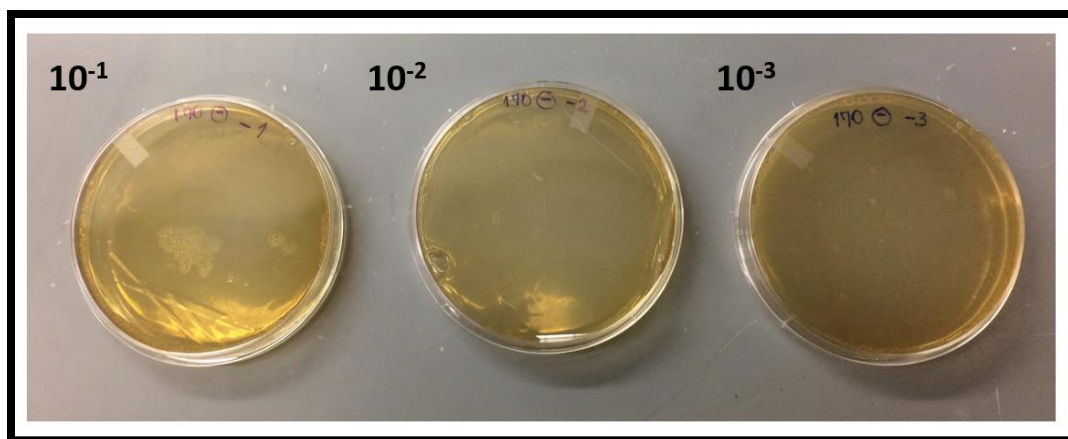


Figure 5. 5 Antibacterial test on nisin-coated Ti64 oxide layer scrubbed using a wet sponge.

5.4.3.2 Test using nisin ZP

As immersion in water during rinsing is a common process in food processing, the amount of nisin retained after immersion in water was examined. To accelerate any diffusive processes, the experiments for release of nisin from Ti64 were carried out at 50°C for 24 hours. Few CFU (only 1 to 2 colonies) grew on the 10^{-1} and 10^{-2} dilutions. Therefore, this immersed nisin-coated sample (Fig. 5.6, up) appeared to provide less antimicrobial benefit compared to the non-immersed sample (Fig. 5.4c), but more benefit compared to the uncoated one (Fig. 5.4a). This could lead to two possibilities: (1) That some nisin was released from the surface and bacteria can attach to those areas not covered by nisin, or (2) That nisin was not released from the surface but the rise of temperature affects to some extent the nisin activity against bacteria. To quantify this we carried out a release test described in the next section.

In the case of SS, as previously mentioned, there was no need to increase temperature since the nisin release was straightforward. After 21 days of immersion in water, the antibacterial test was performed. Few CFU (only 5 – 6 colonies) grew on the 10^{-1} dilutions and only 1 CFU on the

10^{-2} dilutions (Fig. 5.6, down). This means that nisin has been released from the uncracked surface to the release solution, and bacteria were able to attach to those nisin-free regions on the SS surface.

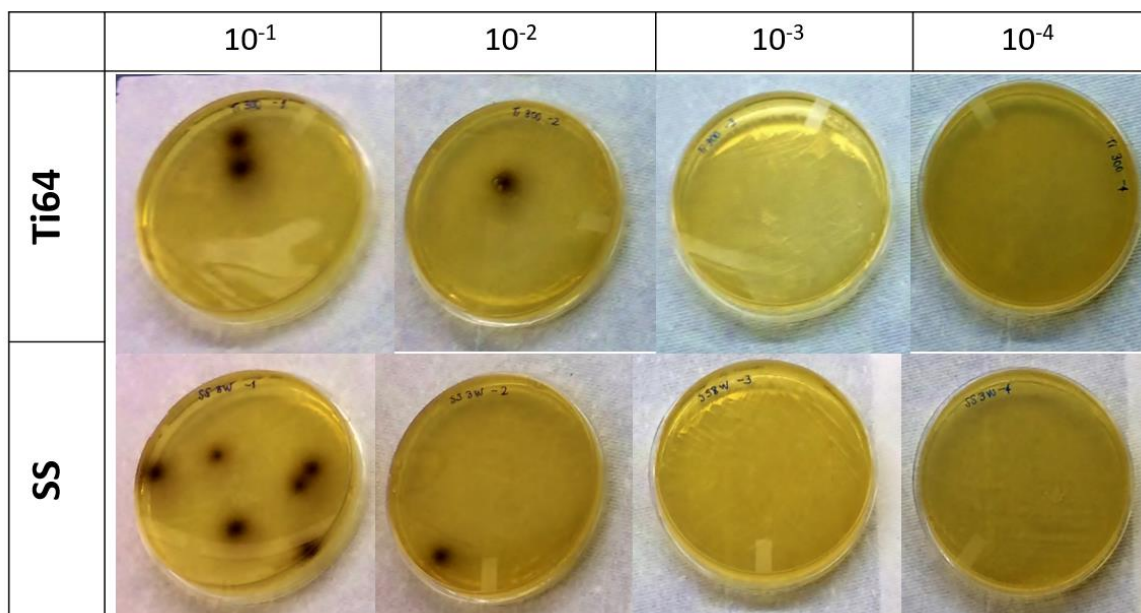


Figure 5. 6 Antibacterial tests performed on nisin-coated Ti64 cracked oxide layer after being immersed in water at 50°C for 24 hours (up), and on nisin-coated SS uncracked oxide layer after being immersed in water at room temperature for 21 consecutive days (down).

5.5 Conclusions

The antimicrobial peptide nisin, when physisorbed onto oxide surfaces grown on Ti-6Al-4V and 304L stainless steel using pulsed laser deposition, displays bactericidal properties. Nisin is effective against *L. monocytogenes* when applied on both materials, and the antibacterial property remains intact even after scrubbing using a sponge, and prevails to a good extent when the material is immersed in water for extended periods of time. These two structures, the stainless steel with a smooth oxide surface and the titanium alloy with microscopic surface cracks, define two extremes of structures for physisorption conditions.

Release tests showed that nisin slowly desorbs from the smooth, uncracked stainless steel surface upon immersion into water, and this desorption process occurs over more than 21 days at room temperature. In the case of the surface cracked titanium alloy, no nisin release was detected even rising temperature to promote the desorption, which we attribute to a good affinity between the peptide nanoparticles and the modified surface and crack walls.

Durability tests on the cracked titanium alloy surface show that nisin is covering the oxide layer, and the characteristic infrared bands for the peptide initially are removed, and then reappear when the surface is scrubbed multiple times, indicating that while mechanical cleaning may remove nisin from the surface of an oxidized metal, the nisin present with the surface cracks can be released over time to re-coat the surface with nisin, providing continued antimicrobial properties to the metal surface. These oxidized structures demonstrate that physisorption of peptides is a viable method to create antibacterial metallic surfaces that could be used in the manufacture of food contact surfaces or other environments where bacteria are present on metal surfaces.

6. APPLICATION OF AN OXIDIZED STAINLESS STEEL SURFACE AS A MEDIUM TO STORE BIOCHEMICAL AGENTS WITH ANTIMICROBIAL PROPERTIES

6.1 Abstract

The aim of this work is to analyze the release kinetics of nisin nanoparticles (an antimicrobial peptide) from cracked and uncracked oxide metallic films, with the purpose to evaluate the viability to develop an antibacterial metallic surface. The material chosen for this work is 304L stainless steel, given its wide usage in the food industry. It has been found that for the uncracked oxide film, the desorption of the peptide is mostly promoted by acidic pH, slowing down at neutral and stopping at basic pH. Rise in temperature contributes to accelerate the desorption process only when pH is acidic. At room temperature and pH 6, there is a linear relationship between the nisin release and time, and this relationship is still linear but faster (higher slope) when the conditions are changed to 50°C and pH 2. On the other hand, for the cracked oxide film, when submitted to 50°C and pH 2, the surface underwent corrosion and, consequently, nisin was liberated into solution, proving that nisin was effectively immobilized into the cracks.

6.2 Introduction

Infectious diseases result from pathogenic microbes (bacteria, fungi, parasites, etc.) and kill more people worldwide than any other single cause [219]. Microbial growth needs to be controlled, especially in the medical and food industries. Operating rooms require a sterile environment because they are filled with the largest number of potentially infectious objects: instruments, the back table, the surgical table, anesthesia equipment, drapes, etc. [220]. In the food industry, raw vegetables [221], dairy products [222] or meat [223] could get contaminated when they are in contact with cutting tables, knives [224], slicers [135], conveyor belts [225], carts to

transport food, etc., reason why all these surfaces need to be cleaned and sanitized often to avoid food contamination.

Despite all cleaning procedures, an estimated 722,000 nosocomial (hospital-acquired) infections occurred only in USA in 2011, resulting in nearly 75,000 deaths [220]. Concerning food, several outbreaks have happened in the last years in food like cantaloupes, ice cream, frozen vegetables and raw milk cheese [226]. It is clear that sterilization and cleaning/sanitation routines are not being effective enough for microbial control.

Antimicrobial agents are used to kill bacteria and other microorganisms. There is extensive research trying to create really effective antimicrobial coatings that preclude microbial attachment to material surfaces or that kill microorganisms as soon as they make contact with the surface (biocidal property). Different antimicrobial agents have been used with this purpose: metallic nanoparticles, N-halamines, quaternary ammonium compounds, essential oils, and also antimicrobial peptides (AMPs).

AMPs have attracted attention as antimicrobial agents due to its natural origin, broad antimicrobial spectrum and for its activity even at very low concentrations. More than 3,000 antimicrobial peptides have been discovered but only one of them, nisin, is legally approved in more than 50 countries to be used as preservative in the food industry [113].

Nisin is a bacteriocin effective against several pathogenic Gram-positive bacteria such as *Listeria monocytogenes* and *Clostridium botulinum*, and it has been demonstrated that when combined with chelators such as ethylenediaminetetraacetic acid (EDTA), heat treatment or freezing, it can also be effective against Gram-negative bacteria such as *Escherichia coli* and *Salmonella spp.* [227].

It exists a special interest in trying to immobilize antimicrobial peptides such as nisin on food contact surfaces to confer antibacterial properties to the surface material. Many works have been done on polymers, trying to create antimicrobial packaging films [228], but some studies have also been done on metals. One of the big challenges to create such coatings is to ensure stability, meaning that the AMP must physically remain active in the film/coating for as long as possible, independently of the environmental conditions the contact surface has to undergo. For this reason, the vast majority of the works make use of plasma techniques and covalently-bonded chemicals to immobilize the AMP.

Lee et al. [229] determined that the migration of nisin from a coated paper stopped after eight days, and the maximum equilibrium concentration of nisin released into solution was in the range of 222 – 241 $\mu\text{g/ml}$. This concentration corresponding to 8.6 – 9.3% of the total nisin content incorporated in the coating layer.

Rossi et al. [230] found that nisin release from whey protein isolate edible films was favored at lower pH and low film thickness, because in thinner films nisin needs to travel a shorter distance to reach the aqueous solution. At pH 7 there was only a small release of nisin because the antimicrobial is below its isoelectric point (pI close to 10), bearing a positive charge, which may interact with the negative whey protein charges (pI 4.2-5.3) in the film. At pH 4, nisin shows an electrostatic repulsion with film proteins, because both molecules have a net positive charge, which favors nisin release to aqueous solution.

Chacko et al. [127] measured the nisin release from a corn zein membrane using high-performance liquid chromatography and determined that the release decreased as the concentration of corn zein increased.

Bastarrachea et al. [216] studied the release kinetics of nisin from biodegradable poly(butylene adipate-co-terephthalate) (PBAT) films into water at different temperatures, finding that the concentration of nisin in solution at equilibrium was higher as the temperature increased, and that the diffusion rates from PBAT were higher if comparing with other materials used in food packaging.

To the extent of our knowledge, there is no work employing a pulsed laser to modify the substrate surface and then using it to “store” an AMP. Thin film fractures have been systematically investigated as a method to generate micro- and nano-scale structures by subjecting them to high residual stresses during the fabrication process [209]. By using the appropriate parameters, lasers are able to create such high residual stresses building features at micro- and nano-scale that can be used to “store” antimicrobial agents or other compounds.

The present work aims to demonstrate that nisin can be physically adsorbed and stored in artificially created cracks on 304L stainless steel, as well as doing an analysis of the release kinetics of nisin from those cracks.

6.3 Experimental

Stainless steel. Two austenitic 304L stainless steel (henceforth SS) coupons (12.5 x 12.5 x 3.4 mm) were irradiated using an Er-doped, glass-fiber laser ($\lambda = 1.54 \mu\text{m}$) with the conditions described in [91]. One of these coupons was irradiated (6 x 6 mm area) at high scan speed (500 mm/s); the second coupon was irradiated (6 x 6 mm area) using varied scan speeds (10, 50, 90 and 130 mm/s). Colored oxide layers appeared as a result of the laser irradiation and these layers are perfectly visible at naked eye; however, scanning electron micrographs were used to confirm that the first coupon (irradiated at 500 mm/s) did not develop cracks, while the second (irradiated at lower scan speeds) developed cracks randomly distributed all over the surface (see Fig. 6.1).

Henceforth the coupons will be named U-SS (for uncracked stainless steel) and C-SS (for cracked stainless steel). The color of the oxide layer is related to the film thickness, which depends on the employed laser scan rate; in this case, goldish color for U-SS, and brown, greenish and pink for C-SS. According to Lawrence [231], these oxide layers are mechanically robust.

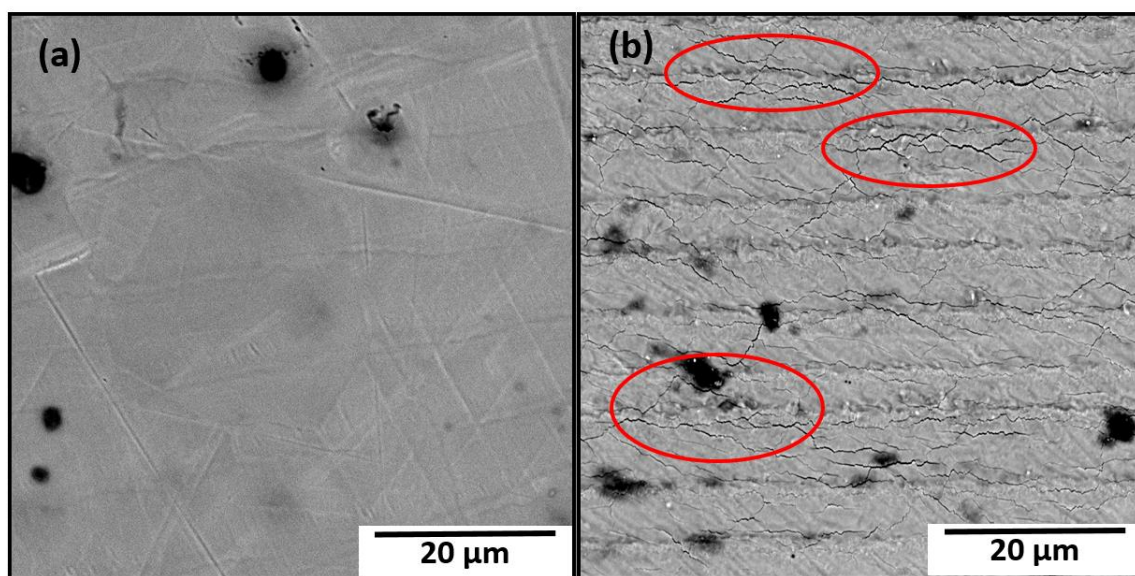


Figure 6. 1 Microstructures corresponding to: (a) U-SS, in which only some scratches and polishing lines are observed on the surface, and (b) C-SS, in which cracks may be observed all over the surface and the areas with more cracks are marked in ovals.

Nisin. Ultrapure nisin Z (Handary SA, Belgium) was used to prepare a solution of 1.0 mg/ml in sterile deionized water. This solution was spread on the fabricated oxide coatings, using vacuum for 10 min with the purpose to infuse the nisin solution, aiming to immobilize the peptide on the surface of U-SS or into the cracks of C-SS. After vacuum treatment, both coupons were immersed for 10 seconds in 3 mL of sterile deionized water with the purpose to remove the “coffee stain” left on the coating after the application of vacuum.

Release tests. Three different release solutions were prepared: One of deionized water ($\text{pH} \approx 6$), one of HCl 0.01M ($\text{pH} \approx 2$) and one of NaOH 0.01M ($\text{pH} \approx 10$). Temperature was varied at two

levels: room temperature (RT) and 50°C, by using a mini-dry bath (Benchmark). Experiments were performed immersing each coupon in 4 mL of release solution and sampling at different intervals of time. A bicinchoninic acid (BCA) kit from G-Biosciences (St. Louis, MO) was used as colorimetric method to determine the amount of nisin released into solution with time. Bovine serum albumin was used as a standard to create a calibration curve, and the regression line for this curve was expressed as following:

$$Y = 0.0017 X + 0.0204 (R^2 = 0.9952) \quad (Eq.6.1)$$

where X ($\mu\text{g/mL}$) is the concentration of nisin, and Y is the absorbance.

A volume of 0.3 mL of release solution was taken at each time interval and placed into refrigeration at 4°C. Once all samples were collected, a volume of 0.1 mL (taken from the 0.3 mL previously sampled) at each time interval was vigorously mixed with 1 mL of the BCA kit's working reagent. For this assay, the reagent is color green and turns into purple when in contact with the peptide. The more purple coloration, the higher the nisin concentration. Absorbance was measured at 562 nm, no more than 10 min after mixing the working reagent with the 0.1 mL of release solution, in a SpectraMax 384 Plus UV/vis spectrophotometer (Materials Science and Engineering, Purdue University, USA) [232], and getting the nisin concentrations based on Eq.(1). All experiments were made by duplicate.

The accumulative release percentage of nisin from the oxide films was calculated using the following equation [233, 234]:

$$\text{Accumulative release (\%)} = \frac{M_t}{M_0} \times 100 \quad (Eq. 6.2)$$

where M_t (μg) is the released nisin at time t , M_0 (μg) is the estimation of the total trapped or entrapped nisin in the oxide layer (surface for U-SS and including into the cracks for C-SS).

6.4 Results and discussion

Release tests were performed by changing temperature and pH of the solution. A summary of the eight tests done can be seen in Fig. 6.2.

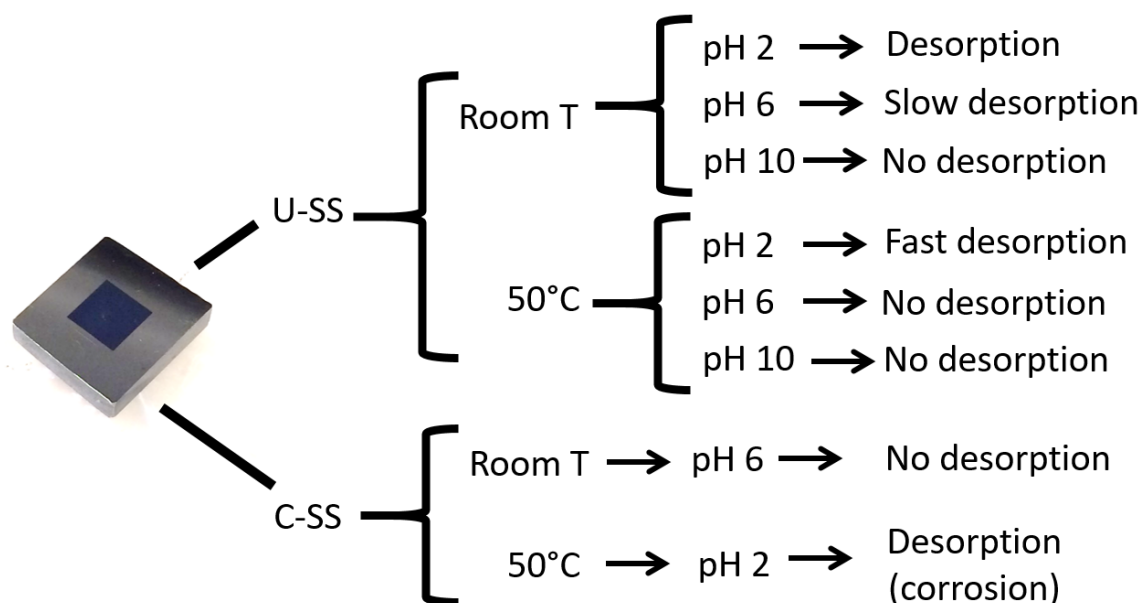


Figure 6. 2 Summary of the tests performed on the stainless steel coupons, changing temperature and pH. It can be seen that nisin release is mainly driven by pH, while rise in temperature only accelerates the reaction. Interesting to notice that slow release was obtained when U-SS was tested at room temperature and pH 6, while there was no release at all when C-SS was submitted to the same conditions; this means that for U-SS there was a slow detachment of nisin nanoparticles from the surface, while for C-SS nisin is immobilized inside the cracks, taking much longer times to travel until the aqueous solution.

U-SS at room temperature and pH 6: The first sample of release solution was taken after 3 days of immersion and the change to purple color was evident even at naked eye. This test was run for 21 consecutive days. The relationship between time and accumulative nisin concentration is linear for this period of time (see Fig. 6.3), and desorption process was still going on even after three weeks.

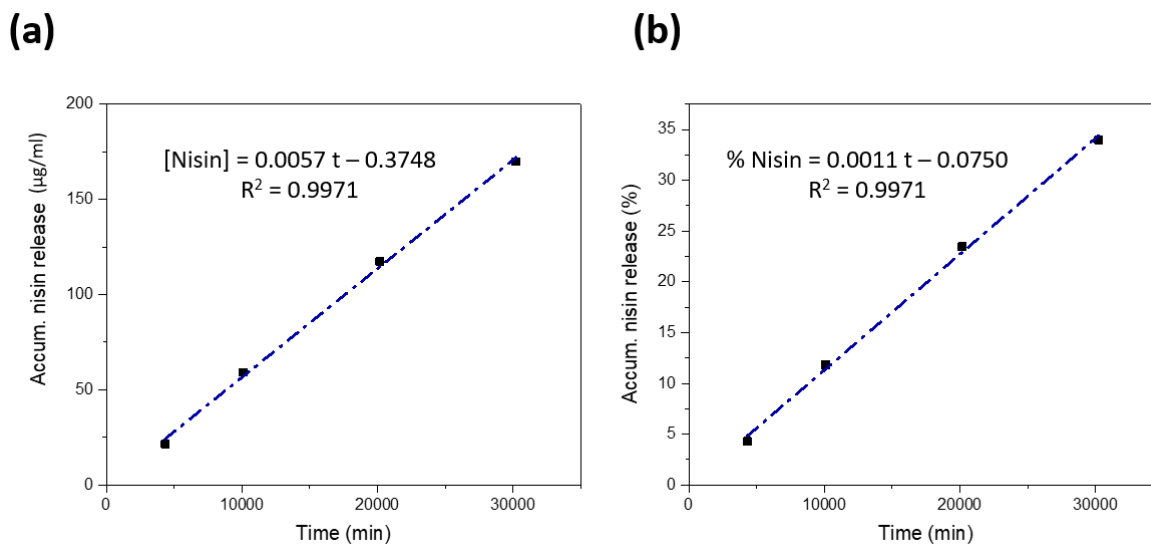


Figure 6. 3 U-SS at room temperature and pH 6. (a) Linear relationship between time and the accumulative nisin release, but even after 21 days there is still desorption; (b) According to calculations, only 34% of the total nisin retained by the oxide film has been released after 21 days, meaning that, if the linear behavior is maintained, all nisin would be released after 63 days of immersion under these conditions.

U-SS at room temperature and pH 10: After 21 consecutive days of immersion, there was no apparent nisin release. This is likely due to the fact that nisin solubility is very low at basic pH, on the order of 0.25 mg/mL at pH 8.5 [120].

U-SS at 50°C and pH 2: Rise in temperature and decrease in pH definitely contributed to accelerate the desorption process from the oxide film. The relationship is still linear and, according to calculations, all the nisin retained on the oxide surface was released in less than 24 hours. According to this result, it is estimated that the total release of nisin under these conditions took approximately 14 hours (Fig. 6.4b). The slope in Fig. 6.4b is two orders of magnitude higher than that in Fig. 6.3b, meaning that by changing conditions to higher temperature and lower pH, the reaction occurs approximately 100 times faster.

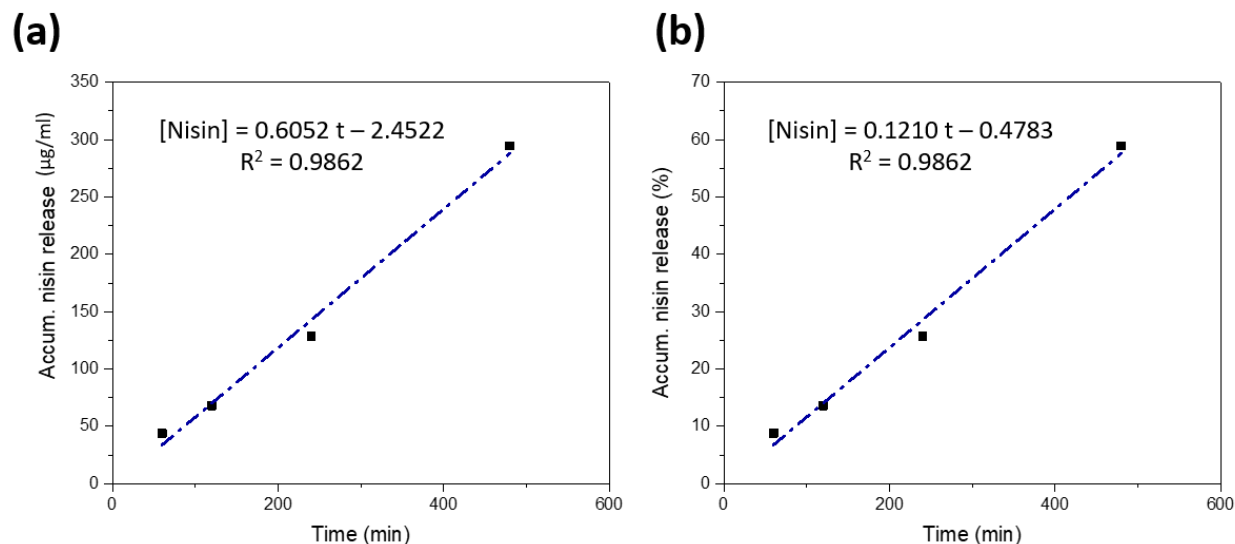


Figure 6. 4 U-SS at 50°C and pH 2. (a) Linear relationship between time and the accumulative nisin release; (b) According to calculations, it would take approximately 14 hours to release all the nisin retained on the oxide layer.

C-SS at room temperature and pH 6: This test was run for 18 consecutive days. There was no nisin desorption in this period of time. When concluding this test, the C-SS coupon was immediately passed to the solution at 50°C and pH 2.

C-SS at 50°C and pH 2: It was planned to take the first sample after 24 hours of immersion. However, the oxide film corroded (Fig. 6.5) by spalling and the test was stopped. Nevertheless, the corrosion helped to demonstrate that nisin was effectively contained into the cracks. When the BCA reagent entered in contact with the release solution, the color instantaneously changed to dark purple (Fig. 6.6).

The tests made using the C-SS coupon prove that physisorption using vacuum is a good method to infuse nisin into cracks as long as the oxide layer is maintained at conditions close to room temperature and pH 6. There is a very good anchor between the nisin nanoparticles and the surface and crack walls that precludes the nisin desorption. Nonetheless, when the conditions turn

harsh (50°C and pH 2), then nisin desorption is promoted and all the peptide comes out of the cracks.

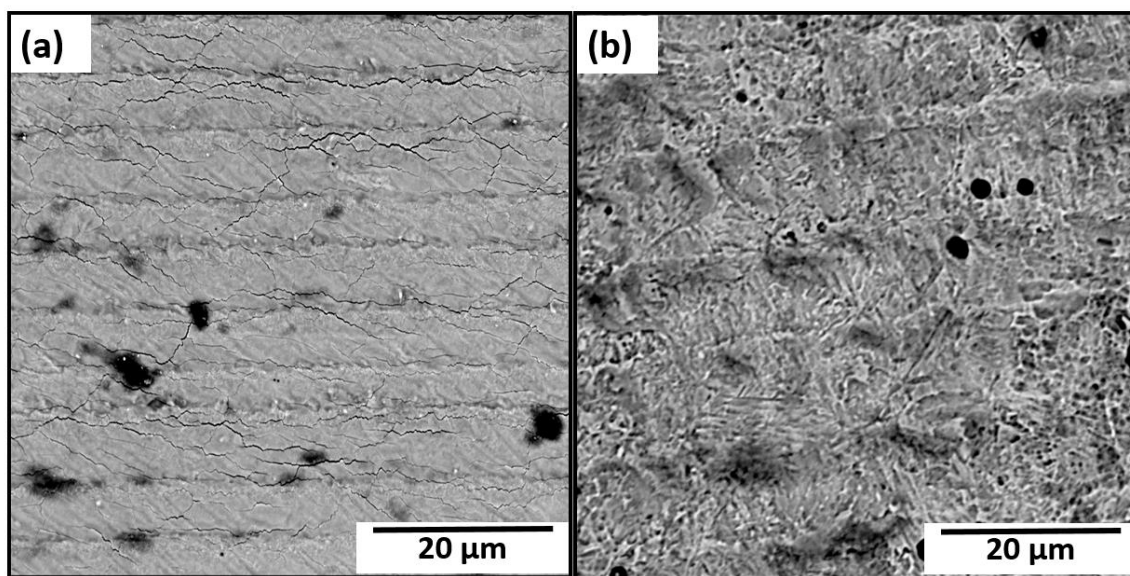


Figure 6. 5 Microstructures corresponding to: (a) C-SS before nisin coating, and (b) C-SS after nisin coating and immersion into solution at 50°C and pH 2, corroded surface, cracks are not there anymore.



Figure 6. 6 Test for C-SS immersed at 50°C and pH 2. (a) BCA reagent is originally green in color, (b) when in contact with the release solution, a purple-colored complex is formed.

Conclusions

Nisin desorption from 304L stainless steel surface is mainly promoted by change in pH. Acidic pH encourage nisin desorption, while neutral and basic pH slow down the diffusion or even stop it. Rise in temperature, when combined with low pH, accelerates the desorption process, but does not seem to be a contributing factor by itself.

Tests made on the cracked stainless steel surface were the real proof that nisin is effectively immobilized into the cracks. This cracked surface did not liberate any nisin even when maintained immersed in water at room T and pH 6 for 18 days, however, as soon as it was submitted to 50°C and pH 2, the oxide layer underwent corrosion and all nisin was effectively released.

In summary, nisin can be effectively “stored” inside artificial cracks created by a nanosecond pulsed laser. Rise in temperature does not significantly affect the nisin immobilization, but low pH encourages the nisin desorption.

CONCLUDING REMARKS AND FUTURE WORK

Although physical adsorption is considered a weak method to try to immobilize an antimicrobial agent on a surface, in the present work, for the first time, it was successfully demonstrated that an antimicrobial peptide can be stored inside artificially created cracks by a pulsed laser on the oxide surface of Ti-6Al-4V and 304L stainless steel. The peptide nanoparticles show such affinity that they may remain attached to the crack walls for more than two weeks as long as pH is kept close to neutral or alkaline.

The biggest challenge in this work was trying to demonstrate that nisin is effectively stored into the interconnected network of cracks of the titanium alloy. Once the Ti-6Al-4V specimen was coated with nisin, even by changing parameters such as concentration, pH and temperature, there was no nisin release from the oxide layer whatsoever. This could lead to two hypotheses; first – and most unlikely – that for some unexpected mechanism the nisin molecule is denatured and, in consequence, it cannot be detected anymore during the colorimetric test, or second, that there is an excellent anchor between nisin nanoparticles and the crack walls of the oxide layer of the titanium alloy. Further investigation would help to determine the real mechanism involved, probably by applying techniques such as glow-discharge optical emission spectroscopy or X-ray photoelectron spectroscopy. If the second possibility is confirmed, this could open the door to new possibilities in which nanoparticles of other natural antimicrobial agents with broader spectrum of action could be practically immobilized on the surface and confer antibacterial properties to materials, hopefully for the entire life of a contact surface.

As stated in other research works, the adoption of antimicrobial nanomaterials – such as silver nanoparticles – in the food industry has been limited due to the unknown implications on human health and on the environment. If it could be demonstrated that nisin remains attached to

the cracked oxide Ti-6Al-4V surface and still imparting biocidal activity, this could represent a novel opportunity to use other antimicrobial agents infused into cracks of food contact surfaces, even if it is not allowed to use the same agents directly on the food matrix. Regulatory issues are the main obstacle for the adoption of new additives or antimicrobials in the food industry.

Given that biofilms represent a problem in different fields – not exclusive to the food industry – and on distinct material surfaces, the chances to explore are boundless. There are hundreds of antimicrobial agents currently under research, and bioengineers are creating even more by modifying the existent ones. This, in combination with the different immobilization techniques, the modifications that can be applied to the material surface, and the variety of target microorganisms, offers a plethora of possibilities for the design of a durable surface that deliver a reliable performance against biofilms without compromising human health or representing a risk to the environment.

It is worth to mention that, unfortunately, many research works only evaluate the antibacterial efficacy under ideal conditions, but a real food processing plant includes drastic changes in temperature, high abrasion, acidic and alkaline environments, reason why, even if costlier, research works closer to real conditions should be performed.

Biomedical applications are taking the leadership in the research and adoption of novel antimicrobial agents, and this is slowly contributing to open new horizons for the food industry as well. The imperative need to find new “natural” antibiotics together with an increasing market for preservatives like nisin seem to be good indicators that the adoption of this peptide on biomedical and/or food contact surfaces is not so distant in the future.

REFERENCES

- [1] H. Zhou, J. Fang, Y. Tian and X. Yang Lu, "Mechanisms of nisin resistance in Gram-positive bacteria," *Ann Microbiology*, vol. 64, pp. 413 - 420, 2014.
- [2] C. Bower, J. McGuire and M. Daeschel, "Influences on the antimicrobial activity of surface-adsorbed nisin," *Journal of Industrial Microbiology*, vol. 15, pp. 227-233, 1995.
- [3] J. Brooks and S. Flint, "Biofilms in the food industry: problems and potential solutions," *International Journal of Food Science and Technology*, vol. 43, pp. 2163-2176, 2008.
- [4] D. Xiao, "Novel delivery systems of nisin to enhance longterm efficacy against foodborne pathogen *Listeria monocytogenes*," *PhD dissertation, University of Tennessee*, 2010.
- [5] M. Najjar, D. Kashtanov and M. Chikindas, " ϵ -poly-L-lysine and nisin A act synergistically against Gram-positive food-borne pathogens *Bacillus cereus* and *Listeria monocytogenes*," *Letters in Applied Microbiology*, vol. 45, pp. 13-18, 2007.
- [6] L. Thomas and J. Delves-Broughton, "Nisin," in *Antimicrobials in Food, 3rd edition*, Taylor & Francis Group, 2005, pp. 237-274.
- [7] Z. Sun, P. Li, F. Liu, H. Bian, D. Wang, X. Wang, Y. Zou, C. Sun and W. Xu, "Synergistic antibacterial mechanism of the *Lactobacillus crispatus* surface layer protein and nisin on *Staphylococcus saprophyticus*," *Nature Scientific Reports*, vol. 7, no. 265, pp. 1-12, 2017.
- [8] E. Zottola and K. Sasahara, "Microbial biofilms in the food processing industry - Should they be a concern?," *International Journal of Food Microbiology*, vol. 23, pp. 125-148, 1994.
- [9] O. Seddiki, C. Harnagea, L. Levesque, D. Mantovani and F. Rosei, "Evidence of antibacterial activity on titanium surfaces through nanotextures," *Applied Surface Science*, vol. 308, pp. 275-284, 2014.
- [10] R. Helbig, D. Gunther, J. Friedrichs, F. Rossler, A. Lasagni and C. Werner, "The impact of structure dimensions on initial bacterial adhesion," *Biomaterials Science*, vol. 4, pp. 1074-1078, 2016.
- [11] M. Salta, J. Wharton, P. Stoodley, S. Dennington, L. Goodes, S. Werwinsky, U. Mart, R. Wood and K. Stokes, "Designing biomimetic antifouling surfaces," *Philosophical Transactions of the Royal Society A*, vol. 368, pp. 4729-4754, 2010.

- [12] D. Guenther, J. Valle, S. Burgui, C. Gil, C. Solano, A. Toledo-Arana, R. Helbig, C. Werner, I. Lasa and A. Lasagni, "Direct laser interference patterning for decreased bacterial attachment," in *Proceedings of SPIE Vol. 9736*, 2016.
- [13] A. Wong, "Biofilms in food processing environments," *Journal of Dairy Science*, vol. 81, pp. 2765-2770, 1998.
- [14] R. Kaur and S. Liu, "Antibacterial surface design - Contact kill," *Progress in Surface Science*, vol. 91, pp. 136-153, 2016.
- [15] C. Sengstock, M. Lopian, Y. Motemani, A. Borgmann, C. Khare, P. Buenconsejo, T. Schildhauer, A. Ludwig and M. Koller, "Structure-related antibacterial activity of a titanium nanostructured surface fabricated by glancing angle sputter deposition," *Nanotechnology*, vol. 25, no. 195101, pp. 1-11, 2014.
- [16] D. Duday, C. Vreuls, M. Moreno, G. Frache, N. Boscher, G. Zocchi, C. Archambeau, C. Van De Weerd, J. Martial and P. Choquet, "Atmospheric pressure plasma modified surfaces for immobilization of antimicrobial nisin peptides," *Surface & Coatings Technology*, vol. 218, pp. 152 - 161, 2013.
- [17] D. Selgas, M. Marin, C. Pin and C. Casas, "Attachment of bacteria to meat surfaces: A review," *Meat Science*, vol. 34, pp. 265-273, 1993.
- [18] J. Chen, "Chapter 7: Thin film coatings and the biological interface," in *Thin Film Coatings for Biomaterials and Biomedical Applications (edited by Prof. Hans Griesser)*, Woodhead Publishing Series in Biomaterials, 2016, pp. 143-164.
- [19] N. Thongyai, "Study of stainless steel surface cleanability," *Master Thesis, King Mongkut's Institute of Technology North Bangkok*, 2005.
- [20] M. Gimeno, P. Pinczowski, M. Perez, A. Giorrello, M. Martinez, J. Santamaria, M. Arruebo and L. Lujan, "A controlled antibiotic release system to prevent orthopedic-implant associated infections: An in vitro study," *European Journal of Pharmaceutics and Biopharmaceutics*, vol. 96, pp. 264-271, 2015.
- [21] N. Guerra, A. Araujo, A. Barrera, A. Torrado, C. Lopez, J. Carballo and L. Pastrana, "Antimicrobial activity of nisin adsorbed to surfaces commonly used in the food industry," *Journal of Food Protection*, vol. 68, no. 5, pp. 1012-1019, 2005.
- [22] T. Garrett, M. Bhakoo and Z. Zhang, "Bacterial adhesion and biofilms on surfaces," *Progress in Natural Science*, vol. 18, pp. 1049 - 1056, 2008.
- [23] C. G. Kumar and S. K. Anand, "Significance of microbial biofilms in food industry: A review," *International Journal of Food Microbiology*, vol. 42, pp. 9 - 27, 1998.

- [24] E. Faure, C. Vreuls, C. Falentin-Daudre, G. Zocchi, C. Van de Weerd, J. Martial, C. Jerome, A. Duwez and C. Detrembleur, "A green and bio-inspired process to afford durable anti-biofilm properties to stainless steel," *Biofouling*, vol. 28, no. 7, pp. 719 - 728, 2012.
- [25] G. Wirtanen and T. Mattila-Sandholm, "Removal of foodborne biofilms - comparison of surface and suspension tests. Part I," *Lebensmittel-Wissenschaft und -Technologie*, vol. 25, pp. 43-49, 1992.
- [26] J. Aveyard, J. Bradley, K. McKay, F. McBride, D. Donaghy, R. Raval and R. D'Sa, "Linker-free covalent immobilization of nisin using atmospheric pressure plasma induced grafting," *Journal of Materials Chemistry B*, vol. 5, pp. 2500-2510, 2017.
- [27] P. Gilbert, A. McBain and A. Rickard, "Formation of microbial biofilm in hygienic situations: a problem of control," *International Biodeterioration & Biodegradation*, vol. 51, pp. 245-248, 2003.
- [28] P. Stoodley, K. Sauer, D. Davies and W. Costerton, "Biofilms as complex differentiated communities," *Annual Review of Microbiology*, vol. 56, pp. 187-209, 2002.
- [29] A. Karimi, D. Karig, A. Kumar and A. Ardekani, "Interplay of physical mechanisms and biofilm processes: Review of microfluidic methods," *Lab Chip*, vol. 15, no. 1, pp. 23-42, 2015.
- [30] L. Li, "Prevention of biofilm formation on food contact surfaces by nanoscale plasma coatings," *Master Thesis, University of Missouri-Columbia*, 2016.
- [31] Q. Bao, N. Nishimura, H. Kamata, K. Furue, Y. Ono, M. Hosomi and A. Terada, "Antibacterial and anti-biofilm efficacy of fluoropolymer coating by a 2,3,5,6-tetrafluoro-phenylenedimethanol structure," *Colloids and Surfaces B: Biointerfaces*, vol. 151, pp. 363-371, 2017.
- [32] L. Bastarrachea and J. Goddard, "Development of antimicrobial stainless steel via surface modification with N-halamines: Characterization of surface chemistry and N-halamine chlorination," *Applied Polymer Science*, pp. 821 - 831, 2013.
- [33] M. Daeschel, J. McGuire and H. Al-Makhlafi, "Antimicrobial activity of nisin adsorbed hydrophilic and hydrophobic silicon surfaces," *Journal of Food Protection*, vol. 55, no. 9, pp. 731-735, 1992.
- [34] A. Hequet, V. Humblot, J. Berjeaud and C. Pradier, "Optimized grafting of antimicrobial peptides on stainless steel surface and biofilm resistance tests," *Colloids and Surface B: Biointerfaces*, vol. 84, pp. 301 - 309, 2011.

- [35] D. Alves and M. Pereira, "Mini-review: Antimicrobial peptides and enzymes as promising candidates to functionalize biomaterial surfaces," *Biofouling*, vol. 30, pp. 483-499, 2014.
- [36] A. Nikiforov, X. Deng, Q. Xiong, U. Cvelbar, N. DeGeyter, R. Morent and C. Leys, "Non-thermal plasma technology for the development of antimicrobial surfaces: a review," *Journal of Physics D: Applied Physics*, vol. 49, pp. 204002(1-8), 2016.
- [37] N. Sangcharoen, W. Klaypradit and P. Wilaipun, "Antimicrobial activity optimization of nisin, ascorbic acid and ethylenediamine tetraacetic acid disodium salt (EDTA) against *Salmonella* Enteritidis ATCC 13076 using response surface methodology," *Agriculture and Natural Resources*, vol. 51, pp. 355-364, 2017.
- [38] Q. Yu, Z. Wu and H. Chen, "Dual-function antibacterial surfaces for biomedical applications," *Acta Biomaterialia*, vol. 16, pp. 1-13, 2015.
- [39] M. Massa, C. Covarrubias, M. Bittner, I. Fuentevilla, P. Capetillo, A. Marttens and J. Carvajal, "Synthesis of new antibacterial composite coating for titanium based on highly ordered nanoporous silica and silver nanoparticles," *Materials Science and Engineering C*, vol. 45, pp. 146-153, 2014.
- [40] C. Zhao, B. Feng, Y. Li, J. Tan, X. Lu and J. Weng, "Preparation and antibacterial activity of titanium nanotubes loaded with Ag nanoparticles in the dark and under the UV light," *Applied Surface Science*, vol. 280, pp. 8-14, 2013.
- [41] M. Clark, "The search for antifoulant alternatives," *Sea Technology*, vol. October, pp. 37-40, 1987.
- [42] M. Gabriel, K. Nazmi, E. Veerman, A. Nieuw and A. Zentner, "Preparation of LL-37-grafted titanium surfaces with bactericidal activity," *Bioconjugate Chemistry*, vol. 17, pp. 548-550, 2006.
- [43] R. Kanchanapally, B. Viraka, S. Sekhar, F. Pedraza, S. Jones, A. Pramanik, S. Reddy, C. Tchounwou, Y. Shi, A. Vangara, D. Sardar and P. Chandra, "Antimicrobial peptide-conjugated graphene oxide membrane for efficient removal and effective killing of multiple drug resistant bacteria," *RSC Advances*, vol. 5, pp. 18881-18887, 2015.
- [44] S. Marshall and G. Arenas, "Antimicrobial peptides: A natural alternative to chemical antibiotics and a potential for applied biotechnology," *Electronic Journal of Biotechnology*, vol. 6, no. 2, pp. 271-284, 2003.
- [45] I. Chopra, "The increasing use of silver-based products as antimicrobial agents: a useful development or a cause of concern?," *Journal of Antimicrobial Chemotherapy*, vol. 59, no. 4, pp. 587-590, 2007.

- [46] P. Chairuangkitti, S. Lawanprasert, S. Roytrakul, S. Aueviriyavit, D. Phummiratch, K. Kulthong, P. Cganvorachote and R. Maniratanachote, "Silver nanoparticles induce toxicity in A549 cells via ROS-dependent and ROS-independent pathways," *Toxicology in Vitro*, vol. 27, pp. 330-338, 2013.
- [47] M. Das, N. Saxena and P. Dwivedi, "Emerging trends of nanoparticles application in food technology: safety paradigms," *Nanotoxicology*, vol. 3, pp. 10-18, 2009.
- [48] L. Bastarrachea, A. Denis-Rohr and J. Goddard, "Antimicrobial food equipment coatings: Applications and challenges," *Annual Review of Food Science and Technology*, vol. 6, pp. 97-118, 2015.
- [49] C. Vreuls, G. Zocchi, G. Garitte, C. Archambeau, J. Martial and C. Van de Weerd, "Biomolecules in multilayer film for antimicrobial and easy-cleaning stainless steel surface applications," *Biofouling*, vol. 26, no. 6, pp. 645-656, 2010.
- [50] R. Mauchauffe, M. Moreno, N. Boscher, C. Van De Weerd, A. Duwez and P. Choquet, "Robust bio-inspired antibacterial surfaces based on the covalent binding of peptides on functional atmospheric plasma thin films," *Journal of Materials Chemistry B*, vol. 2, pp. 5168-5177, 2014.
- [51] E. Faure, P. Lecomte, S. Lenoir, C. Vreuls, C. Van De Weerd, C. Archambeau, J. Martial, C. Jerome, A. Duwez and C. Detrembleur, "Sustainable and bio-inspired chemistry for robust antibacterial activity of stainless steel," *Journal of Materials Chemistry*, vol. 21, pp. 7901 - 7904, 2011.
- [52] C. Vreuls, G. Zocchi, B. Thierry, G. Garitte, S. Griesser, C. Archambeau, C. Van de Weerd, J. Martial and H. Griesser, "Prevention of bacterial biofilms by covalent immobilization of peptides onto plasma polymer functionalized substrates," *Journal of Materials Chemistry*, vol. 20, pp. 8092 - 8098, 2010.
- [53] Y. Hedberg, M. Karlsson, E. Blomberg, I. Wallinder and J. Hedberg, "Correlation between surface physicochemical properties and the release of iron from stainless steel AISI304 in biological media," *Colloids and Surface B: Biointerfaces*, vol. 122, pp. 216-222, 2014.
- [54] B. Somerday, N. Moody, J. Costa and R. Gangloff, "Environment-induced cracking in structural titanium alloys," *Proceedings of the Corrosion/98 Research Topical Symposium, NACE International*, no. 267, pp. 1-17, 1998.
- [55] M. Bezuidenhout, D. Dimitrov, A. van Staden, G. Oosthuizen and L. Dicks, "Titanium-based hip stems with drug delivery functionality through additive manufacturing," *BioMed Research International*, vol. 2015, pp. (ID 134093) 1-11, 2015.

- [56] N. Moody and J. Costa, "A review of microstructure effects on hydrogen-induced sustained load cracking in structural titanium alloys," in *Microstructure/Property Relationships in Titanium Aluminides and Alloys*, The Minerals, Metals & Materials Society, 1991, pp. 587-604.
- [57] Y. Lim, Y. Oshida, C. Andres and M. Barco, "Surface characterizations of variously treated titanium materials," *The International Journal of Oral & Maxillofacial Implants*, vol. 16, no. 3, pp. 333-342, 2001.
- [58] M. Hierro, A. Gallardo, A. Rodriguez, J. Morales and M. Gonzalez, "Experimental approach towards the water contact angle value on the biomaterial alloy Ti6Al4V," *Annales, Universitatis Mariae Curie-Sklodowska*, vol. LXX, no. 1, 2015.
- [59] G. Manivasagam, D. Dhinasekaran and A. Rajamanickam, "Biomedical implants: Corrosion and its prevention - A review," *Recent Patents on Corrosion Science*, vol. 2, pp. 40-54, 2010.
- [60] M. Brown and C. Arnold, "Fundamentals of Laser-Material Interaction and Application to Multiscale Surface Modification," in *Laser Precision Microfabrication*, Berlin Heidelberg, Springer, 2010, pp. 91 - 120.
- [61] J. Ulerich, L. Ionescu, J. Chen, W. Soboyejo and C. Arnold, "Modifications of Ti-6Al-4V surfaces by direct-write laser machining of linear grooves," *Proceedings of SPIE*, vol. 6458, pp. (645819)1-10, 2007.
- [62] C. Ketonis, J. Parvizi, C. Adams, I. Shapiro and N. Hickok, "Topographic features retained after antibiotic modification of Ti alloy surfaces," *Clinical Orthopaedics and Related Research*, vol. 467, no. 7, pp. 1678-1687, 2009.
- [63] E. Zhang, F. Li, H. Wang, J. Liu, C. Wang, M. Li and K. Yang, "A new antibacterial titanium-copper sintered alloy: Preparation and antibacterial property," *Materials Science and Engineering C*, vol. 33, pp. 4280-4287, 2013.
- [64] Z. Liu, X. Liu, U. Donatus, G. Thompson and P. Skeldon, "Corrosion behavior of the anodic oxide film on commercially pure titanium in NaCl environment," *International Journal of Electrochemical Science*, vol. 9, pp. 3558-3573, 2014.
- [65] N. Verissimo, S. Chung and T. Webster, "New nanoscale surface modifications of metallic biomaterials," in *Surface Coating and Modification of Metallic Biomaterials*, Elsevier Ltd., 2015, pp. 249-273.
- [66] I. Pylypchuk, A. Petranovskaya, P. Gorbyk, A. Korduban, P. Markovsky and O. Ivasishin, "Biomimetic hydroxyapatite growth on functionalized surfaces of Ti-6Al-4V and Ti-Zr-Nb alloys," *Nanoscale Research Letters*, vol. 10:338, pp. 1-8, 2015.

- [67] N. Hickok and I. Shapiro, "Immobilized antibiotics to prevent orthopaedic implant infections," *Advanced Drug Delivery Reviews*, vol. 64, pp. 1165-1176, 2012.
- [68] L. Xu, D. Ba, Q. Wang and D. Guo, "New research progressing of surface modification of medical 316L stainless steels," *Eighth International Conference on Thin Film Physics and Applications, Proc. of SPIE*, vol. 9068, pp. 90681L 1-6, 2013.
- [69] C. Gaona, I. Lopez, J. Cabral, P. Zambrano and J. Uruchurtu, "The use of electrochemical noise in the study of nanometric coatings," in *Modern Electrochemical Methods in Nano, Surface and Corrosion Science*, INTECH, 2014, pp. 321-342.
- [70] M. Kulkarni, A. Mazare, P. Schmuki and A. Iglic, "Biomaterial surface modification of titanium and titanium alloys for medical applications," in *Nanomedicine (Chapter 5)*, One Central Press, 2014, pp. 111-136.
- [71] M. Graham, A. Mosier, T. Kiehl, E. Kaloyeros and N. Casy, "Development of antifouling surfaces to reduce bacterial attachment," *Soft Matter*, vol. 9, pp. 6235 - 6244, 2013.
- [72] M. Graham and N. Cady, "Nano and microscale topographies for the prevention of bacterial surface fouling," *Coatings*, vol. 4, pp. 37-59, 2014.
- [73] C. Diaz, P. Schilardi, P. dos Santos, R. Salvarezza and M. Fernandez, "Submicron trenches reduce the *Pseudomonas fluorescens* colonization rate on solid surfaces," *Applied Materials & Interfaces*, vol. 1, no. 1, pp. 136-143, 2009.
- [74] B. Hatton, "Antimicrobial coatings for metallic biomaterials," in *Surface Coating and Modification of Metallic Biomaterials*, Elsevier Ltd., 2015, pp. 379-391.
- [75] E. Ivanova, J. Hasan, H. Webb, V. Tryuong, G. Watson, J. Watson, V. Baulin, S. Pogodin, J. Wang, M. Tobin, C. Lobbe and R. Crawford, "Natural bactericidal surfaces: Mechanical rupture of *Pseudomonas aeruginosa* cells by Cicada wings," *Small*, vol. 8, no. 16, pp. 2489-2494, 2012.
- [76] E. Ivanova, J. Hasan, H. Webb, G. Gervinskas, S. Juodkazis, V. Truong, A. Wu, R. Lamb, V. Baulin, G. Watson, J. Watson, D. Mainwaring and R. Crawford, "Bactericidal activity of black silicon," *Nature Communications*, vol. 4:2838, pp. 1-7, 2013.
- [77] S. Puckett, E. Taylor, T. Raimondo and T. Webster, "The relationship between the nanostructure of titanium surfaces and bacterial attachment," *Biomaterials*, vol. 31, pp. 706-713, 2010.
- [78] J. Hasan and K. Chatterjee, "Recent advances in engineering topography mediated antibacterial surfaces," *Nanoscale*, vol. 7, pp. 15568-15575, 2015.

- [79] J. Genzer and K. Efimenko, "Recent developments in superhydrophobic surfaces and their relevance to marine fouling: a review," *Biofouling*, vol. 22, no. 5-6, pp. 339-360, 2006.
- [80] F. Muller, C. Kunz and S. Graf, "Bio-inspired functional surfaces based on laser-induced periodic surface structures," *Materials*, vol. 9, no. 476, pp. 1-29, 2016.
- [81] U. Manna, N. Raman, M. Welsh, Y. Zayas, H. Blackwell, S. Palecek and D. Lynn, "Slippery liquid-infused porous surfaces that prevent microbial surface fouling and kill non-adherent pathogens in surrounding media: A controlled release approach," *Advanced Functional Materials*, vol. 26, pp. 3599-3611, 2016.
- [82] "Transparency and damage tolerance of patternable omniphobic lubricated surfaces based on inverse colloidal monolayers," *Nature Communications*, vol. 4:2176, pp. 1-10, 2013.
- [83] J. Mori, P. Serra, E. Martinez, G. Sardin, J. Esteve and J. Morenza, "Surface treatment of titanium by Nd:YAG laser irradiation in the presence of nitrogen," *Applied Physics A: Materials Science & Processing [Supplement]*, vol. 69, pp. S699-S702, 1999.
- [84] E. Golosov, V. Emel'yanov, A. Ionin, Y. Kolobov, S. Kudryashov, A. Ligachev, Y. Novoselov, L. Seleznev and D. Siniystn, "Surface modification of titanium by pulsed laser radiation of femtosecond duration," *Inorganic Materials: Applied Research*, vol. 2, no. 3, pp. 206-209, 2011.
- [85] W. Pacquentin, N. Caron and R. Oltra, "Nanosecond laser surface modification of AISI 304L stainless steel: Influence the beam overlap on pitting corrosion resistance," *Applied Surface Science*, vol. 288, pp. 34-39, 2014.
- [86] M. Wautelet, "Laser-assisted reaction of metals with oxygen," *Applied Physics A*, vol. 50, pp. 131-139, 1990.
- [87] M. Bieda, E. Beyer and A. Lasagni, "Direct fabrication of hierarchical microstructures on metals by means of direct laser interference patterning," *Journal of Engineering Materials and Technology*, vol. 132, pp. (031015) 1-6, 2010.
- [88] A. Antonczak, L. Skowronski, M. Trzcinski, V. Kinzhybalo, L. Lazarek and K. Abramski, "Laser-induced oxidation of titanium substrate: Analysis of the physicochemical structure of the surface and sub-surface layers," *Applied Surface Science*, vol. 325, pp. 217-226, 2015.
- [89] P. Gordon, "The tmper colors of steel," *Journal of Heat Treating*, vol. 1, no. 1, p. 93, 1979.
- [90] D. Milovanovic, S. Petrovic, M. Shulepov, V. Tarasenko, B. Radak, S. Miljanic and M. Trtica, "Titanium alloy surface modification by excimer laser irradiation," *Optics & Laser Technology*, vol. 54, pp. 419-427, 2013.

- [91] S. Lawrence, D. Adams, D. Bahr and N. Moody, "Mechanical and electromechanical behavior of oxide coatings grown on stainless steel 304L by nanosecond pulsed laser irradiation," *Surface & Coatings Technology*, vol. 235, pp. 860 - 866, 2013.
- [92] K. Wlodarczyk, M. Ardron, N. Weston and D. Hand, "Nanosecond pulsed laser generation of holographic structures on metals," *Laser-based Micro- and Nanoprocessing X, Proc. of SPIE*, vol. 9736, pp. 97360K 1-8, 2016.
- [93] V. Veiko, G. Odintsova, E. Ageev, Y. Karlagina, A. Loginov, A. Skuratova and E. Gorbunova, "Controlled oxide films formation by nanosecond laser pulses for color marking," *Optics Express*, vol. 22, no. 20, pp. 24342-24347, 2014.
- [94] S. Ahsan, F. AHmed, Y. Kim, M. Lee and M. Jun, "Colorizing stainless steel surface by femtosecond laser induced micro/nano-structures," *Applied Surface Science*, vol. 257, pp. 7771-7777, 2011.
- [95] L. Vazquez, J. Perez, A. Manzano, J. Gonzalez, J. Perez and Y. Vorobiev, "Origin interference colors on austenitic stainless steel," *Inorganic Materials*, vol. 41, no. 9, pp. 1087-1093, 2005.
- [96] S. Ahsan, Y. Kim and M. Lee, "Colorizing of the stainless steel surface by single-beam direct femtosecond laser writing," *Proceedings of SPIE, Frontiers in Ultrafast Optics: Biomedical, Scientific, and Industrial Applications XI*, vol. 7925, pp. (792512) 1-8, 2011.
- [97] M. Thouless, E. Olsson and A. Gupta, "Cracking of brittle films on elastic substrates," *Acta Metallurgica and Materialia*, vol. 40, no. 6, pp. 1287-1292, 1992.
- [98] S. Eto, Y. Miura, J. Tani and T. Fujii, "Effect of residual stress induced by pulsed-laser irradiation on initiation of chloride stress corrosion cracking in stainless steel," *Materials Science & Engineering A*, vol. 590, pp. 433-439, 2014.
- [99] F. Hamadi, E. Amara and H. Kellou, "Characterization of titanium oxide layers formation produced by nanosecond laser coloration," *Metallurgical and Materials Transactions B*, vol. 48B, pp. 1439-1449, 2017.
- [100] M. Heinrich, P. Gruber, S. Orso, U. Handge and R. Spolenak, "Dimensional control of brittle nanoplatelets. A statistical analysis of a thin film cracking approach," *Nanoletters*, vol. 6, no. 9, pp. 2026-2030, 2006.
- [101] "University of Berkeley, Course EE143 Microfabrication Technologies," http://www-inst.eecs.berkeley.edu/~ee143/fa10/handouts/Stress_in_Thin_Films.pdf. [Online]. [Accessed 13 7 2015].

- [102] D. Mattox, "Atomistic film growth and resulting film properties: Residual film stress," *Vacuum Technology & Coating*, pp. 22-23, November 2001.
- [103] M. Fusi, E. Maccallini, T. Caruso, C. Casari, A. Bassi, C. Bottani, P. Rudolf, K. Prince and R. Agostino, "Surface electronic and structural properties of nanostructured titanium oxide grown by pulsed laser deposition," *Surface Science*, vol. 605, pp. 333-340, 2011.
- [104] G. Li, J. Li, X. Li, Z. Zhu, Y. Hu, J. Chu and W. Huang, "Evolution of titanium surfaces irradiated by femtosecond laser pulses with different wavelengths," *Proceedings of SPIE, International Conference on Optics in Precision Engineering and Nanotechnology*, vol. 8769, pp. (87691V) 1-5, 2013.
- [105] J. Martin, "EPA takes action to protect public from an illegal nano silver pesticide in food Containers; Cites NJ Company for Selling Food containers with an unregistered pesticide warns large retailers not to sell these products," 2014. [Online]. Available: <https://archive.epa.gov/epapages/newsroom>. [Accessed 13 May 2018].
- [106] K. Glinel, P. Thebault, V. Humblot, C. Pradier and T. Jouenne, "Antibacterial surfaces developed from bio-inspired approaches," *Acta Biomaterialia*, vol. 8, pp. 1670-1684, 2012.
- [107] J. Green, T. Fulghum and M. Nordhaus, "Immobilized antimicrobial agents: A critical perspective, No. 3, Vol. 1," in *Science against microbial pathogens: communicating current research and technological advances*, Formatex Research Center, 2011, pp. 84-98.
- [108] L. Karam, C. Jama, P. Dhulster and N. Chihib, "Study of surface interaction between peptides, materials and bacteria for setting up antimicrobial surfaces and active food packaging," *Journal of Materials and Environmental Science*, vol. 4, no. 5, pp. 798-821, 2013.
- [109] A. Abts, A. Mavaro, J. Stindt, P. Bakkes, S. Metzger, A. Driessen, S. Smits and L. Schmitt, "Easy and rapid purification of highly active nisin," *International Journal of Peptides*, pp. (175145) 1-9, 2011.
- [110] L. Yin, M. Edwards, J. Li, C. Yip and C. Deber, "Roles of hydrophobicity and charge distribution of cationic antimicrobial peptides in peptide-membrane interactions," *The Journal of Biological Chemistry*, vol. 287, no. 10, pp. 7738-7745, 2012.
- [111] M. Hamad, F. Di Lorenzo, A. Molinaro and M. Valvano, "Aminoarabinose is essential for lipopolysaccharide export and intrinsic antimicrobial peptide resistance in *Burkholderia cenocepacia*," *Molecular Microbiology*, vol. 85, no. 5, pp. 962-974, 2012.
- [112] W. Shafer, L. Martin and J. Spitznagel, "Cationic antimicrobial proteins isolated from human neutrophil granulocytes in the presence of diisopropyl fluorophosphate," *Infection and Immunity*, vol. 45, pp. 29-35, 1984.

- [113] L. Juncioni, A. Faustino, P. Gava and T. Vessoni, "Nisin biotechnological production and application: a review," *Trends in Food Science & Technology*, vol. 20, pp. 146-154, 2009.
- [114] C. Cheigh and Y. Pyun, "Nisin biosynthesis and its properties," *Biotechnology Letters*, vol. 27, pp. 1641-1648, 2005.
- [115] G. Kaur, T. Singh and R. Malik, "Antibacterial efficacy of nisin, pediocin 34 and enterocin FH99 against *Listeria monocytogenes* and cross resistance of its bacteriocin resistant variants to common food preservatives," *Brazilian Journal of Microbiology*, vol. 44, no. 1, pp. 63-71, 2013.
- [116] D. Field, P. Cotter, R. Ross and C. Hill, "Bioengineering of the model lantibiotic nisin," *Bioengineered*, vol. 6, pp. 187-192, 2015.
- [117] J. Lubelski, R. Rink, R. Khusainov, G. Moll and O. Kuipers, "Biosynthesis, immunity, regulation, mode of action and engineering of the model lantibiotic nisin," *Cellular and Molecular Life Sciences*, vol. 65, pp. 455-476, 2008.
- [118] M. Imran, A. Revol-Junelles, M. De Bruin, C. Paris, E. Breukink and S. Desobry, "Fluorescent labeling of nisin Z and assessment of anti-listerial action," *Journal of Microbiological Methods*, vol. 95, pp. 107-113, 2013.
- [119] L. Zhou, A. van Heel and O. Kuipers, "The length of a lantibiotic hinge region has profound influence on antimicrobial activity and host specificity," *Frontiers in Microbiology*, vol. 6, no. 11, pp. 1-8, 2015.
- [120] W. Liu and J. Hansen, "Some chemical and physical properties of nisin, a small-protein antibiotic produced by *Lactococcus lactis*," *Applied and Environmental Microbiology*, vol. 56, pp. 2551-2558, 1990.
- [121] K. Scherer, I. Wiedemann, C. Ciobanasu, H. Sahl and U. Kubitscheck, "Aggregates of nisin with various bactoprenol-containing cell wall precursors differ in size and membrane permeation capacity," *Biochimica et Biophysica Acta*, vol. 1828, pp. 2628 - 2636, 2013.
- [122] H. Hasper, B. De Kruijff and E. Breukink, "Assembly and stability of nisin - lipid II pores," *Biochemistry*, vol. 43, pp. 11567-11575, 2004.
- [123] L. Bi, L. Yang, G. Narsimhan, A. Bhunia and Y. Yao, "Designing carbohydrate nanoparticles for prolonged efficacy on antimicrobial peptide," *Journal of Controlled Release*, vol. 150, pp. 150-156, 2011.
- [124] X. Qi, G. Poernomo, K. Wang, Y. Chen, M. Chan-Park, R. Xu and M. Wook, "Covalent immobilization of nisin on multi-walled carbon nanotubes: superior antimicrobial and anti-biofilm properties," *Nanoscale*, vol. 3, pp. 1874-1880, 2011.

- [125] "Aplin and Barrett Ltd. Technical information sheet: the safety of nisin as a food additive. Technical data reference No. 2/88," Aplin & Barrett Ltd., Dorset, United Kingdom, 1988.
- [126] C. Bower, J. McGuire and M. Daeschel, "Suppression of *Listeria monocytogenes* colonization following adsorption of nisin onto silica surfaces," *Applied and Environmental Microbiology*, vol. 61, no. 3, pp. 992-997, 1995.
- [127] J. Chacko, M. Lalpuria, J. Floros and R. Anantheswaran, *Controlled release of nisin from biopolymer films*, The Pennsylvania State University - General Mills Inc..
- [128] M. Esteban, A. Aznar, P. Fernandez and A. Palop, "Combined effect of nisin, carvacrol and a previous thermal treatment on the growth of *Salmonella enteritidis* and *Salmonella senftenberg*," *Food Science and Technology International*, vol. 19, no. 4, pp. 357-364, 2012.
- [129] A. Alishahi, "Antibacterial effect of chitoan nanoparticle loaded with nisin for the prolonged effect," *Journal of Food Safety*, vol. 34, pp. 111-118, 2014.
- [130] J. Shin, J. Gwak, P. Kamarajan, J. Fenno, A. Rickard and Y. Kapila, "Biomedical applications of nisin," *Journal of Applied Microbiology*, vol. 120, pp. 1449-1465, 2016.
- [131] T. Krivorotova, A. Cirkovas, S. Maciulyte, R. Straneviciene, S. Budriene, E. Serviene and J. Sereikaite, "Nisin-loaded pectin nanoparticles for food preservation," *Food Hydrocolloids*, vol. 54, pp. 49-56, 2016.
- [132] W. Guiga, Y. Swesi, S. Galland, E. Peyrol, P. Degraeve and I. Sebti, "Innovative multilayer antimicrobial films made with Nisaplin or nisin and cellulosic ethers: Physico-chemical characterization, bioactivity and nisin desorption kinetics," *Innovative Food Science and Emerging Technologies*, vol. 11, pp. 352-360, 2010.
- [133] J. Reunanen and P. Saris, "Microplate bioassay for nisin in foods, based on nisin-induced green fluorescent protein fluorescence," *Applied and Environmental Microbiology*, vol. 69, no. 7, pp. 4214 - 4218, 2003.
- [134] C. Lin, K. Takeuchi, L. Zhang, C. Dohm, J. Meyer, P. Hall and M. Doyle, "Cross-contamination between processing equipment and deli meats by *Listeria monocytogenes*," *Journal of Food Protection*, vol. 69, no. 1, pp. 71-79, 2006.
- [135] D. Chen, T. Zhao and M. Doyle, "Transfer of foodborne pathogens during mechanical slicing and their inactivation by levulinic acid-based sanitizer on slicers," *Food Microbiology*, vol. 38, pp. 263-269, 2014.

- [136] L. Karam, C. Jama, A. Mamede, A. Fahs, G. Louarn, P. Dhulster and N. Chihib, "Study of nisin adsorption on plasma-treated polymer surfaces for setting up materials with antibacterial properties," *Reactive & Functional Polymers*, vol. 73, pp. 1473 - 1479, 2013.
- [137] C. Lee, D. An, S. Lee, H. Park and D. Lee, "A coating for use as an antimicrobial and antioxidative packaging material incorporating nisin and alpha-tocopherol," *Journal of Food Engineering*, vol. 62, pp. 323 - 329, 2004.
- [138] A. van Staden, A. Brand and L. Dicks, "Nisin F-loaded brushite bone cement prevented the growth of *Staphylococcus aureus* in vivo," *Journal of Applied Microbiology*, vol. 112, pp. 831-840, 2012.
- [139] H. Hasper, N. Kramer, J. Smith, J. Hillman, C. Zachariah, O. Kuipers, B. De Kruijff and E. Breuknik, "An alternative bactericidal mechanism of action for lantibiotic peptides that target Lipid II," *Science*, vol. 313, pp. 1636-1637, 2006.
- [140] D. Xiao, P. Davidson and Q. Zhong, "Spray-dried zein capsules with coencapsulated nisin and thymol as antimicrobial delivery system for enhanced antilisterial properties," *Agricultural and Food Chemistry*, vol. 59, pp. 7393-7404, 2011.
- [141] P. Knerr and W. van der Donk, "Discovery, biosynthesis, and engineering of lantipeptides," *Annual Review of Biochemistry*, vol. 81, pp. 479-505, 2012.
- [142] S. Hsu, E. Breukink, E. Tischenko, M. Lutters, B. de Kruijff, R. Kaptein, A. Bonvin and N. van Nuland, "The nisin-lipid II complex reveals a pyrophosphate cage that provides a blueprint for novel antibiotics," *Nature Structural & Molecular Biology*, vol. 11, pp. 963-967, 2004.
- [143] R. Rink, J. Wierenga, A. Kuipers, L. Kluskens, A. Driessen, O. Kuipers and G. Moll, "Dissection and modulation of the four distinct activities of nisin by mutagenesis of rings A and B and by C-terminal truncation," *Applied and Environmental Microbiology*, vol. 73, pp. 5809-5816, 2007.
- [144] M. Gee, M. Burton, A. Grevis, M. Akhter, S. McArthur, E. Palombo, J. Wade and A. Clayton, "Imaging the action of antimicrobial peptides on living bacterial cells," *Scientific Reports*, vol. 3:1557, pp. 1-6, 2013.
- [145] O. Tokarsky and D. Marshall, "Mechanism of synergistic inhibition of *Listeria monocytogenes* growth by lactic acid, monolaurin and nisin," *Applied and Environmental Microbiology*, vol. 74, no. 23, pp. 7126-7129, 2008.
- [146] H. Liu, H. Pei, Z. Han, G. Feng and D. Li, "The antimicrobial effects and synergistic antibacterial mechanism of the combination of ϵ -polylysine and nisin against *Bacillus subtilis*," *Food Control*, vol. 47, pp. 444-450, 2015.

- [147] A. Khan, K. Vu, B. Riedl and M. Lacroix, "Optimization of the antimicrobial activity of nisin, Na-EDTA and pH against gram-negative and gram-positive bacteria," *LWT - Food Science and Technology*, vol. 61, pp. 124 - 129, 2015.
- [148] D. Xiao, M. Davidson, D. D'Souza, J. Lin and Q. Zhong, "Nisin extraction capacity of aqueous ethanol and methanol from a 2.5% preparation," *Journal of Food Engineering*, vol. 100, pp. 194 - 200, 2010.
- [149] M. Adhikari, G. Das and A. Ramesh, "Retention of nisin activity at elevated pH in an organic acid complex and gold nanoparticle composite," *Chemical Communications*, vol. 48, pp. 8928 - 8930, 2012.
- [150] A. Scannell, C. Hill, R. Ross, S. Marx, W. Hartmeier and E. Arendt, "Development of bioactive food packaging materials using immobilised bacteriocins Lacticin 3147 and Nisaplin," *International Journal of Food Microbiology*, vol. 60, pp. 241-249, 2000.
- [151] B. Jarvis, "Resistance to nisin and production of nisin-inactivating enzymes by several *Bacillus* species," *Journal of General Microbiology*, vol. 47, no. 1, pp. 33-48, 1967.
- [152] M. Arakha, S. Borah, M. Saleem, A. Jha and S. Jha, "Interfacial assembly at silver nanoparticle enhances the antibacterial efficacy of nisin," *Free Radical Biology and Medicine*, vol. 101, pp. 434-445, 2016.
- [153] M. Zohri, M. Alavidjeh, I. Haririan, M. Ardestani, S. Ebrahimi, H. Sani and S. Sadjadi, "A comparative study between the antibacterial effect of nisin and nisin-loaded chitosan/alginate nanoparticles on the growth of *Staphylococcus aureus* in raw and pasteurized milk samples," *Probiotics & Antimicrobial Proteins*, vol. 2, pp. 258-266, 2010.
- [154] Markets and Markets Research Private Ltd., April 2016. [Online]. Available: <https://www.marketsandmarkets.com/Market-Reports/nisin-market-29041412.html>. [Accessed 7 May 2018].
- [155] C. Shi, X. Zhao, R. Meng, Z. Liu, G. Zhang and N. Guo, "Synergistic antimicrobial effects of nisin and p-Anisaldehyde on *Staphylococcus aureus* in pasteurized milk," *LWT - Food Science and Technology*, vol. 84, pp. 222-230, 2017.
- [156] N. Joo, K. Ritchie, P. Kamarajan, D. Miao and Y. Kapila, "Nisin, an apoptogenic bacteriocin and food preservative, attenuates HNSCC tumorigenesis via CHAC1," *Cancer Medicine*, vol. 1, no. 3, pp. 295-305, 2012.
- [157] W. Brumfitt, M. Salton and J. Hamilton, "Nisin, alone and combined with peptidoglycan-modulating antibiotics: activity against methicillin-resistant *Staphylococcus aureus* and vancomycin-resistant enterococci," *Journal of Antimicrobial Chemotherapy*, vol. 50, pp. 731-734, 2002.

- [158] T. Sivarooban, N. Hettiarachchy and M. Johnson, "Inhibition of *Listeria monocytogenes* using nisin with grape seed extract on turkey frankfurters stored at 4 and 10 C," *Journal of Food Protection*, vol. 70, no. 4, pp. 1017-1020, 2007.
- [159] A. Brandt, A. Castillo, K. Harris, J. Keeton, M. Hardin and T. Taylor, "Inhibition of *Listeria monocytogenes* by food antimicrobials applied singly and in combination," *Journal of Food Science*, vol. 75, no. 9, pp. M557-M563, 2010.
- [160] A. Bag and R. Chattopadhyay, "Synergistic antibacterial and antibiofilm efficacy of nisin in combination with p-coumaric acid against food-borne bacteria *Bacillus cereus* and *Salmonella typhimurium*," *Letters in Applied Microbiology*, vol. 65, pp. 366-372, 2017.
- [161] F. Rusmini, Z. Zhong and J. Feijen, "Protein immobilization strategies for protein biochips," *Biomacromolecules*, vol. 8, pp. 1775 - 1789, 2007.
- [162] D. Kim and A. Herr, "Protein immobilization techniques for microfluidic assays," *Biomicrofluidics*, 2013.
- [163] P. Chua, K. Neoh, Z. Shi and E. Kang, "Structural stability and bioapplicability assessment of hyaluronic acid-chitosan polyelectrolyte multilayers on titanium substrates," *Journal of Biomedical Materials Research Part A*, pp. 1061-1074, 2008.
- [164] V. Humblot, J. Yala, P. Thebault, K. Boukerma, A. Hequet, J. Berjeaud and C. Pradier, "The antibacterial activity of Magainin I immobilized onto mixed thiols self-assembled monolayers," *Biomaterials*, vol. 30, pp. 3503-3512, 2009.
- [165] E. Scallan, R. Hoekstra, F. Angulo, R. Tauxe, M. Widdowson, S. Roy, J. Jones and P. Griffin, "Foodborne illness acquired in the United States - Major pathogens," *Emerging Infectious Diseases*, vol. 17, no. 1, pp. 7-15, 2011.
- [166] S. Lewis, A. Gilmour, T. Fraser and R. McCall, "Scanning electron microscopy of soiled stainless steel inoculated with single bacterial cells," *International Journal of Food Microbiology*, vol. 4, pp. 279-284, 1987.
- [167] P. Herald and E. Zottola, "Attachment of *Listeria monocytogenes* to stainless steel surfaces at various temperatures and pH values," *Journal of Food Science*, vol. 53, pp. 1549-1552, 1988.
- [168] "Effect of cleaners and sanitizers on *Listeria monocytogenes* attached to product contact surfaces," *Journal of Food Protection*, vol. 55, pp. 246-251, 1992.
- [169] R. Brewer, M. Adams and S. Park, "Enhanced inactivation of *Listeria monocytogenes* by nisin in the presence of ethanol," *Letters in Applied Microbiology*, vol. 34, pp. 18-21, 2002.

- [170] L. Thomas and J. Wimpenny, "Investigation of the effect of combined variations in temperature, pH, and NaCl concentration on nisin inhibition of *Listeria monocytogenes* and *Staphylococcus aureus*," *Applied and Environmental Microbiology*, vol. 62, no. 6, pp. 2006-2012, 1996.
- [171] K. Nam, I. Park and S. Ko, "Patterning by controlled cracking," *Nature*, vol. 485, pp. 221-224, 2012.
- [172] S. Mani and T. Saif, "Mechanism of controlled crack formation in thin-film dielectrics," *Applied Physics Letters*, vol. 86, pp. 201903(1-3), 2005.
- [173] R. Seghir and S. Arscott, "Controlled mud-crack patterning and self-organized cracking of polydimethylsiloxane elastomer surfaces," *Scientific Reports*, p. 5:14878, 2015.
- [174] S. Lawrence, D. Adams, D. Bahr and N. Moody, "Deformation and fracture of a mudflat-cracked laser-fabricated oxide on Ti," *Journal of Materials Science*, vol. 48, pp. 4050-4058, 2013.
- [175] F. Variola, J. Yi, L. Richert, J. Wuest, F. Rosei and A. Nanci, "Tailoring the surface properties of Ti6Al4V by controlled chemical oxidation," *Biomaterials*, vol. 29, pp. 1285-1298, 2008.
- [176] Y. Lim, Y. Sohida, C. Andres and M. Barco, "Surface characterizations of variously treated titanium materials," *The International Journal of Oral & Maxillofacial Implants*, vol. 16, pp. 333-342, 2001.
- [177] V. Tarasenko, S. Alekseev, A. Fedenev, I. Goncharenko, N. Koval, K. Oskomov, V. Orlovskii, N. Sochugoy and M. Shulepoy, "Study o IR and UV - lasers interaction with metal surfaces," *Gas and Chemical Lasers and Intense Beam Applications III*, vol. 4631, pp. 234-243, 2002.
- [178] E. Akman and E. Cerkezoglu, "Compositional and micro-scratch analyses of laser induced colored surface on titanium," *Optics and Lasers in Engineering*, vol. 84, pp. 37-43, 2016.
- [179] J. Hutchinson and Z. Suo, "Mixed mode cracking in layered materials," *Advances in Applied Mechanics*, vol. 29, pp. 63-146, 1992.
- [180] Z. Xia and J. Hutchinson, "Crack patterns in thin films," *Journal of the Mechanics and Physics of Solids*, vol. 48, pp. 1107-1131, 2000.
- [181] T. Guo, L. Qiao, X. Pang and A. Volinsky, "Brittle film-induced cracking of ductile substrates," *Acta Materialia*, vol. 99, pp. 273-280, 2015.

- [182] A. Pérez del Pino, P. Serra and J. Morenza, "Oxidation of titanium through Nd:YAG laser irradiation," *Applied Surface Science*, Vols. 197-198, pp. 887-890, 2002.
- [183] D. Adams, R. Murphy, D. Saiz, D. Hirschfeld, M. Rodriguez, P. Kotula and B. Jared, "Nanosecond pulsed laser irradiation of titanium: Oxide growth and effects on underlying metal," *Surface & Coatings Technology*, vol. 248, pp. 38-45, 2014.
- [184] C. Huang, J. Bow, Y. Zheng, S. Chen, N. Ho and P. Shen, "Nonstoichiometric titanium oxides via pulsed laser ablation," *Nanoscale Research Letters*, vol. 5, pp. 972-985, 2010.
- [185] I. Hall and C. Hammond, "Fracture toughness and crack propagation in titanium alloys," *Materials Science and Engineering*, vol. 32, pp. 241-253, 1978.
- [186] B. Kim, C. Moraes, J. Huang, M. Thouless and S. Takayama, "Fracture-based micro- and nanofabrication for biological applications," *Biomaterials Science*, vol. 2, pp. 288-296, 2014.
- [187] P. Wojciechowski and M. Mendiola, "Fracture and cracking phenomena in thin films adhering to high-elongation substrates," *Thin Films for Emerging Applications*, vol. 16, pp. 271-282, 1992.
- [188] M. Thouless, "Modeling the development and relaxation of stresses in films," *Annual Review of Materials Science*, vol. 25, pp. 69-96, 1995.
- [189] J. Zhou, S. Huang, L. Zuo, X. Meng, J. Sheng, Q. Tian, Y. Han and W. Zhu, "Effects of laser peening on residual stresses and fatigue crack growth properties of Ti-6Al-4V titanium alloy," *Optics and Lasers in Engineering*, vol. 52, pp. 189-194, 2014.
- [190] M. Hu, M. Thouless and A. Evans, "The decohesion of thin films from brittle substrates," *Acta Metallurgica*, vol. 36, pp. 1301-1307, 1988.
- [191] M. Thouless, Z. Li, N. Douville and S. Takayama, "Periodic cracking of films supported on compliant substrates," *Journal of Mechanics and Physics of Solids*, vol. 59, pp. 1927-1937, 2011.
- [192] A. Pineau, A. Benzerga and T. Pardoen, "Failure of metals III: Fracture and fatigue of nanostructured metallic materials," *Acta Materialia*, vol. 107, pp. 508-544, 2016.
- [193] A. Volinsky, N. Moody and W. Gerberich, "Interfacial toughness measurements for thin films on substrates," *Acta Materialia*, vol. 50, pp. 441-466, 2002.
- [194] J. Huang, B. Kim, S. Takayama and M. Thouless, "The control of crack arrays in thin films," *Journal of Materials Science*, vol. 49, pp. 255-268, 2014.

- [195] M. Drory and A. Evans, "Experimental observations of substrate fracture caused by residually stressed films," *Journal of American Ceramic Society*, vol. 73, pp. 634-638, 1990.
- [196] M. Niinomi, "Mechanical properties of biomedical titanium alloys," *Materials Science and Engineering A*, vol. A243, pp. 231-236, 1998.
- [197] V. Cain, L. Thijs, J. Humbeeck, B. Van Hooreweder and R. Knutsen, "Crack propagation and fracture toughness of Ti6Al4V alloy produced by selective laser melting," *Additive Manufacturing*, vol. 5, pp. 68-76, 2015.
- [198] Z. Liu and G. Welsch, "Effects of oxygen and heat treatment on the mechanical properties of alpha and beta titanium alloys," *Metallurgical Transactions A*, vol. 19A, pp. 527-542, 1988.
- [199] D. Meyn, "Effect of hydrogen on fracture and inert-environment sustained load cracking resistance of α - β titanium alloys," *Metallurgical Transactions*, vol. 5, pp. 2405-2414, 1974.
- [200] E. Tal-Gutelmacher and D. Eliezer, "Hydrogen-assisted degradation of titanium based alloys," *Materials Transactions*, vol. 45, pp. 1594-1600, 2004.
- [201] B. Yilbas, A. Coban, R. Kahraman and M. Khaled, "Hydrogen embrittlement of Ti-6Al-4V alloy with surface modification by TiN coating," *International Journal of Hydrogen Energy*, vol. 23, no. 6, pp. 483-489, 1998.
- [202] M. Dubravka, A. Ruzica, V. Branka, D. Krnjaic, P. Jelena and S. Sara, "M. Dubravka, A. Ruzica, V. Branka, D. Krnjaic, P. Jelena and S. Sara, "Scanning electron microscopy of *Listeria monocytogenes* biofilms on stainless steel surfaces," *Acta Veterinaria*, vol. 59, no. 4, pp. 423-435, 2009.
- [203] R. Donlan, "Biofilms: Microbial life on surfaces," *Emerging Infectious Diseases*, vol. 8, no. 9, pp. 881-890, 2002.
- [204] N. Jakubovics, R. Shields, N. Rajarajan and J. Burgess, "Life after death: the critical role of extracellular DNA in microbial biofilms," *Letters in Applied Microbiology*, pp. 1-9, 2013.
- [205] M. Vukomanovic, V. Zunic, S. Kunej, B. Jancar, S. Jeverica, R. Podlipec and D. Suvorov, "Nano-engineering the antimicrobial spectrum of lantibiotics: Activity of nisin against Gram negative bacteria," *Scientific Reports*, vol. 7:4324, pp. 1-13, 2017.

- [206] C. Vreuls, G. Zocchi, H. Vandegaart, E. Faure, C. Detrembleur, A. Duwez, J. Martial and C. Van De Weerd, "Biomolecule-based antibacterial coating on a stainless steel surface: multilayer film build-up optimization and stability study," *Biofouling*, vol. 28, no. 4, pp. 395 - 404, 2012.
- [207] J. Weimer, M. Walsh and X. Wang, "Influence of a poly-ethylene glycol spacer on antigen capture by immobilized antibodies," *Journal of Biochemical and Biophysical Methods*, vol. 45, pp. 211-219, 2000.
- [208] J. Peyre, V. Humblot, C. Methivier, J. Berjeaud and C. Pradier, "J. Peyre, V. Humblot, C. Methivier, J. Berjeaud and C. Pradier, "Co-grafting of amino-poly(ethylene glycol) and magainin I on a TiO₂ surface: Tests of antifouling and antibacterial activities," *The Journal of Physical Chemistry B*, vol. 116, no. 2012, pp. 13839-13847.
- [209] T. Cao, A. Wang, X. Liang, H. Tang, G. Auner, S. Salley and S. Ng, "Patterned immobilization of antibodies in mechanically induced cracks," *Journal of Physical Chemistry B*, vol. 112, pp. 2727-2733, 2008.
- [210] A. Hamad, "Effects of different laser pulse regimes (nanosecond, picosecond and femtosecond) on the ablation of materials for production of nanoparticles in liquid solution," in *High Energy and Short Pulse Lasers (Chapter 12)*, INTECH, 2016, pp. 305-325.
- [211] A. Epstein, T. Wong, R. Belisle, E. Boggs and J. Aizenberg, "Liquid-infused structured surfaces with exceptional anti-biofouling performance," *Proceedings of the National Academy of Sciences of the United States of America*, vol. 109, no. 33, pp. 13182-13187, 2012.
- [212] T. Wong, S. Kang, S. Tang, E. Smythe, B. Hatton, A. Grinthal and J. Aizenberg, "Bioinspired self-repairing slippery surfaces with pressure-stable omniphobicity," *Nature*, vol. 477, pp. 443-447, 2011.
- [213] N. McCallum, C. Howell, P. Kim, D. Sun, R. Friedlander, J. Ranisau, O. Ahanotu, J. Lin, A. Vena, B. Hatton, T. Wong and J. Aizenberg, "Liquid-infused silicone as a biofouling-free medical material," *ACS Biomaterials Science & Engineering*, vol. 1, pp. 43-51, 2014.
- [214] P. Sikder, N. Koju, Y. Ren, V. Goel, T. Phares, B. Lin and S. Bhaduri, "Development of single-phase silver-doped antibacterial CDHA coatings on Ti6Al4V with sustained release," *Surface & Coatings Technology*, vol. 342, pp. 105-116, 2018.
- [215] H. Espejo and D. Bahr, "Substrate cracking in Ti-6Al-4V driven by pulsed laser irradiation and oxidation," *Surface & Coatings Technology*, vol. 322, pp. 46-50, 2017.

- [216] L. Bastarrachea, S. Dhawan, S. Sablani and J. Powers, "Release kinetics of nisin from biodegradable poly(butylene adipate-co-terephthalate) films into water," *Journal of Food Engineering*, vol. 100, pp. 93-101, 2010.
- [217] K. Mattick, K. Durham, G. Domingue, F. Jorgensen, M. Sen, D. Schaffner and T. Humphrey, "The survival of foodborne pathogens during domestic washing-up and subsequent transfer onto washing-up sponges, kitchen surfaces and food," *International Journal of Food Microbiology*, vol. 85, pp. 213-226, 2003.
- [218] R. Breed and W. Dotterer, "The number of colonies allowable on satisfactory agar plates," *Journal of Bacteriology*, vol. 1, pp. 321-331, 1916.
- [219] K. Huang, C. Yang, S. Huang, C. Chen, Y. Lu and Y. Lin, "K. Huang, C. Yang, S. Huang, C. Chen, Y. Lu and Y. Lin, "Recent advances in antimicrobial polymers: A mini-review," *International Journal of Molecular Sciences*, vol. 17, no. 1578, pp. 1-14, 2016.
- [220] M. Cloutier, D. Mantovani and F. Rosei, "Antibacterial coatings: Challenges, perspectives, and opportunities," *Trends in Biotechnology*, vol. 33, no. 11, pp. 637-652, 2015.
- [221] Y. Fu, A. Deering, A. Bhunia and Y. Yao, "Pathogen biofilm formation on cantaloupe surface and its impact on the antibacterial effect of lauroyl arginate ethyl," *Food Microbiology*, vol. 64, pp. 139-144, 2017.
- [222] H. Ksontini, F. Kachouri and M. Hamdi, "Dairy biofilm: Impact of microbial community on raw milk quality," *Journal of Food Quality*, vol. 36, no. 4, pp. 282-290, 2013.
- [223] J. Wang, "Characteristics and practices that may lead to *Listeria monocytogenes* contamination in retail delis," *PhD thesis, Purdue University*, 2014.
- [224] E. van Asselt, A. de Jong, R. de Jonge and M. Nauta, "Cross-contamination in the kitchen: estimation of transfer rates for cutting boards, hands and knives," *Journal of Applied Microbiology*, vol. 105, no. 5, pp. 1392-1401, 2008.
- [225] R. Scheffler, "Preventive measures to reduce the risk of cross contamination on direct food contact surfaces of conveyor belts," *Journal of Hygienic Engineering and Design*, vol. 5, pp. 3-5, 2013.
- [226] "Centers for Disease Control and Prevention," <https://www.cdc.gov/foodsafety/outbreaks/index.html>. [Online]. [Accessed 2 06 2018].
- [227] A. Gharsallaoui, N. Oulahal, C. Joly and P. Degraeve, "Nisin as a food preservative: part 1: Physicochemical properties, antimicrobial activity, and main uses," *Critical Reviews in Food Science and Nutrition*, vol. 56, pp. 1262-1274, 2016.

- [228] S. Singh, I. Park, Y. Shin, M. Lee and Y. Lee, "Antimicrobial seafood packaging: a review," *Journal of Food Science and Technology*, vol. 53, no. 6, pp. 2505-2518, 2016.
- [229] C. Lee, D. An, H. Park and D. Lee, "Wide- spectrum antimicrobial packaging materials incorporating nisin and chitosan in the coating," *Packaging Technology and Science*, vol. 16, no. 3, pp. 99-106, 2003.
- [230] G. Rossi, J. Han, B. Garcia , E. Castaño and C. Regalado, "Effect of temperature, pH and film thickness on nisin release from antimicrobial whey protein isolate edible films," *Journal of Science and Food Agriculture*, vol. 89, pp. 2492-2497, 2009.
- [231] S. Lawrence, D. Adams, D. Bahr and N. Moody, "Environmental resistance of oxide tags fabricated on 304L stainless steel via nanosecond pulsed laser irradiation," *Surface & Coatings Technology*, vol. 285, pp. 87-97, 2016.
- [232] L. Bastarrachea, S. Dhawan, S. Sablani and J. Powers, "Release kinetics of nisin from biodegradable poly(butylene adipate-co-terephthalate) films into water," *Journal of Food Engineering*, vol. 100, pp. 93-101, 2010.
- [233] H. Wang, R. Zhang, H. Zhang, S. Jiang, H. Liu, M. Sun and S. Jiang, "H. Wang, R. Zhang, H. Zhang, S. Jiang, H. Liu, M. Sun and S. Jiang, "Kinetics and functional effectiveness of nisin loaded antimicrobial packaging film based on chitosan/poly(vinyl alcohol)," *Carbohydrate Polymers*, vol. 127, pp. 64-71, 2015.
- [234] H. Wang, H. Liu, C. Chu, Y. She, S. Jiang, L. Zhai, S. Jiang and X. Li, "Diffusion and antibacterial properties of nisin-loaded chitosan/poly(L-lactic acid) towards development of active food packaging film," *Food Bioprocessing Technology*, vol. 8, pp. 1657-1667, 2015.

VITA

Jesús Héctor Morales Espejo graduated from Instituto Tecnológico y de Estudios Superiores de Monterrey Campus Eugenio Garza Sada in Monterrey, México, in 1999. He obtained a B.E. in Chemical Engineering, with a minor in Industrial Engineering, from Instituto Tecnológico y de Estudios Superiores de Monterrey Campus Monterrey in December 2003.

He worked for the cement and agrochemical industry in Mexico, while doing an online Master in Quality and Productivity, getting his degree in June 2009.

Later, he was awarded with an Erasmus Mundus scholarship to begin master studies in Europe, doing his first year at Université de Lille 1 Sciences et Technologies (Lille, France) and second year at Università di Bologna (Bologna, Italy), getting his M.S. in Advanced Chemical Spectroscopy degree in July 2011.

He began doctoral studies at Purdue University with Dr. David Bahr in August 2014 and completed doctoral studies in 2018. His doctoral research focused on the development of antibacterial surfaces by desorption of an antimicrobial peptide on modified surfaces of stainless steel and titanium alloy.